


5-2014

The regulation of microRNA biogenesis by ribosome-interacting proteins

Brian Pickering

Follow this and additional works at: http://digitalcommons.library.tmc.edu/utgsbs_dissertations

 Part of the [Cancer Biology Commons](#), [Medicine and Health Sciences Commons](#), and the [Molecular Biology Commons](#)

Recommended Citation

Pickering, Brian, "The regulation of microRNA biogenesis by ribosome-interacting proteins" (2014). *UT GSBS Dissertations and Theses (Open Access)*. Paper 460.

This Dissertation (PhD) is brought to you for free and open access by the Graduate School of Biomedical Sciences at DigitalCommons@The Texas Medical Center. It has been accepted for inclusion in UT GSBS Dissertations and Theses (Open Access) by an authorized administrator of DigitalCommons@The Texas Medical Center. For more information, please contact laurel.sanders@library.tmc.edu.

**THE REGULATION OF MICRORNA BIOGENESIS BY RIBOSOME-
INTERACTING PROTEINS**

by

Brian F. Pickering, Ph.D.

APPROVED:

Dihua Yu, M.D., Ph.D.
Supervisory Professor

Ann-Bin Shyu, Ph.D.

Dos Sarbassov, Ph.D.

Min Gyu Lee, Ph.D.

Richard Behringer, Ph.D.

APPROVED:

Dean, The University of Texas
Graduate School of Biomedical Sciences at Houston

**THE REGULATION OF MICRORNA BIOGENESIS BY RIBOSOME-
INTERACTING PROTEINS**

**A
DISSERTATION**

Presented to the Faculty of
The University of Texas
Health Science Center at Houston

and

The University of Texas MD Anderson Cancer Center
Graduate School of Biomedical Sciences

In Partial Fulfillment
of the Requirements
for the Degree of

DOCTOR OF PHILOSOPHY

by

Brian Frederick Pickering, BS, PhD

Houston, Texas

May, 2014

Dedication

I dedicate this dissertation to my father, Fred Pickering, who passed away shortly after the start of my graduate studies.

Acknowledgements

There were many people involved in my studies without whom this work would not be possible.

I would like to thank my mentors, Dr. Michael Van Dyke and Dr. Dihua Yu for providing me the opportunity to pursue my interests and for their support throughout my tenure.

Many lab mates have contributed significantly both in their help with experiments and intellectual input. I owe much of my success to Sumaiyah Rehman for making some key observations and beginning the studies associated with the miR-200 family biogenesis project. She has also been the primary person I discussed data interpretation, troubleshooting, and alternative approaches. Ping Li was a valuable asset in providing assistance on experiments, as was Sonali Joshi. I would like to thank all of the members of the Yu laboratory, past and present, for their valuable input.

I am indebted to my various committee members who have always given me constructive advice that propelled my projects along. My advisory committee members: Drs. Ann-Bin Shyu, Miles Wilkinson, Seth Corey, and William Mattox, as well as my Supervisory Committee members: Drs. Ann-Bin Shyu, Dos Sarbassov, Min Gyu Lee, and Richard Behringer always pointed my research in the right direction. I owe a special thanks to Dr. Ann-Bin Shyu who took extra time out of his schedule to discuss my project outside of committee meetings and whose advice always changed my entire viewpoint.

I would like to acknowledge our collaborators Dr. Mien-Chie Hung, Dr. Chien-Chen Liu, Wei-Yi Hsu, and Fuu-Jen Tsai for the help with mass spectrometry and Dr. Jun Yao for bioinformatics assistance.

To my family I owe much of my success for sculpting me into the person I am today, especially my mother, Barbara, for being the strongest and most inspirational person I know.

I must thank my friends both local and out of state for putting up with me and taking my mind off work when it seemed overwhelming.

Abstract

The regulation of microRNA biogenesis by ribosome-interacting proteins

Brian Frederick Pickering, Ph.D.

Supervisory Professor: Dihua Yu, MD, Ph.D.

MicroRNA (miRNA) are small, non-coding RNAs that affect gene expression through degradation of complementary mRNA targets or inhibition of translation. As they affect approximately 50% of all cellular processes, miRNA are tightly regulated by the cell through transcriptional and post-transcriptional mechanisms. Transcribed miRNA are capped and polyadenylated (referred to as pri-miRNA) which are cleaved by Drosha and DGCR8 to generate 60-90 nucleotide precursor miRNA. The precursors are cleaved again by Dicer and loaded into the RNA-induced silencing complex (RISC) of which Argonaute 2 is the functional component. Many of the proteins involved in miRNA biogenesis share a common role in ribosomal RNA regulation. Here we characterize two ribosome-associated proteins that are important for miRNA biogenesis. In one study, we identified nucleolin as a positive regulator of pri-miR-15a/miR-16-1 biogenesis. Nucleolin expression is inversely proportional to mature miR-15a/miR-16-1 expression. While nuclear localization of nucleolin increases miR-15a/16-1 expression, cytoplasmic localization of nucleolin decreases it in a mechanism dependent on the interaction of nucleolin with Drosha and DGCR8. Furthermore, pri-miR-15a/miR-16-1 is bound by nucleolin, which facilitates its processing *in vitro*. In another study, we analyzed TCGA patient datasets to uncover a miRNA signature associated with ZEB1/2 expression that

refutes current models of miR-200 family (miR-200a/b/c, miR-141, miR-429) regulation. In breast cancer cell lines with low miR-200 expression an abundance of primary and precursor species exist. We found these precursors are able to regulate other miR-200 family members in a coherent feedforward loop, independent of transcription, by titrating away a repressor complex. We identified the repressor as Receptor of Ribosome Binding Protein 1 (RRBP1) by developing a new technique to capture endogenous protein-RNA complexes *in vivo* called Cross-linking and PNA Pulldown (CLaPP) assay. RRBP1 inversely correlates with miR-200 expression in cell lines and through gain- and loss-of-function studies. TGF- β treatment transcriptionally increased RRBP1 abundance resulting in loss of miR-200 expression. Lastly, RRBP1 was found to directly associate with miR-200 precursors through iCLIP analysis.

In summary, the ribosome-associated proteins nucleolin and RRBP1 were identified and characterized as two novel proteins involved in miRNA biogenesis, each forming feedforward miRNA loops that regulate distinct cellular processes.

Table of Contents

Dedication.....	iii
Acknowledgements.....	iv
Abstract.....	v
Table of Contents.....	vii
List of Figures.....	x
List of Tables.....	xii
1. Chapter 1: Introduction.....	1
1.1. MicroRNA.....	1
1.1.1. MiRNA function.....	1
1.1.2. Transcriptional regulation of miRNA.....	2
1.1.3. Epigenetic regulation of miRNA.....	3
1.1.4. MiRNA biogenesis: the microprocessor complex.....	4
1.1.5. Exportin-5/Ran-GTP.....	5
1.1.6. Dicer/TRBP/PACT.....	5
1.1.7. Argonaute and the RISC complex.....	7
1.1.8. Regulation of miRNA biogenesis by accessory proteins.....	9
1.1.9. Non-canonical biogenesis of miRNA.....	12
1.1.10. Modification of miRNA nucleotides.....	12
1.1.11. Turnover of miRNA.....	14
1.1.12. MiRNA regulatory networks.....	14
1.1.13. The role of miRNA in cancer.....	17
1.2. Mechanisms for studying protein-RNA interactions.....	18
1.2.1. Protein-centric techniques for studying protein-RNA interactions.....	20
1.2.1.1. RNA immunoprecipitation (RIP).....	20
1.2.1.1. Crosslinking and immunoprecipitation (CLIP).....	20
1.2.2. RNA-centric techniques for studying protein-RNA interactions.....	22
1.2.2.1. Biotinylated RNA pulldown.....	22
1.2.2.2. MS2-tagged RNA pulldown.....	22
1.2.2.3. Poly-(A) affinity capture of RNA-binding proteins.....	23
1.2.2.4. ChIRP and RAP antisense tiling pulldown.....	23
1.2.2.5. Peptide nucleic acids (PNAs).....	24
1.3. Rationale for the study.....	24
Chapter 2: Materials and Methods.....	27
2.1. Cell culture.....	27
2.2. Antibodies and drugs.....	27
2.3. Plasmids and siRNA transfections.....	27
2.4. RNA extraction and qRT-PCR.....	28
2.5. Northern blotting.....	28
2.6. Cellular fractionation.....	29
2.7. Immunoprecipitation.....	29

2.8. RNA immunoprecipitation.....	30
2.9. <i>In vitro</i> miRNA processing assay.....	31
2.10. Dual luciferase assay.....	32
2.11. Poly-A+ purification.....	32
2.12. RNA size fractionation.....	32
2.13. High stringency northern blotting.....	32
2.14. Cloning of inducible lentiviral plasmids.....	33
2.15. Cross-linking and PNA Pulldown Assay (CLaPP).....	33
2.16. Identification of RRBP1-bound RNAs by iCLIP.....	35
Chapter 3: Nucleolin interacts with the microprocessor to affect biogenesis of miR-15a/miR-16-1.....	39
3.1. Introduction.....	39
3.2. Results.....	41
3.2.1. The expression of miR-15a and miR-16 correlates with nucleolin expression.....	41
3.2.2. Induced cytoplasmic nucleolin inhibits processing of primary miRNA.....	44
3.2.3. Knockdown of nucleolin ablates processing of primary miRNA.....	48
3.2.4. Nucleolin interacts with the components of the microprocessor independent of RNA.....	51
3.2.5. Nucleolin binds to primary miR-15a and miR-16.....	54
3.2.6. Nucleolin affects the processing of primary miRNA <i>in vitro</i>	57
3.3. Discussion.....	59
Chapter 4: Identification of RRBP1 as a repressor of miR-200 biogenesis and a novel miRNA-mediated coherent feedforward loop.....	63
4.1. Introduction.....	63
4.2. Results.....	63
4.2.1. TCGA analysis of miRNA in patients stratified by ZEB1/2 expression.....	63
4.2.2. Analysis of pri- and mature miR-200 family in breast cancer cell lines.....	67
4.2.3. ZEB1/2 maintain transcriptional repression of the miR-200 family.....	71
4.2.4. TGF- β stimulation or p53 loss do not alter pri- or pre-miR-200 expression.....	74
4.2.5. Knockdown of ZEB1/2 in 14-3-3 ζ overexpressing cells.....	77
4.2.6. Pre-miRNA levels remain unchanged in miR-200 low cells.....	79
4.2.7. Re-expression of the miR-200 clusters.....	84
4.2.8. Coherent feedforward regulation of miR-200 biogenesis.....	88
4.2.9. Development of Cross-linking and PNA Pulldown (CLaPP) assay.....	97
4.2.10. Identification of RRBP1 by CLaPP.....	102
4.2.11. Characterization of RRBP1 as a repressor of miR-200 biogenesis.....	106
4.2.12. TGF- β induces expression of RRBP1.....	110
4.2.13. Characterizing RRBP1 binding to miR-200 by iCLIP.....	112
4.2.14. Detection of pre-miRNA sequences in iCLIP libraries by PCR.....	119
4.3. Discussion.....	121
Chapter 5: Summary and Future Directions.....	127

5.1. Summary.....	127
5.2. Future studies.....	134
Appendix.....	136
Bibliography	143
Vita	166

List of Figures:

Fig. 1. An overview of regulations of miRNA biogenesis.....	11
Fig. 2. MicroRNA regulatory networks.....	16
Fig. 3. Transcriptional regulation of the miR-200 family.....	19
Fig. 4. An overview of ribosomal RNA biogenesis regulated by miRNA processing enzymes.....	26
Fig. 5. Nucleolin expression correlates with miR-15a and miR-16 expression	43
Fig. 6. Decreased association of nucleolin with the microprocessor complex affects miRNA processing.....	45
Fig. 7. Treatment with all <i>trans</i> retinoic acid (ATRA) induces nuclear localization of nucleolin and increased miRNA expression.....	47
Fig. 8. Primary miRNA processing is inhibited in the absence of nucleolin.....	50
Fig. 9. Nucleolin interacts with the microprocessor complex.....	53
Fig. 10. Nucleolin binds to pri-miR-15/16.....	56
Fig. 11. Nucleolin directly affects processing of primary miR-15a and miR-15.....	58
Fig. 12. Model of the bipartite regulation of bcl-2 by nucleolin.....	62
Fig. 13. Correlation between miRNA in ZEB1/2 high and low patient samples.....	65
Fig. 14. Expression of pri-miR-200 vs. ZEB1/2 high and low patient datasets.....	66
Fig. 15. MiRNA and protein expression in breast cancer cell lines.....	68
Fig. 16. Loss of mature miR-200 expression does not alter pre-miR-200 levels and increases pri-miR-200.....	70
Fig. 17. ZEB 1 and ZEB2 transcriptionally repress the miR-200b/a/429 promoter.....	73
Fig. 18. TGF- β treatment or p53 loss downregulate miR-200 post-transcriptionally.....	75
Fig. 19. Knockdown of ZEB1 and ZEB2 fails to restore miR-200 expression.....	78
Fig. 20. Validation of miR-200 precursor.....	81
Fig. 21. Poly-(A)+ selected RNA northern blot and qRT-PCR.....	83
Fig. 22. Re-expression of miR-200 clusters induces upregulation of endogenous clusters independent of transcription.....	87
Fig. 23. Time course dependent induction of individual miR-200 members upregulates other members independent of transcription.....	90
Fig. 24. ZEB1 expression in each of the miR-200 expressing clones during induction timecourse.....	92
Fig. 25. Co-upregulation of miRNA following miR-200a induction.....	93
Fig. 26. Co-upregulation of miRNA following miR-200b induction.....	94
Fig. 27. Co-upregulation of miRNA following miR-200c induction.....	95
Fig. 28. Co-upregulation of miRNA following induction of non-targeting shRNA.....	96
Fig. 29. Specific capture and detection of pre-miR-200 sequences with antisense PNAs.....	100
Fig. 30. An overview of the CLaPP assay.....	101
Fig. 31. Coomassie stain of gel after PNA capture.....	103
Fig. 32. Overview of RRBP1 domain structure.....	105
Fig. 33. RRBP1 expression in breast cancer cell line panel.....	107
Fig. 34. Gain-of-function analysis of RRBP1 on miR-200 expression.....	108
Fig. 35. Knockdown of RRBP1 increases miR-200 expression.....	109

Fig. 36. TGF- β treatment induces RRBP1 expression.....	111
Fig. 37. Expression validation of RRBP1 clones for iCLIP.....	114
Fig. 38. Optimization of crosslinking conditions for RRBP1.....	115
Fig. 39. Triplicate iCLIP analysis of p130 and p180 isoforms.....	116
Fig. 40. Library amplification of RRBP1-bound RNA.....	118
Fig. 41. Detection of pre-miR-200 family members from iCLIP library.....	120
Fig. 42. Model of RRBP1 regulation of miR-200 in luminal and basal-like breast cancers.....	124
Fig. 43. Model of repressor titrating miRNA upregulation.....	125
Fig. 44. TGF- β induced loss of miR-200 via multiple mechanisms.....	126

List of Tables:

Table 1. Antisense PNA sequences used in CLaPP assay.....	96
Table 2. Comparison of hybridization temperatures for PNAs and RNAs with the same base sequences.....	96

1. Introduction

1.1. MicroRNAs

MicroRNAs (miRNA) are short ~21 nucleotide non-coding RNA that negatively affect protein expression by either degrading complementary mRNAs, inhibit mRNA translation, or by inhibiting initiation of the translational machinery (1). The first miRNA identified was by Victor Ambros' group when they isolated a small RNA that regulated lineage commitment in *C. elegans* (2). Since then miRNAs have been found in higher eukaryotes all with similar mechanisms of regulation of and by miRNAs. They regulate upwards of 50% of cellular mRNAs and every major disease studied to date has altered miRNA expression patterns (3). Yet with all that we have learned about miRNAs in two decades of research, new insights are continually being uncovered changing paradigms of miRNAs function, regulation, and impact in disease and development.

1.1.1. MiRNA function

MicroRNAs undergo multiple steps of processing before the functional mature miRNA is generated. The process begins with transcription by RNA pol II generating a 5' capped polyadenylated transcript referred to as a primary microRNA (pri-miRNA) (4, 5). While RNA pol II transcribes the majority of miRNAs there are a small fraction (~5%) that are transcribed by RNA pol III and which are associated with Alu repeat regions (6, 7). These pri-miRNA can be tens of kilobases in length. The first step of post-transcriptional biogenesis is orchestrated by Drosha and DiGeorge's Syndrome Critical Region 8 (DGCR8) proteins called the microprocessor complex (8, 9). The miRNA forms a double stranded

hairpin structure and DGCR8 binds to the flanking ssRNA within ~30 nucleotides from the hairpin. Drosha cleaves ~11 nucleotides from the junction between ssRNA and dsRNA to generate the 60-90 nucleotide precursor miRNA (pre-miRNA) that has a two nucleotide 3' overhang (10, 11). The pre-miRNA is exported to the cytoplasm after binding to Exportin5 and Ran-GTP where it is recognized by Dicer that cleaves the remaining loop structure by measuring the distance from the two nucleotide overhang and cleaving the opposite end (12, 13). Argonaute 2 (Ago2) binds the double stranded RNA, which is now approximately 21 nucleotides with two nucleotide overhangs at either end, and separates the two strands (14). Ago2 binds the functional strand, called the guide strand, while the complementary strand, called the passenger strand, is degraded. Ago2 guides the now mature miRNA to find its mRNA targets dictated by an 8-nucleotide seed region in the 5' of the miRNA that is complementary to target (15). Perfect complementarity results in endolytic cleavage of the mRNA target while incomplete complementarity can result in stalling of the ribosome on the mRNA, inhibition of the ribosomal initiation complex altogether, or deadenylation and exonuclease degradation.

The biogenesis pathways for miRNAs were fleshed out soon after their discovery but since then it has become apparent that these pathways are not linear as initially described and are controlled by many other regulatory factors.

1.1.2. Transcriptional regulation of miRNAs

MiRNAs are transcribed predominantly by RNA pol II but the genes encoding them can have unique gene structures. In the simplest case miRNAs can be found as separate gene

entities with their own promoter. Changes in the activity of their transcription factor directly affect the generation of the pri-miRNA. Things become a bit more complex when one considers that miRNA can reside within protein coding genes. The location can either be in an intron or within an exon. Intronic RNAs require the transcription factor of the host protein-coding gene to generate the RNA but can then be differentially spliced out to make the pri-miRNA. Some intronic miRNAs can also have their own separate promoter within the intron allowing for transcription to occur from either the host gene promoter or their own promoter (16). Exonic miRNAs are hairpins that exist within the coding region of a protein-coding gene. Cleavage of the hairpin often can disrupt the coding sequence negatively impacting the expression of host gene (17).

1.1.3. Epigenetic regulation of miRNA

Epigenetic modification can be broadly grouped into methylation of the DNA through CpG islands and histone modifications. Nearly half of all miRNA genes are associated with CpG islands though not all are necessarily methylated (18). Loss of both DNA methyltransferases, DNMT1 and DNMT3b, in a double knockout restored only 6% miRNAs in HCT116 cells (19). Treatment with 5-aza-2'-deoxycytidine (5-AzaC) increased the expression of only 13 miRNAs suggesting that CpG methylation may not be a dominant mechanism by which cells regulate miRNA expression (20). Combining treatments to reverse CpG methylation along with histone deacetylase inhibition (HDACi) restored again restored approximately 5% of all miRNAs suggesting epigenetic modification by both DNA methylation and histone modifications play only a minor role in miRNA expression

regulation (21). Additionally, HDAC inhibition may in reality be regulating post-transcriptional biogenesis by altering the acetylation of DGCR8 (22)

1.1.4. miRNA biogenesis: the microprocessor complex

The post-transcriptional biogenesis of miRNAs is a multi-step process involving multiple protein complexes in both the nucleus and the cytoplasm. The first step of processing, cleavage by Drosha and DGCR8, occurs simultaneously with transcription (23). Drosha is the enzymatic component of the complex and cleaves miRNA via an RNase III domain in an endonuclease reaction. DGCR8 is thought to stabilize the RNA to give a proper alignment and allow Drosha processing. Evidence suggests that DGCR8 binds RNAs in a non-specific manner giving it a large repertoire of structures and sequences in which it can bind (24). As the core components of miRNA processing, the cell tightly regulates the levels of Drosha and DGCR8. Drosha negatively regulates the expression of DGCR8 by cleavage of a hairpin structure in the 5' UTR of the DGCR8 mRNA (17, 25). DGCR8 stabilizes Drosha via a protein-protein interaction (17). Therefore, increases in DGCR8 lead to stabilization of Drosha that in turn cleaves the mRNA of DGCR8 reducing both their levels. Processing of miRNAs is not the only function of the microprocessor complex (26). An analysis of DGCR8-interacting RNAs demonstrated that mRNAs, snoRNAs, and lncRNAs are all targets of DGCR8 (27). Similarly, not all miRNAs require the microprocessor complex for their expression (28).

Drosha and DGCR8 are subject to post-translational modifications in addition to expression regulation. Drosha is phosphorylated on Ser300 and Ser302, which is necessary

for its nuclear localization. Mutations at either one of these sites to alanine inhibits nuclear localization and decreases miRNA biogenesis (29). DGCR8 is phosphorylated at 28 different residues by Erk1/2 which increases protein expression (30). Phosphorylation does not alter the miRNA processing ability of DGCR8 but does stimulate a pro-growth miRNA profile in HeLa cells. In addition to phosphorylation, DGCR8 can also be acetylated and deacetylation by HDAC1 increases mature miRNA expression (22).

1.1.5. Exportin-5/Ran-GTP

After processing of the primary miRNA by the microprocessor the pre-miRNA is exported out of the nucleus by Exportin-5 and Ran-GTP in complex (12). Exportin5, long thought to be a minor transporter of tRNAs, binds to the dsRNA stem of miRNA and has a propensity for RNAs with a protruding 3' end such as the product from cleavage by the microprocessor complex (31, 32). Exportin-5 has been shown to generate a truncated product due to microsatellite instability in various cancers. The truncated mutant does not possess the final 22 amino acids of the protein and this causes miRNA precursors to be trapped in the nucleus and fail to generate mature miRNA (33).

1.1.6. Dicer/TRBP/PACT

Once the precursors are in the cytoplasm they are recognized by another RNase III enzyme, Dicer. Dicer is a conserved protein found in single-celled eukaryotes as simple as *Schizosaccharomyces pombe*. Interestingly, while yeast contain Dicer they do not make miRNAs but possess the ability to generate RNAi (34). Dicer is a large protein at around 200

kDa that cleaves the terminal loop of precursor miRNAs. The PAZ domain binds to the protruding 3' end and the distance between the catalytic RNase III domains and the PAZ (~65 Å) determines the length of the dsRNA product at around 22 nucleotides (35, 36).

Mice with Dicer knocked out are embryonic lethal, presumably due to depletion of stem cells indicating Dicer, and by extension miRNAs, are necessary for maintaining stem cell populations in early development of mice (37). In ovarian cancer, patients with low Dicer expression were associated with poor clinical outcomes as well as chemotherapy resistance (38). In that study several mutations were identified but did not correlate with expression data indicating other mechanisms leading to down-regulation of Dicer. Similarly, decreased Dicer expression was found in breast cancer and prostate cancer patients (39, 40). In prostate cancer the tumors as a whole had increased Dicer expression yet metastases had significantly lower Dicer expression indicating hemizygous expression of Dicer may give tumor cells a selective advantage for metastasis. One mechanism uncovering the regulation of Dicer expression was via the p53 protein family member TAp63 that serves as a transcriptional activator of Dicer (41). Loss of TAp63 in patient tumors and mouse models resulted in lower levels of Dicer and an increased incidence of metastasis.

In mammals, Dicer interacts with TAR RNA-binding protein (TRBP) and PACT. TRBP and PACT are not necessary for miRNA processing but have positive and negative effects, respectively (42, 43). Moreover, binding of either of these two proteins generates non-redundant altered cleavage, the product of which is referred to as isomiRs.

Phosphorylation of TRBP by Erk increases the stability of the complex between Dicer and TRBP and results in increased expression of pro-growth related miRNAs (44). TRBP not

only affects bindings and processing of precursors to Dicer but is necessary to exchange the cleaved dsRNA from Dicer to Ago2 in the formation of the RNA-induced silencing complex (RISC) (45).

1.1.7. Argonaute and the RISC complex

Argonaute 2 (Ago2, also known as eukaryotic translation initiation factor 2C, 2 (EIF2C2)) is the major constituent of the effector complex of miRNA known as RISC. Evidence suggests Ago2 receives the dsRNA with 5' and 3' overhangs from the Dicer complex with TRBP bound to the more thermodynamically stable end of the miRNA and Ago2 binding to the other end (46, 47). The two miRNA strands are separated into the guide strand (functional) and the passenger strand (degraded). Separation of the strands is due to the RNA helicase activity of Ago2. Studies as to how the guide strand is selected point towards thermodynamic stability, specifically at the 5' end (48, 49).

Ago2 works in conjunction with GW182 (also known as TNRC6) through two phenylalanines to recruit the Pan2-Pan3 and Ccr4-Caf1 deadenylase complexes that deadenylates mRNAs in a biphasic manner coupled with decapping to trigger mRNA decay (50). GW182 contains several domains in the carboxy-terminus including an RNA Recognition Motif (RRM) and a PAM2 motif that recognizes poly(A) binding protein C (PABPC) that coats the poly(A) site of mRNA. The interaction between GW182 and PABPC is required for both translational repression and for miRNA mediated deadenylation (51).

Given its importance in regulating global protein expression, it is not surprising that Ago2 undergoes extensive post-translational modifications. There are seven different

phosphorylation sites that have been identified. Phosphorylation of Ser387 by p38 results in increased accumulation of Ago2 in P-bodies (52). Tyrosine phosphorylation at Tyr529 in the MIDI domain resulted in decreased binding to miRNAs and reduced accumulation in P-bodies presumably due to electrostatic repulsion from the negatively charged phosphate (53). This site is also highly conserved between different species suggesting a critical point of regulation. Akt3 phosphorylates Ser387 in the L2 region increasing its association with GW182 and increasing translational repression (54). Also in the L2 region of Ago2 Tyr393 was found to be phosphorylated by EGFR under hypoxia. This resulted in a identification of an miRNAs regulated by hypoxia-dependent EGFR-suppressed maturation (mHESM) signature of hypoxia-regulated miRNAs that have a unique loop structure that may be important for recognition by phosphorylated Ago2 (55).

Ubiquitylation of Ago2 appears to be a means to regulate miRNA pathway activity. The mouse E3 ubiquitin ligase lin-41 co-localizes with Ago2 and Dicer in P-bodies and ubiquitylates them both *in vitro* and *in vivo* (56). Gain and loss of function of lin-41 resulted in decrease and increased Ago2 expression, respectively and correlated with miRNA processing. Ago2 is bound by the autophagy receptor NDP52 and ubiquitylated resulting in reduced Ago2. Interestingly, it was only miRNA-free complexes that were targeted to autophagosomes suggesting under nutrient stress conditions miRNA regulation is still key but ubiquitylation decreases inefficiency (57).

Upon induction of cellular stress the Argonaute family of proteins is poly(ADP-ribosylated) by PARP-13 increasing stress granule localization and decreasing miRNA suppression of mRNA (58). This is a reversible process wherein the removal of pADPr is

mediated by PARG. Conversely, Ago2 is stabilized and miRNA-suppressive activity is increased upon hydroxylation of Pro700 by the type I collagen prolyl-4-hydroxylase (C-P4H (I)) (59).

1.1.8. Regulation of miRNA biogenesis by accessory proteins

The core components of the miRNA processing pathway are necessary for global expression of miRNAs; however, a number of accessory proteins are able to transiently bind to the core components at all stages of biogenesis to both positively and negatively regulate miRNA biogenesis. By far the most heavily regulated step of processing known to date is the processing of pri-miRNA by the microprocessor complex. Perhaps this is due to the increased presence of *cis* regulatory elements lacking in later stages of processing or it may simply be due to a gap in knowledge regarding the complexities of later stages of processing.

Arsenite-resistance protein 2 (ARS2) regulates miRNA processing at the very beginning by binding to Drosha and stabilizing pri-miRNA as they are processed co-transcriptionally (60, 61).

The regulation of pri-let-7 by Lin28 is one of the best-studied accessory molecules. Lin28 binds to the terminal loop of pri-let-7 which inhibits proper processing by the microprocessor complex (62). In an additional level of regulation Lin28 also recruits the terminal poly(U) polymerases TUT4 and TUT7 to uridylate the 3' end of the let-7 precursor which can no longer be processed by Dicer and is targeted for degradation by DIS3L2 an oligo(U)-binding and processing exoribonuclease (63–67). Loss of mature let-7 is one of the mechanisms by which Lin28 functions as a stem cell factor.

Two RNA helicases, p68 and p72, are necessary for the processing of multiple pri-miRNA through their interaction with Drosha (68, 69). While these proteins are not capable of processing pri-miRNAs alone it is thought they facilitate processing by Drosha via structurally stabilizing the pri-miRNA. Of the two, p68 also interacts with p53 upon DNA damage and TGF- β activated SMAD signal transducer (69, 70). In a similar mechanism to SMADs, SNIP1 interacts with Drosha and may increase processing of pri-miR-21 (71).

Post-transcriptional processing of miRNAs can exhibit an extraordinary level of precision as is the case for hnRNP A1, which facilitates the exclusive processing of pri-miR-18a from the polycistronic miRNA cluster miR-17~92 (72). Accessory protein factors also compete for the same binding sites as with hnRNP A1 and KSRP on the terminal loop of pri-let-7a. hnRNP A1 binds the loop and inhibits processing by Drosha while simultaneously inhibiting KSRP, a positive regulator of pri-miR-let-7a biogenesis (73), from binding the same region (74). KSRP, in addition to regulating pri-miRNA, is one of the few accessory proteins known to regulate pre-miRNA biogenesis (75–77).

Estrogen receptors ER α and ER β both have a role in miRNA biogenesis through interacting with p68 and Drosha (78, 79). Following along with their known antagonistic roles in cancer outcomes ER α and ER β demonstrate opposite effects in miRNA biogenesis.

ILF2 and ILF3 (also known as NF45 and NF90, respectively) function together to repress a subset of miRNA (80). ILF3 may interact with the microprocessor through DGCR8 in an RNA-dependent manner to transfer pre-miRNA from the microprocessor to Exportin-5 (81).

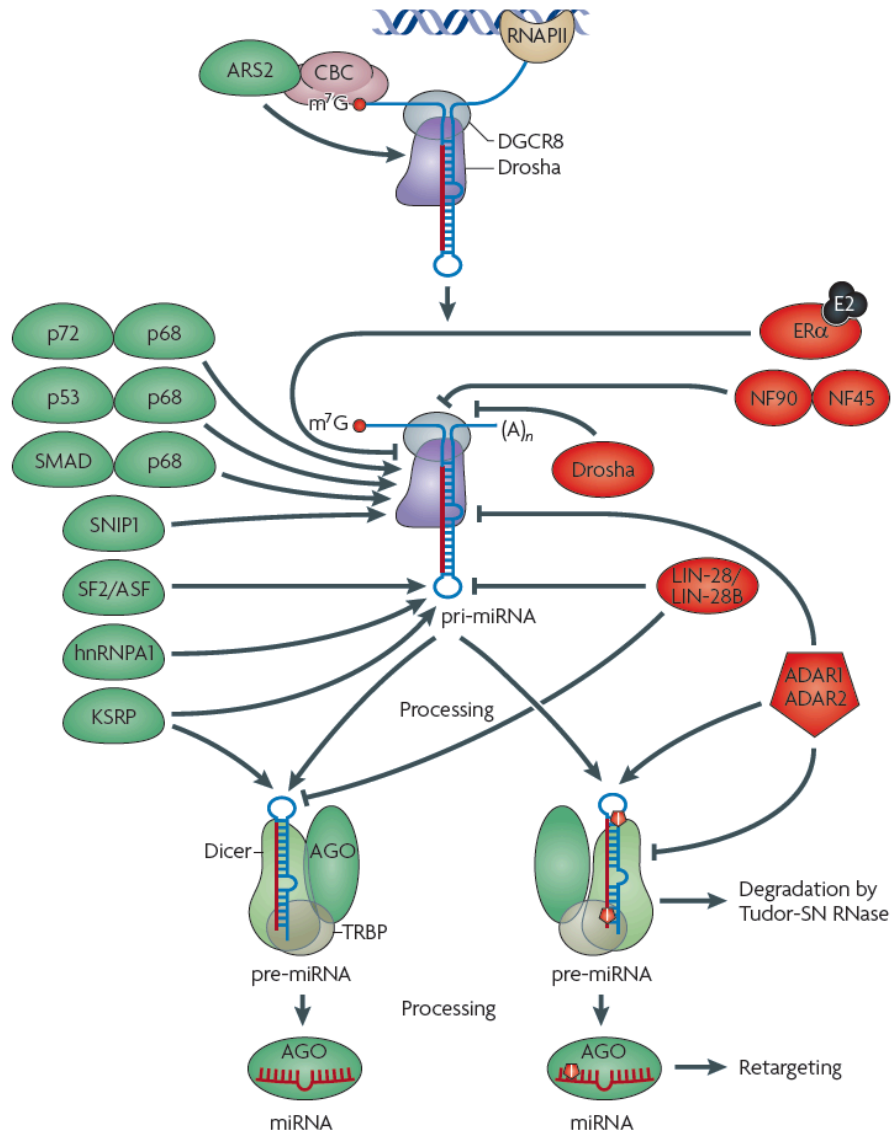


Fig. 1. An overview of regulators of miRNA biogenesis.

The core processing machinery is represented by Drosha/DGCR8 to process pri-miRNAs while Dicer/Ago/TRBP process pre-miRNA. Accessory molecules in green and red are activators and inhibitors of biogenesis, respectively. RNA modifications are indicated by a red 'I'. Reprinted by permission from Macmillan Publishers Ltd: *Nat Rev. Genet.* (Krol J *et al.* 2010 Sep;11(9): 597-610.), copyright (2010).

1.1.9. Non-canonical biogenesis of miRNA

While the core machinery processes the majority of miRNAs there are exceptions that bypass one or more steps. Often this is possible due to structural features in the hairpin loop that allow loading directly into downstream processing complexes. MiR-451 skips Dicer processing by being directly trimmed by Ago2 following Drosha processing (82–84). Poly (A)-specific ribonuclease (PARN) was identified as the enzyme responsible for trimming the 3' end of miR-451 for proper RISC loading (85). Interestingly, trimming was not always to the optimal length for RISC indicating RISC can accommodate RNAs of varying lengths. A limited number of miRNAs are transcribed as pre-miRNA with 5' caps that are able to directly be processed by Dicer (86). These pre-miRNAs are exported out of the nucleus using Exportin-1 instead of Exportin-5. Certain miRNA classes can be cleaved from their primary transcripts not by the microprocessor but rather via the spliceosome machinery (87, 88). Termed mirtrons, these miRNA merge with the canonical pathway at Exportin-5 and are loaded into Dicer to complete their maturation.

1.1.10. Modification of miRNA nucleotides

In addition to regulating miRNA biogenesis in *trans* as determined by protein complexes, cells also regulate miRNA biogenesis in *cis* by modifying nucleotides that affect biogenesis or targeting. These alterations can range from altering nucleotides at the 5' or 3' end of the pre- or mature miRNA, or by altering the internal nucleotides, which often occurs at the pri- or pre-miRNA level. Collectively, these modifications are referred to as non-templated additions (NTAs).

Double-stranded RNA-specific adenosine deaminase, or ADARs, are enzymes that convert adenosine nucleotides to inosine nucleotides by hydrolyzing the the C6 amine (89). The resulting inosine is structurally similar to guanosine, which can alter base pairing and recognizing by other proteins. Editing of pri-miR-142 inhibits processing from Drosha and facilitates cleavage by Tudor-SN, a nuclease that recognizes inosine-uracil pairs in dsRNA (90). However, some miRNA demonstrate enhanced processing upon A-to-I editing suggesting ADARs may have a significant influence on miRNA activity (91). Editing of miRNAs in their seed region can also alter the mRNAs that are targeted (92).

While ADARs modify internal nucleotides of miRNAs multiple enzymes catalyze modifications to the 5' or 3' ends. Uridylation of miRNAs on their 3' end was found to inhibit processing by Dicer and resulted in degradation (63, 65). TUT4 and TUT6 are part of a family of terminal uridyl transferases and are the key enzymes involved in uridylating miRNAs. High-throughput sequencing revealed extensive uridylation of multiple miRNAs including mono-, di-, tri-, and poly-uridylated species (93). Whereas uridylation destabilizes miRNAs, adenylation functions to stabilize them. GLD-2 is a poly(A) polymerase that stabilizes adenylated miRNAs; however, poly-adenylated miRNAs may have reduced capacity to load into the RISC complex, which may affect their activity (94, 95). 2'-O-methylation of miRNAs is found in plants and stabilizes miRNAs by preventing uridylation-mediated cleavage (96, 97). However, human miRNAs are methylated on their 5' end. BCDIN3D is a RNA-methyltransferase that phospho-dimethylates 5' monophosphate precursor miRNAs (98). 5' methylation inhibits Dicer recognition and processing. Taken

together, the complexity of miRNA NTA generates an exquisite diversity of ways in which cells can regulation miRNA levels in *cis* (99).

1.1.11. Turnover of miRNAs

The diversity of processes regulated by miRNA cover those which require a rapid response such as apoptosis and neurological signaling to processes requiring constant miRNA levels such as stem cell maintenance. As such, miRNAs have variable half-lives from hours to days (100). Relatively little is known as to what proteins are responsible for turnover. In plants, degradation of mature miRNA is mediated by small RNA degrading nuclease 1 (SDN1), which is a 3' to 5' exoribonuclease (101). Conversely, animals utilize a 5' to 3' exoribonuclease, XRN-2, which requires separation of the miRNA from the RISC complex before it can be degraded (102).

1.1.12. MiRNA regulatory networks

The multi-tiered nature of miRNA processing coupled with regulation miRNA exert on gene expression allows cells to form distinct regulatory loops to maintain or react to a variety of cellular processes. The networks are often composed of a transcription factor-miRNA-target gene relationship. In the broadest sense, these networks can be either feedforward or feedback loops that serve to propagate a signal or mitigate long-lasting effects, respectively (Fig 2). For example, in the development of *Drosophila* sensory organs the transcription factor Pnt-P1 is activated by EGF to serve as a transcriptional repressor of Yan, ultimately leading to differentiation (103). Pnt-P1 also stimulates the transcription of

miR-7, which in turn inhibits Yan forming a coherent feedforward loop (104). This pathway is conserved in humans suggesting that these networks may have evolved early on and are necessary for proper development (105). Incoherent feedforward loops function in noise buffering to maintain a signal at appropriate levels (106). Nodal signaling, which determines left and right axial structures, regulated by an incoherent feedforward loop where Oct4 activates transcription of the Nodal antagonist Lefty and its negative regulator, the miR-290-miR-295 cluster (107). As a result, Lefty levels are constantly kept in check. E2F1 transcriptionally activates and is negatively regulated by the miR-17~92 cluster of miRNA forming a single negative feedback loop to regulate cellular proliferation (108, 109). Perhaps the best-characterized double-negative feedback loop exists between ZEB1 and ZEB2 (also known as Sip1) and the miR-200 family (composed of miR-200a/b/c, miR-141, and miR-429). ZEB1 and ZEB2 function as transcriptional repressors of the two genomic clusters of the miR-200 family (see Fig 3.) and contain multiple miR-200 binding sites in their 3' UTR (110, 111). In epithelial cells, ZEB1/2 levels remain low resulting in an abundance of miR-200. Upon treatment with TGF- β , ZEB1/2 are transcriptionally upregulated by SMAD2 resulting in loss of miR-200 transcription and an epithelial-to-mesenchymal transition (112).

Recently, a hypothesis regarding RNA-directed miRNA regulation has been proposed referred to as the competing endogenous RNA (ceRNA) hypothesis (113). It postulates that the relative abundance of the mRNA targets can alter the effects of miRNAs by serving as molecular 'sponges' to dilute the effects of miRNA on other target genes. PTEN was found to be regulated by ZEB2 levels in a ceRNA-dependent manner and this was largely due to

effects from the miR-200 family (114). The expression of ZEB2 lead to increased Akt activation resulting in cellular transformation. This represents the first instance of an mRNA dictating miRNA effects in a manner independent of transcription.

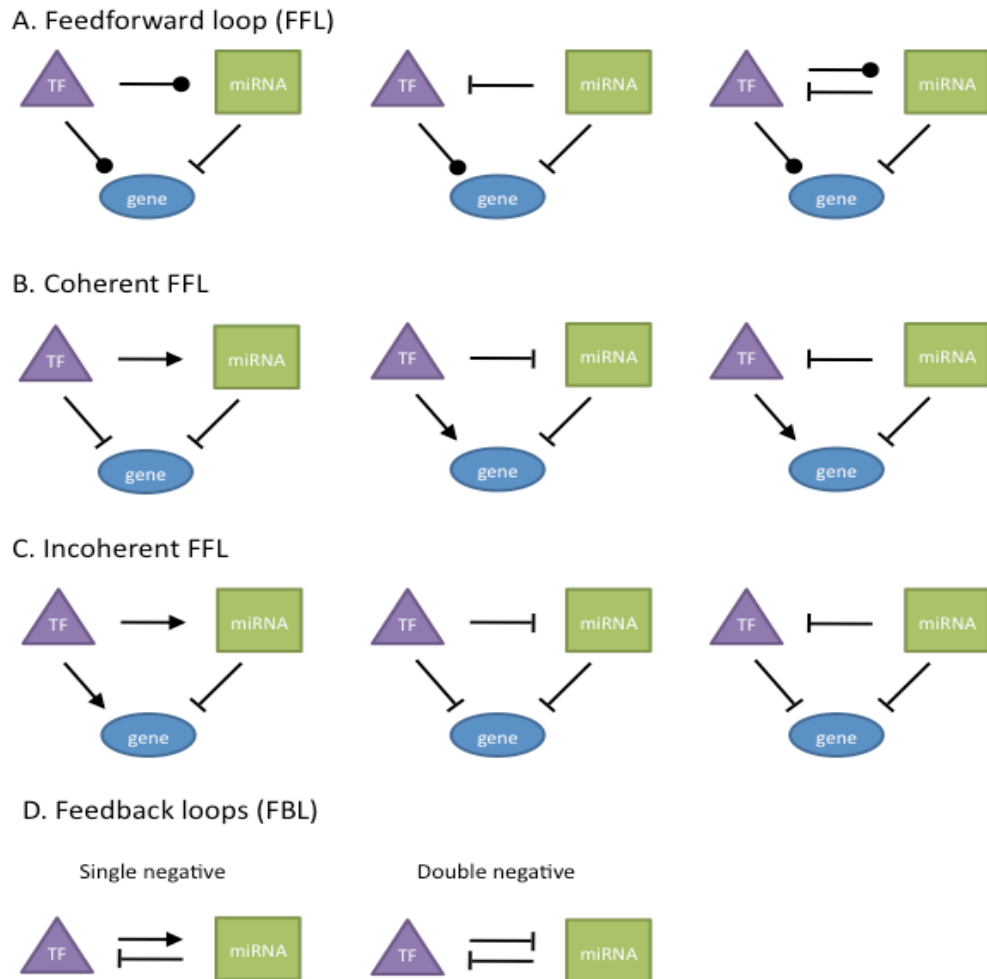


Fig 2. MicroRNA regulatory networks.

A) Representation of generic FFLs. Line with dots at the end can be transcriptional activators or repressors. B) Coherent FFLs two paths have the same effect on a common target. C) Incoherent FFLs the target gene is both activated and inactivated through the actions of the transcription factor (TF). D) Feedback loops can be either single or double negative. Single negative keep FBLs keep expression of either in check while double negative FBLs can have a runaway effect in favor of either TF or miRNA.

1.1.13 The role of the miRNA in cancer

Since their discovery, miRNA have been found to be critical regulators of disease and development. Their role in cancer has been particularly well-established (112, 115–117). Much like their protein-coding counterparts, miRNAs can function as tumor suppressors or oncogenes depending on the genes they regulate.

MiR-15a and miR-16-1 are transcribed as a bicistronic primary miRNA. The gene encoding them is embedded within the DLEU2 non-coding RNA, which part of the fragile genomic region 13q14.3 prone to translocating (118). MiR-15a/16-1 negatively regulates the expression of the anti-apoptosis *BCL2* gene to function as a tumor suppressor (119). However, when expression of miR-15a/16-1 is lost the resulting high levels of bcl-2 can lead to resistance to chemotherapy (120). Moreover, induction of miR-15a/16-1 by all *trans* retinoic acid in acute promyelocytic leukemic induced differentiation via down-regulation of *BCL2* (121). In the development of *Xenopus* embryos, miR-15 and miR-16 function to establish a dorso-ventral gradient of Nodal ligand expression where more dorsal features have decreased miR-15/16 expression and consequently increased SMAD2 signaling (122). Cancer cells often hijack cellular programs whose origins lie in development and exploit them to their own advantage. The miR-15/16 cluster is no exception to this and represents one of the earliest examples of cancer cells manipulating miRNA with dual roles in development and disease.

The miR-200 family represents another excellent example of miRNAs with clear developmental origins that go awry in cancer. This family has garnered extensive attention, in part, because of its contributing role in cancer metastasis, which remains the leading cause

of mortality from cancer (123). The miR-200 family was found to have two separate but equally important roles in metastasis. In the first stage within the primary tumor, low miR-200 levels at the invasive front decrease E-cadherin expression increasing the potential of cells to metastasize (124–126). However, once the cancer cell reaches the site of metastasis miR-200 levels are restored in a mesenchymal-to-epithelial transition (MET) (127, 128). These findings indicate a pleiotropic role in miR-200 function and argue that understanding their regulation may unlock new insights into the metastatic process.

The miR-200 family consists of five miRNAs expressed from two different genomic clusters (Fig. 3). Each cluster is under extensive transcriptional regulation, both positively and negatively. Of the transcription factors listed in Fig. 3 only three are negative regulators of miR-200 family transcription: Slug, ZEB1, and ZEB2 (111, 129). ZEB1 and ZEB2 work in concert to inhibit miR-200 expression via binding to multiple E-box domains in the two chromosomal loci. The ZEB1/2-miR-200 axis also forms a distinct double-negative feedback loop whose balance is perturbed upon induction from external stimuli (*e.g.* TGF- β or BMPs), which often commits the cell to either an epithelial or mesenchymal lineage.

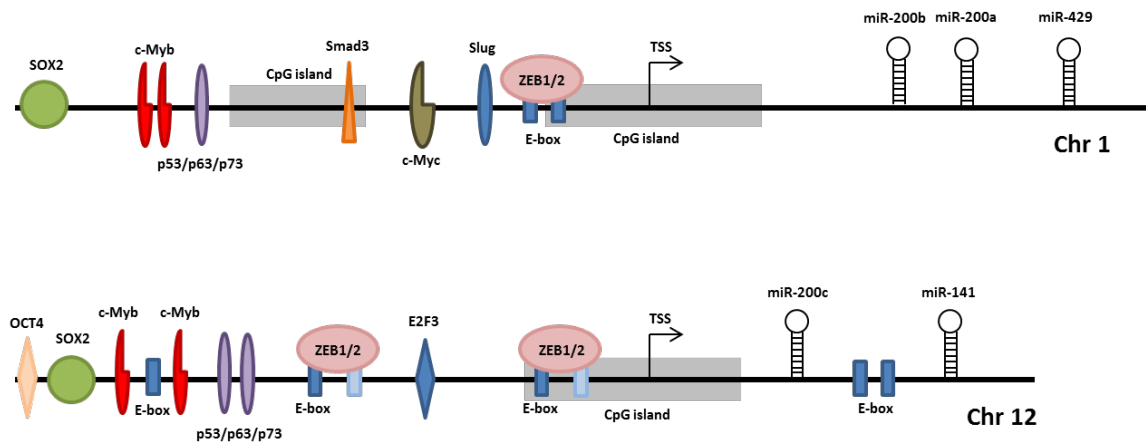


Fig. 3. Transcriptional regulation of the miR-200 family.

A graphical representation of the various transcription factors that bind to the miR-200b/a/429 cluster or the miR-200c/141 cluster. All transcription factors listed are activators except Slug and ZEB1/2. TSS = transcription start site. Not drawn to scale.

1.2 Mechanisms for studying protein-RNA interactions

Following the sequencing of the human genome and development of evermore advanced sequencing technologies, a new world of RNA biology that lay hidden beyond our reaches due to technical limitations is suddenly exploding with richness. The following sections describe the advances that have been made in developing new tools to identify and characterize novel protein-RNA interactions. These sections are broken down into two broad categories: protein-centric and RNA-centric

1.2.1 Protein-centric techniques to study protein-RNA interactions

1.2.1.1 RNA immunoprecipitation (RIP)

One of the earliest advances to address whether a particular protein interacts with a particular RNA without relying on *in vitro* techniques was RNA immunoprecipitation (130). This technique built upon existing technologies at the time for chromosome immunoprecipitation (ChIP) with the extra step of reverse transcription. While ChIP and RIP are powerful techniques in their own right, they rely on chemical crosslinkers, which can result in significant background from non-specific covalent bonding during fixation. Another shortcoming of RIP was the target sequence must be known to some extent. However, this was fixed with the development of RIP-Chip and RIP-seq that catalog bound RNAs through microarray hybridization or RNA deep sequencing (131, 132).

1.2.1.2 Crosslinking and Immunoprecipitation (CLIP)

The next major advancement in the identification of RNAs bound by a particular protein was through the use of UV crosslinking RNAs to the protein. UV crosslinking had long been used in *in vitro* studies to analyze protein binding through gel shifts or filter binding assays. It has the distinct advantage of generating a near zero distance covalent bond between protein and RNA; however, that covalent bond is irreversible preventing separating the RNA from the protein in downstream analyses. Work in the lab of Robert Darnell conducted by Jernej Ule used this principle to his advantage to develop the CLIP methodology (133).

Later variants of the protocol incorporated high-throughput sequencing (HITS-CLIP) and increased crosslinking efficiency by the use of photoactivatable ribonucleosides (PAR-CLIP) (134, 135). Importantly, the inclusion of next-gen sequencing in these techniques not only allowed the identification of all the RNAs bound by a protein but also the exact location in which it interacts. This can be done computationally through identifying mutations induced as a result of downstream applications. In HITS-CLIP, the protein-RNA complex is extracted from nitrocellulose via proteinase K digestion, which leaves a couple of amino acids still covalently linked to the RNA. As the reverse transcriptase is moving along the RNA it encounters the amino acids and skips over the nucleotide to complete the cDNA synthesis. Therefore, nucleotides missing in the sequencing data indicate the exact location the protein was bound. A similar bioinformatic analysis can be done with PAR-CLIP since the incorporation of 4-thiouridine or 6-thioguanosine in the RNA to facilitate crosslinking results in a thymidine to cytosine or guanosine to adenosine transition, respectively (136).

The latest iteration of CLIP technologies is individual-nucleotide resolution CLIP, or iCLIP (137). iCLIP takes advantage of the fact that 85% of the time the reverse transcriptase does not skip over crosslinked sites, rather it falls off generating a truncated product. The key difference in iCLIP is circularization of cDNAs to identify the exact site of reverse transcriptase termination. Different technologies can be joined together, for example, using photoactivatable nucleosides with iCLIP to generate PAR-iCLIP.

Taken together, the latest advancement in RNA sequencing technologies allow an unprecedented view into the RNA-binding landscape of proteins.

1.2.2 RNA centric methods for studying protein-RNA interactions

1.2.2.1. Biotinylated RNA pulldown

The use of biotinylated RNAs generated by *in vitro* transcription represents an easy method in which to identify proteins that bind to a particular RNA. In this assay, cell extracts are mixed with synthetic biotinylated RNA probes that are captured through streptavidin beads or pre-bound in a column. However, the advantage of simplicity is often outweighed by the significant drawbacks including binding of non-specific, highly abundant RNA binding proteins and the capture probes are often in large excess and not physiological levels giving a high false-positive and false-negative return.

1.2.2.2. MS2-tagged RNA capture

To overcome issues of spatial disruption during lysis and non-physiological RNA levels a new technique was developed using the MS2 aptamer fused to an mRNA of interest.

The technique is known as RNA-binding protein purification and identification (RaPID) (138). The MS2 aptamer has a K_d of approximately 3 nM for the MS coat protein allowing very specific purification of low abundant species.

1.2.2.3. Poly(A) affinity capture of RNA-binding proteins

Much like CLIP took advantage of the highly specific UV-induced crosslinks between protein and RNA to identify RNAs bound to specific protein, Castello and colleagues applied UV crosslinking and RNA capture to characterize genome-wide protein-RNA complexes (139, 140). The assay is based upon the principle that RNA pol II substrates are polyadenylated and established protocols for the purification of poly-(A) RNA using oligo-dT beads. When cells are crosslinked *in vivo* before lysis poly-(A) capture the RNA one can evaluate the repertoire of RNA binding proteins as they exist in their cellular context. A similar protocol was adapted to identify newly poly-adenylated RNAs by spiking cells with 2-ethynyl adenosine before treating with biotin-azide and capturing with streptavidin beads (141). While the later technique was used to profile RNAs by sequencing it is easy to extrapolate this technique could be combined with UV crosslinking to identify RBPs bound to newly polyadenylated RNAs.

1.2.2.4. ChIRP and RAP antisense tiling pulldown

The capture of poly-(A) RNA does not allow any specificity in target RNAs captured. The techniques of ChIRP (Chromatin Isolation by RNA Purification) and RAP (RNA Antisense Purification) both utilize multiple antisense biotinylated RNA probes that

hybridize to their target RNA and are captured by streptavidin beads (142, 143). The use of multiple antisense RNAs that are ‘tiled’ against the target RNA allow the target RNA to be captured even if a particular antisense probe is blocked by structural features or are precluded by bound proteins.

1.2.2.5. Peptide Nucleic Acids (PNAs)

An alternative to using antisense RNAs are capture probes are peptide nucleic acids (PNAs). As the name implies, PNAs contain the normal nitrogenous bases but instead of a sugar phosphate backbone PNAs contain an uncharged peptide backbone (144). This unique chemistry allows PNAs to hybridize to complementary sequences in the absence of salts to neutralize the negative charge of a sugar phosphate backbone. As such, PNAs display amazing strand invasive capability to hybridize to even highly structured RNAs. While PNAs have not been used to capture protein-bound RNAs, they have been used to capture highly structured, non-polyadenylated RNAs (tRNAs) from a complex milieu of other cellular RNAs with very high sensitivity and specificity (145)

1.3 Rationale for the study

Many of the proteins involved in miRNA biogenesis were originally characterize in the ribosomal RNA biogenesis pathway (Fig. 4). Drosha was first characterized as RNase III necessary for pre-rRNA processing (146). The RNA helicases p68 and p72 are responsible for 5.8S rRNA biogenesis (68). *Candida albicans* Dicer is necessary for cleavage of 3’ unprocessed rRNA (147). Loss of expression of Ago2 inhibits pre-rRNA processing,

specifically in the conversion of pre-5.8S rRNA (148). Lastly, HITS-CLIP analysis of RNA bound by DGCR8 indicated 21% of all RNA species bound are rRNA (27). In this study, we identify and characterize two ribosome-associated proteins, nucleolin and receptor of ribosome binding protein 1 (RRBP1), with novel miRNA processing functions in the cell.

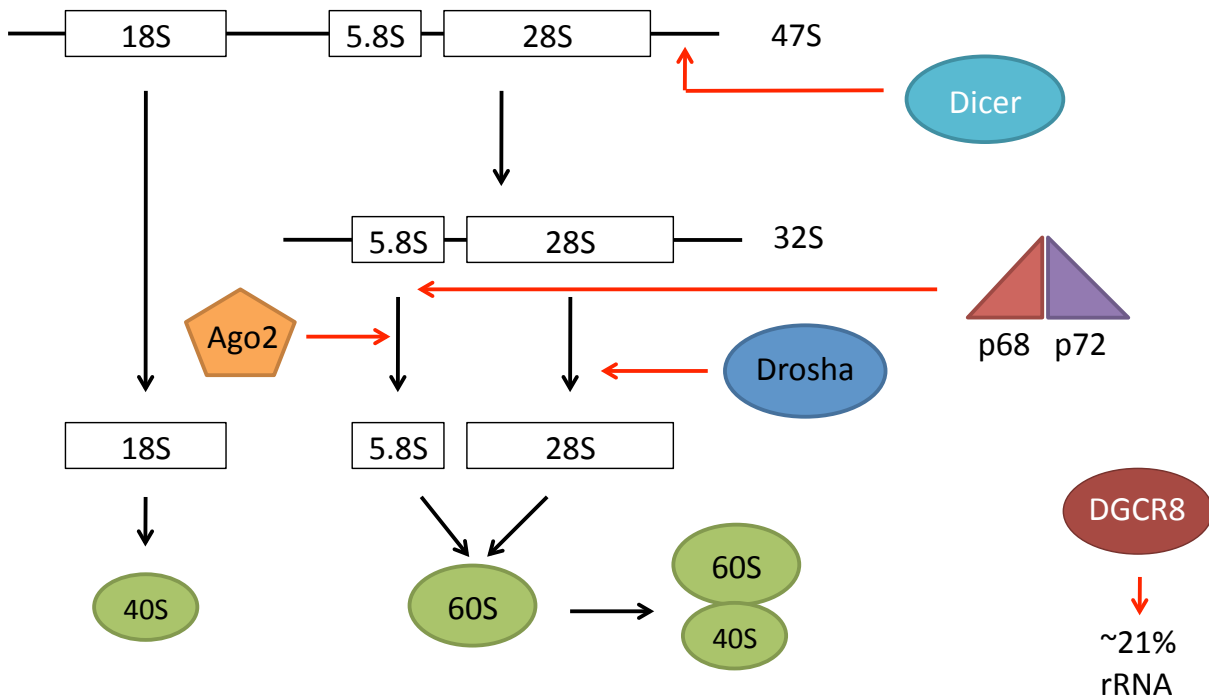


Fig. 4. An overview of ribosomal RNA biogenesis regulated by miRNA processing enzymes. A simplified model of rRNA processing is represented beginning with the conversion of the transcribed 47S rRNA precursor, which gets processed in through multiple stages to generate the 40S and 60S ribosomal subunits that associate to form the functional 80S ribosome. White boxes represent RNA sequences present in the mature rRNAs and black lines are cleaved and degraded flanking RNA sequences. Dicer is responsible for degradation of the cleaved flanking sequences while Drosha, Ago2, p68, and p72 are necessary for proper formation of individual precursors. Approximately 21% of all RNAs bound by DGCR8 are rRNA sequences, though no specific step in rRNA biogenesis has been attributed to it.

Chapter 2: Materials and Methods

2.1. Cell Culture

All cell lines were purchased from ATCC (Manassas, VA) and maintained in the recommended media. HEK293 were used to generate stable expressing lines while HEK293FT cells were used for lentiviral production. Cell lines included non-transformed MCF-10A and MCF-12A; breast cancer cells MB-MDA-361, MB-MDA-453, MCF-7, T47D, MB-MDA-231, BT-549, Hs578T, and MB-MDA-435. MOLM-13 and HL-60 cells were grown in RPMI with 10% heat-inactivated FBS.

2.2. Antibodies and drugs

Antibodies to nucleolin (clone 4E2, MBL International, 1:1000), FLAG M2 (Sigma-Aldrich, 1:1000), HA (clone 16B12, Covance, 1:1000), Drosha (Cell Signaling, D28B1, 1:500), GAPDH (Santa Cruz, SC-32233, 1:1000), and PARP (Santa Cruz, SC-1019, 1:1000), RRBP1 (Genetex, GTX101844, 1:1000), β -actin (Sigma Aldrich, 1:5000), ZEB1 (Novus Biologicals, NBP1-05987, 1:500), E-cadherin (Santa Cruz, 1:1000), p53 (Santa Cruz, 1:500) were obtained from the suppliers indicated. Parthenolide was purchased from Sigma-Aldrich.

2.3 Plasmids and siRNA transfection

The pCMV2-FLAG-NCL was generously donated by Paula Bates (U. Louisville) and previously described (148). The TAP-tagged DGCR8 expression vector was generated by the Tuschl lab and was obtained through Addgene (Plasmid ID: 10921)(149). Cells stably transfected with the pCMV2-FLAG-NCL plasmid were selected for three weeks with 800 μ g/ml G418 and maintained with 200 μ g/ml G418. Cells transfected with pFLAG/HA-

DGCR8 were selected in 10 µg/ml puromycin for one week and maintained with 1 µg/ml. The Plasmid for RRBP1 (p130 isoform) was purchased from Origene. The p180 isoform was a gift from Dr. Ogawa-Goto (150) and was sub-cloned into the same pCMV6 backbone as the p130 isoform. Stable lines for p130 and p180 isoforms were generated by transfecting MCF-10A cells with 10 µg of plasmid with GenJet Ver II, allowing them to grow for 48 hours, and selecting with 400 µg/ml G418 for one week. Primary miRNA for *in vitro* processing assays were reverse transcribed from cDNA using SuperScript III first strand cDNA synthesis kit (Invitrogen) and PCR products included approximately 200 nt of the flanking sequences. The gel purified products were inserted into the pGEM-T-easy vector (Promega) by TA cloning and inserts verified by sequencing. Small interfering RNA were purchased from Dharmacon and Sigma-Aldrich and routinely achieved >70% knockdown efficiency. Transfections were carried out using Pepmute (SignaGen) with 30 nM siRNA for 72 to 96 hours before knockdown experiments were carried out.

2.4. RNA Extraction and qRT-PCR

RNA was extracted using Trizol according to the manufacturer's instructions. For mature miRNA analysis, RNA was reverse transcribed and quantified using the TaqMan miRNA Assay kit (Applied Biosystems) according to the manufacturer's instructions. Pri-miRNA and mRNA expression were reverse transcribed with random hexamers using the High Capacity cDNA kit (Applied Biosystems). Kapa Biosystems Sybr green or Probe mastermixes were used for qPCR.

2.5. Northern blotting

10 µg of RNA was run on a 15% PAGE-urea gel and transferred to Brightstar-plus positively charged nylon membranes (Ambion, Inc.) by semidry transfer. The membrane was crosslinked using a Stratalinker 1800 (Stratagene) at 0.12 J/cm² followed by baking for 30 minutes at 80 °C. Membranes were pre-hybridized in Ultrahyb-Oligo (Ambion) for 30 minutes at 42 °C before the addition of 10⁶ cpm of ³²P-labelled synthetic LNA probes (Exiqon) and incubated overnight at 42 °C. Membranes were washed two times for 30 minutes at 37 °C in 2× SSC and 0.5% SDS before being exposed on a phosphorimaging screen overnight.

2.6. Cellular fractionation

Cells were trypsinized and washed three times with PBS. Three packed cell volumes (pcv) of cytoplasmic extraction (CE) buffer (10 mM HEPES pH 7.9, 10 mM KCl, 0.1 mM EDTA pH 8.0, 0.1 mM EGTA, 1 mM DTT) was used to resuspend the pellet. After 15 minutes on ice, NP-40 was added to a final concentration of 0.3%, gently mixed, and centrifuged at 4 °C for 1 minute at 10,000 × g. The supernatant was saved as the cytoplasmic fraction. The pellet was washed once with two volumes of CE buffer. The pellet was resuspended in 1 volume of nuclear extract buffer (20 mM Tris pH 7.9, 400 mM NaCl, 0.2 mM EDTA pH 8.0), incubated for 30 minutes on ice, and centrifuged for 5 minutes at 10,000 × g. The supernatant was saved as the nuclear extract and the pellet discarded.

2.7. Immunoprecipitation

HEK293 cells stably expressing either FLAG/HA-DGCR8 or FLAG-NCL were collected, washed with PBS, and lysed in NP-40 whole cell extraction buffer (20 mM HEPES pH 8.0, 150 mM NaCl, 0.1% NP-40, 1 mM EDTA, 1 mM phenylmethylsulfonyl fluoride

[PMSF], and 1 $\mu\text{g}/\text{mL}$ each of leupeptin, pepstatin, and aprotonin). 2.5 μg of antibody was added to the 500 μl immunoprecipitation overnight at 4 $^{\circ}\text{C}$. RNase A (20 $\mu\text{g}/\text{ml}$) treatments were overnight at 4 $^{\circ}\text{C}$. 50 μl of Protein A/G agarose (Santa Cruz) was added to the lysates for 2 hours at 4 $^{\circ}\text{C}$. Beads were washed three times in lysis buffer (20 mM HEPES pH 8.0, 150 mM NaCl, 0.1% NP-40) and boiled in 60 μl of 2 \times Laemmli sample buffer. 20 μl of the boiled beads and 10% of input and supernatant were resolved by SDS-PAGE, and Western blotted with the described antibodies.

2.8. RNA immunoprecipitation

RNA immunoprecipitation (RIP) was carried out as previously described with slight modifications (30). HEK293 cells were trypsinized, washed twice with PBS and resuspended in 10 ml PBS. Cells were crosslinked with 1% formaldehyde for 10 minutes followed by quenching with 0.25 M glycine for 10 minutes at room temperature and washed twice with PBS. The pellet was resuspended in buffer A (5 mM PIPES [pH 8.0], 85 mM KCl, 0.5% NP-40) and incubated on ice for 10 minutes. Nuclei were collected by spinning at 2500 \times g for 5 minutes at 4 $^{\circ}\text{C}$. The pellet was washed once with buffer A without NP-40. The nuclear pellet was resuspended in 500 μl of buffer B (1% SDS, 10 mM EDTA, 50 mM Tris [pH 8.1]) and sonicated. Insoluble material was pelleted at 14,000 \times g for 10 minutes at 4 $^{\circ}\text{C}$. The supernatant was diluted into IP buffer (0.01% SDS, 1.1% Triton X-100, 1.2 mM EDTA, 16.7 mM Tris [pH 8.1], 167 mM NaCl) and incubated with 5 μg of FLAG antibody overnight at 4 $^{\circ}\text{C}$. Beads were washed once with low-salt wash (0.1% SDS, 1% Triton X-100, 2 mM EDTA, 20 mM Tris [pH 8.1], 150 mM NaCl), high-salt wash (same as low-salt but with 500 mM NaCl), LiCl wash (0.25 M LiCl 1% NP-40, 1% Na Deoxycholate, 1 mM

EDTA, 10 mM Tris [pH 8.1]), and twice with TE buffer. Immunoprecipitated complexes were eluted from the beads by treatment with 100 µl elution buffer (50 mM Tris-HCl [pH 7.5], 10 mM EDTA, 1% SDS) at 65 °C for 10 minutes. Samples were reverse crosslinked by incubation for 2 hours at 42 °C and 6 hours at 65 °C in 0.5× elution buffer plus 0.5 mg/ml proteinase K. RNA was extracted with Trizol and reverse transcribed in a 20 µl final volume using the high capacity cDNA kit (Applied Biosystems) with random primers. Following reverse transcription, 5 µl of sample was analyzed by PCR with 500 nM primer concentration and the reaction allowed to proceed for 30-35 cycles before 10 µl of product was analyzed on a 2% agarose gel.

2.9. *In vitro* miRNA processing assay

The processing assay was carried out as described previously (151). Labeled primary miRNA were generated using the maxiscript kit (Ambion) according to the manufacturer's instructions. Briefly, 1 µg of linearized plasmid was labeled with ³²P-labeled UTP. RNA products were gel purified and eluted in 0.5 M NH₄OAc, 1 mM EDTA, 2% SDS, overnight at 37°C followed by ethanol precipitation. All *in vitro* transcribed probes were made fresh for each experiment. HEK293 cells were treated with siRNA for 48 hours before being collected. Cells were washed in PBS and resuspended in IVP lysis buffer (50 mM Tris [pH 8.0], 100 mM KCl, 0.2 mM EDTA) and sonicated. Insoluble material was pelleted by spinning at 14,000 rpm for 10 minutes at 4°C. 15 µl of cell extract were mixed with 3 µl 64 mM MgCl₂, 3 µl labeled pri-miRNA (~3×10⁴ cpm), 1 U/µl SUPERase-in (Ambion) and the final volume brought to 30 µl with DEPC-water. For rescue experiments, 5 or 10 µl of beads from a FLAG-nucleolin immunoprecipitation were added to the reaction. The reaction

was incubated for 90 minutes at 37°C before the RNA was extracted with Trizol LS (Invitrogen). Purified RNA was run on a 12.5% denaturing PAGE and exposed to a phosphorimager overnight.

2.10. Dual luciferase assay

1×10^5 cells were plated onto 6-well plates and co-transfected with 500 ng of miR-200b/a/429 reporters pGL3-321/+120 or pGL3-321/+120 Ebox Mut2 firefly luciferase plasmids (111) and 20 ng of pGL4-TK Renilla luciferase constructs (Promega) with GenJet ver. II (SignaGen). Dual luciferase reporter assay system (Promega) was performed 24 hr after transfection according to the manufacturer's instructions, and luciferase activity was measured with a TD-20/20 luminometer. Each assay was performed in triplicate, and all firefly luciferase values were normalized to renilla luciferase readings.

2.11. Poly-(A)+ RNA purification

Poly-A+ RNA purification from MCF-10A.vec and MCF-10A.ζ cells utilized the Poly (A)Purist™ Kit (Ambion) according to the manufacturer's instructions. Each purification was done using one 10-cm culture plate of cells.

2.12. RNA size fractionation

RNA were fractionated into high (>200 nt) and low (<200 nt) fractions using RNazol (MBL) and the small RNA isolation protocol according to the manufacturer's instructions.

2.13. High stringency northern blotting

Trizol purified RNA was fractionated by 10% acrylamide (19:1) denaturing $1 \times$ TBE-urea electrophoresis and transferred to Hybond+ nylon membranes by semi-dry transfer in $0.5 \times$ TBE for 1.5 hours at 20 volts. The membranes were crosslinked with 120 mJ/cm^2 UV₂₅₄ and

baked at 80°C for 30 minutes. Membranes were prehybridized with pre-hyb buffer (6× SSC, 0.1% SDS, 5× Denhardt's solution) at 50°C for 1 hour to overnight then incubated with 12.5 pmol of ³²P-labeled locked nucleic acids (Exiqon) in UltraHyb-Oligo hybridization solution (Ambion) overnight. Washing of the membranes was as follows: 1× SSC 55°C, 1× SSC 60°C, 1× SSC 65°C, 0.1× SSC 65°C. Each wash was for 15 minutes. Membranes were then exposed to a phosphorimager for 24-48 hours and scanned on a Typhoon Trio imager.

2.14. Cloning of inducible miRNA lentiviral plasmids

The pTRIPz doxycycline inducible lentiviral plasmid was linearized with XhoI and MluI, releasing a non-targeting shRNA. Individual primary miRNA sequences were cloned from the pLenti-miR-200b/a/429 or pLenti-miR-200c/141 constructs (System Biosciences, Inc.) to include an additional 50 nucleotides of flanking nucleotides on either side of the stem-loop structures cataloged in MiRBase. Primers are as follows

200aF 5' GCACTCGAGGGCTGCTCACCGCTCC 3',

200aR 5' GCAACGCGTCCGCTCGGCCCTCC 3',

200bF 5' GCACTCGAGCAGGAGGACGAGGCC 3',

200bR 5' GCAACGCGTAGCGGGCTGTGTGGG 3',

200cF 5' GCACTCGAGCAGGGATCTGCAGCTTTTCC 3',

200cR 5' GCAACGCGTAAGTGGGGAGGGGGCT 3'.

2.15. Crosslinking and Peptide Nucleic Acid Pulldown Assay (CLaPP)

MCF-12A vector or 14-3-3 ζ overexpressing cells were plated on 500 cm² dishes at ~80% confluency (5 × 10⁷ cells) in 100 mls of culture medium. One plate was used per antisense peptide nucleic acid. 100 μ M 4-thiouridine was added to the plates and incubated

for 24 hours. Before UV crosslinking, cells were washed twice with 25 mls ice cold PBS with the second wash remaining on the cells. The cells were crosslinked with 450 mJ/cm² of UV_{365nm} on ice and then gently scraped into a 50 ml conical tube and the cells pelleted. The cell pellet was lysed in 2 mls CLaPP lysis buffer (50 mM HEPES [pH 7.4], 0.1% lithium dodecyl sulfate, 10 mM LiCl, 10 mM Ribonucleoside Vanadyl Complex (NEB)). Lysates were incubated for 10 minutes on ice then centrifuged at 20,000 × g for 15 min at 4°C. The pellets were discarded and the supernatant treated with 2 µl TurboDNase at 37°C for 10 minutes.

Peptide nucleic acids that were antisense to the basal stem of specific precursor miRNA (see Table 1 for sequences) were added to a final concentration of 1 nmol in 2 mls and incubated for 30 minutes at 55°C to allow hybridization of PNAs to their target RNAs. After hybridization the samples were brought down to room temperature and 50 µl pre-equilibrated Nanolink 0.8 µm streptavidin magnetic beads were added to the lysates and incubated for 30 minutes at 37°C. The beads were washed once in CLaPP low salt wash (50 mM HEPES [pH 7.4], 0.5% LDS), once in CLaPP high salt wash (50 mM HEPES [pH 7.4], 0.5% LDS, 500 mM LiCl), once in low salt wash, once in CLaPP lysis buffer, and once in RNase digestion buffer (50 mM Tris [pH 7.4], 50 mM NaCl, 0.01% Triton X-100, 5 mM MgCl₂). Beads were resuspended in 20 µl RNase digestion buffer containing 1 unit RNase A, 40 units RNase T1, 0.002 units RNase V1 and digestion allowed to proceed for 10 minutes at 37°C before stopped by the addition of NuPAGE loading buffer. Samples were heated at 70°C before being loaded onto a 4-12% NuPAGE gradient gel and run in MOPS running buffer. Samples were stained with coomassie blue to avoid detection of partially

undigested RNAs by silver staining. Individual protein bands were excised from the gel and send for mass spectrometry identification.

2.16. Identification of RRBP1-bound RNAs by iCLIP

HEK293 cells were transfected with 5 µg of pCMV6-p130 or pCMV6-p180 and 24 hours later each plate was split 1:2 and incubated with 100 µM 4-thiouridine (Sigma) for an additional 24 hours. The cells were washed with PBS twice and UV-crosslinked cells irradiated with 450 mJ/cm² of UV₃₆₅ while on ice. Cells were scraped and centrifuged at 150 × g for two minutes at 4°C and the PBS removed. Cell pellets were snap frozen in liquid nitrogen and stored at -80°C for later use.

After thawing, cell pellets were lysed in iCLIP lysis buffer (50 mM HEPES [pH 7.4], 100 mM NaCl, 1% NP-40, 0.5% sodium deoxycholate, 0.1% sodium dodecyl sulfate, protease inhibitor cocktail), followed by sonicating three times at 3 watts in 10 s bursts while on wet ice. After sonication the lysates were mixed with a 1:250 dilution of RNase I (100 units/µl) in PBS along with 2 µl TurboDNase and incubated at 37°C for 5 minutes. The lysates were centrifuged at 20,000 × g for 15 minutes at 4°C. A 15 µl aliquot was saved as input protein levels and the remainder of the supernatant was incubated with 10 µg biotinylated FLAG antibody pre-bound to Nanolink 0.8 µm magnetic streptavidin beads for two hours at 4°C. The beads were collected on a DynaMag magnetic rack and 15 µl of supernatant collected to determine immunoprecipitation efficiency. The beads were washed twice in high salt wash buffer (50 mM HEPES [pH 7.4], 1 M NaCl, 1% NP-40, 0.5% sodium deoxycholate, 0.1% sodium deoxycholate), and washed three times in PNK buffer (20 mM HEPES [pH 7.4], 0.2% Tween-20, 10 mM MgCl₂).

The 3' end of the RNA was dephosphorylated by incubating the beads with 0.5 μ l T4 PNK, 0.5 μ l RNasin, 15 μ l DEPC-H₂O, 5 μ l 5 \times PNK dephosphorylation buffer (350 mM Tris [pH 6.5], 50 mM MgCl₂, 5 mM DTT) for 20 minutes at 37°C. The beads were washed once with PNK wash buffer, twice with high salt wash buffer, and twice with PNK wash buffer.

The L3 adapter sequence (5' [phos] AGATCGGAAGAGCGGTTCAG/ddC/) that were 5' phosphorylated and protected on the 3' end with dideoxycytosine were adenylated using the DNA adenylation kit (NEB) following the manufacturer's instructions and made to a final concentration of 20 pmol/ μ l. The adapters were ligated to the 3' end of the dephosphorylated RNA by T4 RNA ligase in iCLIP ligation buffer (50 mM HEPES [pH 7.4] 10 mM MgCl₂, 1 mM DTT, 10% PEG 400). The reaction was incubated in a thermomixer at 1100 RPM at 16°C for 16 hours. The beads were washed once with PNK wash buffer, twice with high salt wash buffer, and twice in PNK wash buffer.

Ligated protein:RNA complexes were 5' phosphorylated with γ -³²P ATP with PNK for detection and isolated of crosslinked RNA. The reaction was washed once in PNK wash buffer and RRBP1 was eluted from the beads by incubating at 70°C in NuPAGE loading buffer for 5 minutes. Samples were run on a 4-12% NuPAGE bis-tris gel in MOPS NuPAGE running buffer then transferred to a 0.45 μ m nitrocellulose membrane in 2 \times MOPS transfer buffer by semi-dry transfer. The membrane was washed in PBS and exposed to x-ray film at -80°C for one hour to detect crosslinked complexes. The film was used as a mask to cut fragments from nitrocellulose that were incubated with proteinase K in PK buffer (100 mM HEPES [pH 7.4], 50 mM NaCl, 10 mM EDTA) for 20 minutes at 37°C and then incubated

with PK buffer plus 7 M urea for an additional 20 minutes. Released RNA was isolated by addition of 400 μ l phenol/chloroform [pH 6.7] and separation in a Phase Lock Gel Heavy tube according to the manufacturers instructions. The aqueous layer was precipitated by adding 40 μ l 3 M sodium acetate [pH 5.5] and 1 ml 100% ethanol with 0.75 μ l glycoblue and stored at -20°C overnight. RNA was precipitated by spinning at 20,000 \times g for 20 minutes at 4°C and washed with 80% ethanol.

RNA pellets were resuspended in 5 μ l H₂O and mixed with 1 μ l barcoded reverse transcription primer and 1 μ l 10 mM dNTP mix then heated to 70°C for 5 minutes and returned to 25°C. Superscript III reverse first strand mix was added according to the manufacturer's instruction and incubated at 25°C for 5 min, 42°C for 20 minutes, 50°C for 40 minutes, 80°C for 5 minutes, and the temperature held at 4°C. RNA was degraded from the cDNA mix by adding 1.65 μ l 1M NaOH and incubating at 98°C for 20 minutes and neutralized by adding 20 μ l 1 M HEPES [pH 7.4]. cDNA was precipitated by adding 350 μ l TE, 40 μ l NaOAc, 0.75 μ l glycoblue, and 100% ethanol at -20°C overnight.

cDNA was isolated into high, medium, and low molecular weights by running precipitates on a pre-cast 6% TBE-urea gel. Gel slices were isolated using bromophenol blue and xylene cyanol dyes as markers corresponding to nucleotides ranging from 70-150 nucleotides. The cDNA was eluted from the gel fragments by first fragmenting slices through a 0.65 ml tube with a hole punched in the bottom by a 21-gauge syringe and spinning at 16,000 \times g for 2 minutes into a 1.5 ml tube then incubating the fragments in 10 mM Tris [pH 8.0], 0.3 M NaCl, 10 mM EDTA for two days at 4°C. The eluted cDNA was separated

from gel fragments by spinning in a Costar cellulose acetate spin filter with a 1 cm Whatman glass pre-filtered inserted in the top and spinning at 16,000 × g for 2 minutes. Eluted cDNA was precipitated overnight at -20°C by adding 0.75 µl glycoblue and 1 ml 100% ethanol.

The cDNA was circularized using the CircLigase II kit (Epicentre Bio) by incubating at 60°C for one hour. The BamHI cut oligonucleotide (GTTCAGGATCCACGACGCTCTTC/ddc/) was then annealed by adding 10 pmol of the oligonucleotide with 3 µl Fast digest buffer (Thermo) and the volume brought to 30 µl. Annealing was achieved by incubating at 95°C for 2 minutes and successively decreasing the temperature 1°C every 20 seconds until the temperature reached 25°C. Circular cDNA was linearized by adding 2 µl BamHI (NEB) to each reaction and incubated for 30 minutes at 37°C followed by 5 minutes at 80°C. The digested cDNA was precipitated as previously described.

Library amplification using the Solexa P5 and P3 sequencing primers was accomplished using the Accurprime Supermix I following the program (94°C 2 min, 27-35 cycles of: 94°C 15 s, 65°C 30 s, 68°C, 30 s, and a final extension of 3 minutes at 68°C. Optimal cycles were determined by gel analysis and the remainder of the library prepared using the optimized cycles. The individual barcoded samples were pooled and gel purified as described above, ethanol precipitated, and resuspended in 30 µl of 10 mM Tris for Illumina single read 50-nucleotide sequencing.

This chapter is based upon: Pickering BF, Yu D, Van Dyke MW. (2011). Nucleolin protein interacts with microprocessor complex to affect biogenesis of microRNAs 15a and 16. *J Biol Chem.* **286**(51): 44095-103.

Copyright declaration from *the Journal of Biological Chemistry*: “Authors are automatically granted copyright permission to use an article in a thesis/dissertation.”

Chapter 2: Nucleolin interacts with the microprocessor to affect biogenesis of miR-15a/miR-16-1.

3.1. Introduction

MicroRNA (miRNA) are short ~21 nucleotide single-stranded noncoding RNA that affect gene expression by inhibiting translation or degrading mRNA targets by binding to their 3' untranslated region (3'UTR) (1). Transcripts from miRNA-encoding genes generate primary miRNA (pri-miRNA) that vary in size from one to tens of kilobases and contain a 5' cap and a poly (A) tail. These pri-miRNA are processed in the microprocessor complex composed of Drosha and DGCR8 into 60-90 nucleotide precursor miRNA (pre-miRNA) (8). After being exported to the cytoplasm by Exportin5 and Ran-GTP, pre-miRNAs are cleaved by Dicer, which transfers the double stranded RNA to the Argonaut complex to generate the mature miRNA (12–14).

The miRNA biogenesis pathway is tightly regulated with numerous other proteins transiently associating with the individual complexes to either stimulate or inhibit processing. For example, transient interaction of p53, p68 and p72 with Drosha increases the processing of a subset of miRNA (69, 70). Negative regulators of miRNA processing include the

estrogen receptor, NF45/NF90 complexes, and Lin28 (62, 78, 80). The AU-rich binding protein KSRP can interact with both the microprocessor and Dicer complexes and affect their function (75, 76). The effect of these regulators on miRNA processing can be very specific, as is the case of hnRNP A1, which facilitates the specific processing of miR-18a from the polycistronic miRNA miR-17~92 and Lin28, which blocks the biogenesis of let-7 family miRNA (62, 152). While KSRP and Lin28 are the only two regulatory proteins known to affect Dicer, most of the transient effectors characterized thus far interact exclusively with the microprocessor complex, suggesting that this may be a critical step in the regulation of miRNA expression.

An interesting parallel exists between miRNA biogenesis and ribosomal RNA (rRNA) biogenesis with a number of proteins having important roles in both pathways. Drosha was originally identified for its role in rRNA biogenesis, cleaving the 48S pre-rRNA into the 12S rRNA intermediate (146). Both p68 and p72 are responsible for cleavage of the 12S rRNA to generate the mature 5.8S rRNA species (68, 153). Additionally, Dicer has recently been found to associate with the chromatin encoding rRNA (154). Depletion of either Dicer or Ago2 results in an accumulation of 5.8S rRNA species indicating they are necessary for processing (155). Recently, it was found that Drosha co-localizes with nucleolin in the nucleolus to increase the biogenesis of a mouse long non-coding RNA *mrhl*, which is a 2.8 kilobase RNA that gets cleaved into an 80 nucleotide RNA that can be further processed into a 21 nucleotide RNA by Dicer (156). Strikingly, this pathway, like that of rRNA biogenesis, is very similar to the miRNA biogenesis pathway with regards to proteins and RNA substrates.

Nucleolin has long been known as a protein critical for rRNA biogenesis (157). Evidence suggests that it may also have a role as an accessory protein in miRNA biogenesis. Nucleolin is predominantly a nucleolar-localized protein; however, in a number of different cancers nucleolin is found largely in the cytoplasm (158–161). In the cytoplasm, nucleolin functions to stabilize the mRNA of bcl-2, thereby inhibiting apoptosis (158). When cytoplasmic levels of nucleolin are decreased upon treatment with all-*trans* retinoic acid (ATRA) the levels of miR-15a and miR-16 increase in both acute promyelocytic leukemia (APL) cell lines and patients with APL treated with ATRA (121, 161). MiR-15a and -16 have been shown to target bcl-2 mRNA and are greatly decreased in chronic lymphocytic leukemia, where nucleolin is predominantly localized to the cytoplasm (119, 158).

Therefore, we sought out to investigate the role of nucleolin in controlling the expression of miR-15a and miR-16. We determined how overall expression of nucleolin and its cellular localization impacts miRNA expression. Additionally, we characterized nucleolin's interaction with components of the biogenesis pathway and with miRNA directly.

3.2. Results

3.2.1. The expression of miR-15a and miR-16 correlates with nucleolin expression

To determine whether nucleolin expression impacts the levels of miRNA, nucleolin was knocked down with siRNA and cancer associated mature miRNA assessed by qRT-PCR. As a positive control, Drosha was also knocked down (Fig. 5A). As expected, all mature miRNA were decreased in Drosha knockdown to 25-50% of control siRNA cells (Fig. 5C). In nucleolin knockdown cells, five miRNA were significantly reduced. Because none of the miRNA tested were increased upon loss of nucleolin we investigated whether nucleolin

directly controlled their expression through processing. Primary miRNA levels were analyzed since loss of proteins involved in processing typically cause an increase in primary miRNA while mature miRNA decrease (8, 68). All primary miRNA increased in Drosha knockdown while only two primary miRNA, miR-15a and miR-16, increased in the absence of nucleolin. This suggests nucleolin may directly control the expression of these two miRNA while the other miRNA decreased in the absence of nucleolin may be through indirect mechanisms. To determine if the opposite held true when nucleolin is increased, MCF-7 cells were stably transfected with a CMV-driven expression vector containing FLAG-tagged nucleolin and determined miRNA expression by real-time PCR. We were able to achieve about a two-fold increase in nucleolin expression (Fig 5B). Upon overexpression of nucleolin, the levels of mature miR-15a and miR-16 increased approximately 2.5 fold (Fig. 4D). Two other miRNA, miR-100 and miR-31 increased significantly with miR-31 increasing nearly 80-fold. This increase may be transcriptionally regulated because the pri-miRNA for miR-31 significantly increased in nucleolin overexpressing cells. Pri-miRNA for miR-15 and miR-16 also increase, however; this may be indirectly regulated through c-myc. Nucleolin can inhibit c-myc through formation of a G-quadruplex in c-myc's promoter and c-myc can transcriptionally inhibit miR-15a and miR-16 (162, 163). An interesting observation was that nucleolin expression inversely correlates to Drosha expression (Fig. 5A and 5C). It is possible this relationship is the cells way of compensating for altered ribosome biogenesis, as this is a common function between the two. We speculate that upon loss of nucleolin the cell tries to compensate by increasing Drosha and while nucleolin is plentiful there is less of

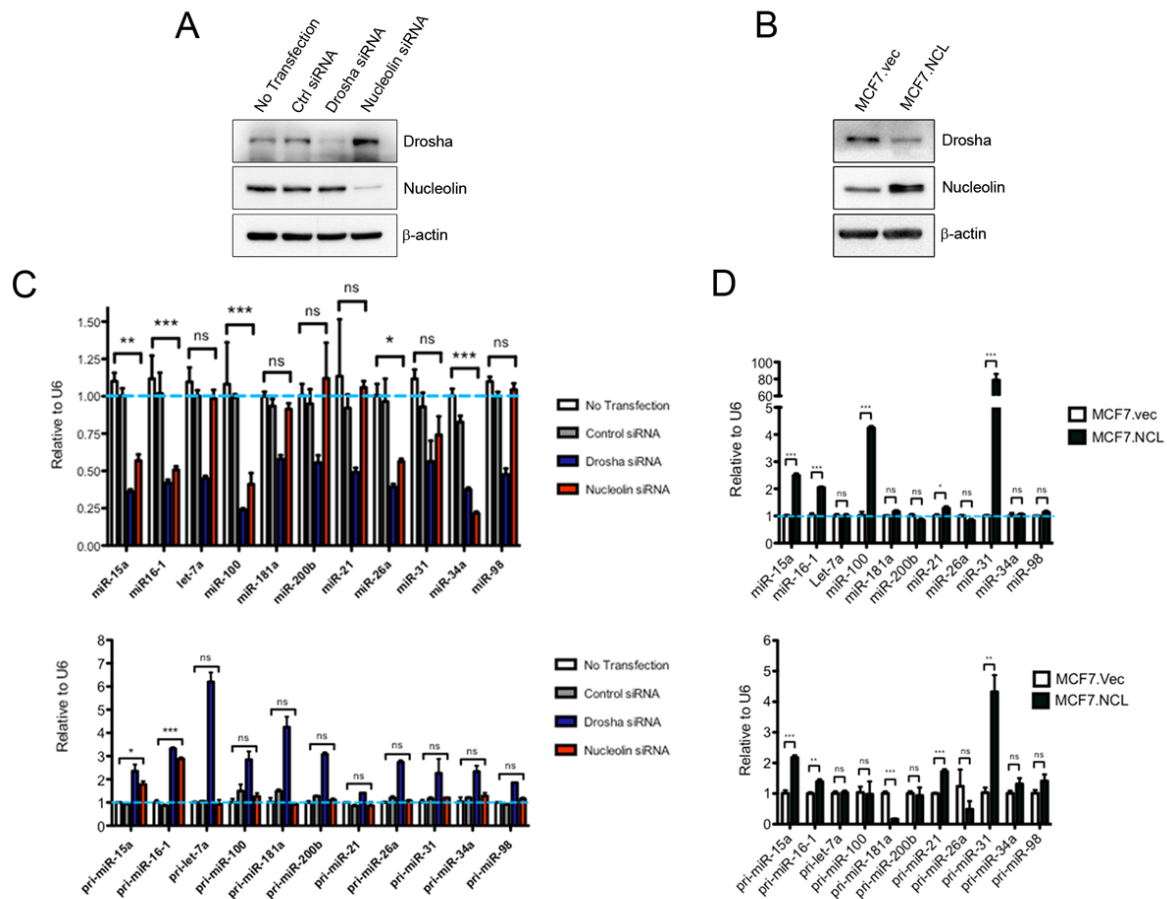


Figure 5. Nucleolin expression correlates with miR-15a and miR-16 expression.

A) Expression of Droscha and nucleolin 72 hours following siRNA treatment B) Expression of stably expressed FLAG-tagged nucleolin in MCF-7 cells. C) Real time PCR analysis of mature miRNA (top) and primary miRNA (bottom) in cells with Droscha or nucleolin knocked down. Results are normalized to U6 snoRNA expression. D) Real time PCR analysis of mature miRNA (top) and primary miRNA (bottom) in cells overexpressing nucleolin. Error bars = SEM

a need for Drosha in ribosome biogenesis. All together, these data are consistent with the hypothesis that nucleolin plays an ancillary role in the biogenesis of miR-15a and miR-16.

3.2.2. Induced cytoplasmic nucleolin inhibits processing of primary miRNA

Clinical data from CLL patients shows that nucleolin is localized primarily in the cytoplasm, which leads to increased bcl-2 mRNA levels (158). Because miR-15a and miR-16 are known to target bcl-2 mRNA, we sought to determine whether cytoplasmic nucleolin could lead to decreased levels of miR-15a and miR-16. We found that when MOLM-13 acute myelogenous leukemia cells are treated with parthenolide, a natural product small molecule that affects multiple signal transduction pathways, it induces a dramatic increase in cytoplasmic nucleolin levels (Fig. 6A). Analysis of mature miRNA by qRT-PCR revealed a significant decrease in both miR-15a and miR-16 concurrent with cytoplasmic localization of nucleolin (Fig. 6B). To determine whether treatment with parthenolide decreased the transcription of these miRNA the pri-miRNA were amplified by PCR. Astonishingly, we found not a decrease but rather an increase in the pri-miRNA precursor of miR-15a and miR-16 (Fig. 6C). Given this finding, we analyzed the precursor species by Northern blot and found that levels of the pre-miR-15 and -16 precursors decreased similarly that of the mature miRNA following parthenolide treatment (Fig. 6D). These data are similar to that observed when either Drosha or DGCR8 are knocked down, resulting in a decrease of mature species and an increase in the primary precursors (8). While it was clear that nucleolin increased in cytoplasmic localization, it appeared nucleolin did not decrease in nuclear expression despite the miRNA expression indicating this. Nucleolin normally resides

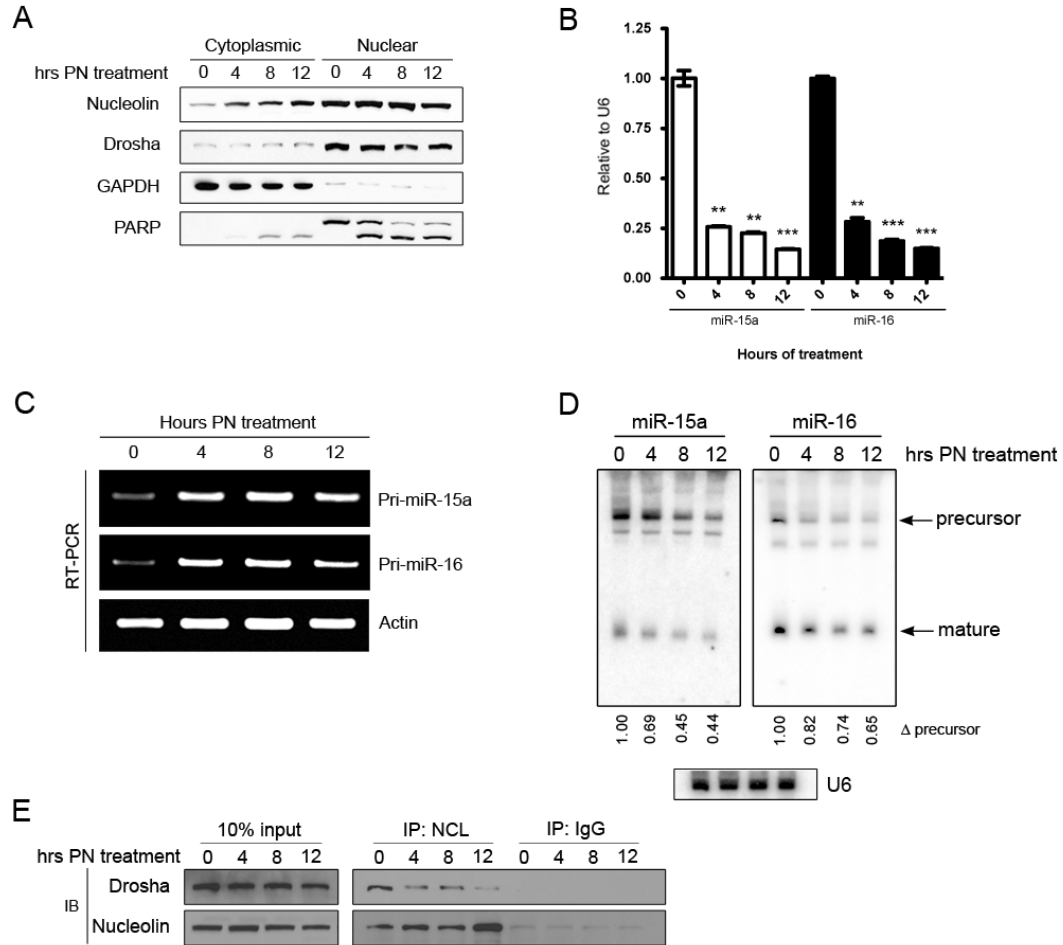


Figure 6. Decreased association of nucleolin with the microprocessor complex affects miRNA processing.

A) MOLM-13 cells were treated with 10 μ M parthenolide (PN) for the times indicated. The efficiency of cellular fractionation was determined using GAPDH and PARP. Cleaved PARP is visible in the cytoplasm after 8 hours of treatment. B) Expression of mature miRNA following treatment with PN for the times indicated as determined by qRT-PCR and normalized to U6 snoRNA expression. Error bars = SEM. C) PCR of primary miRNA following treatment with PN with actin as a loading control. D) Northern blot analysis of RNA from MOLM13 cells treated with PN. Quantitation of precursor species is indicated below each lane and is normalized to U6. E) Western blot of nucleolin immunoprecipitation from nuclear extracts to interrogate the interaction of nucleolin with Drosha in the nucleus following PN treatment.

in the nucleolus and is not evenly dispersed throughout the nucleus. Upon activation of p53, nucleolin leaves the nucleolus (164). We previously reported that parthenolide potently activates p53 (165). It has been reported that Drosha co-localizes with nucleolin in the nucleolus and so we hypothesized that the interaction between nucleolin and Drosha is decreased upon re-localization of nucleolin out of the nucleolus. To determine this MOLM13 cells were treated with parthenolide and nucleolin immunoprecipitated from nuclear extracts. We found that nucleolin interacts with Drosha and this interaction is disrupted upon treatment with parthenolide (Fig. 6E). From these data we concluded that nucleolin facilitates the processing of miR-15a and miR-16 likely through the microprocessor complex, which is localized exclusively in the nucleus. Upon cellular stress nucleolin alters its localization and is spatially separated from the microprocessor complex, which is responsible for the cleavage of primary miRNA to generate the precursor. We suspect that in the absence of nucleolin the microprocessor can less effectively cleave the primary species resulting in the observed buildup of the pri-miRNA for miR-15a and miR-16. Conversely, when the acute promyelocytic leukemia (APL) HL-60 cell line was treated with all-*trans* retinoic acid (ATRA), nucleolin was observed to move from the cytoplasm to the nucleus (Fig. 7A). The increased nuclear localization of nucleolin was accompanied by significant increases in mature miR-15a/16 (Fig. 7B). The primary miRNA were not increased in these cells following treatment (Fig. 7C) indicating post-transcriptional regulation.

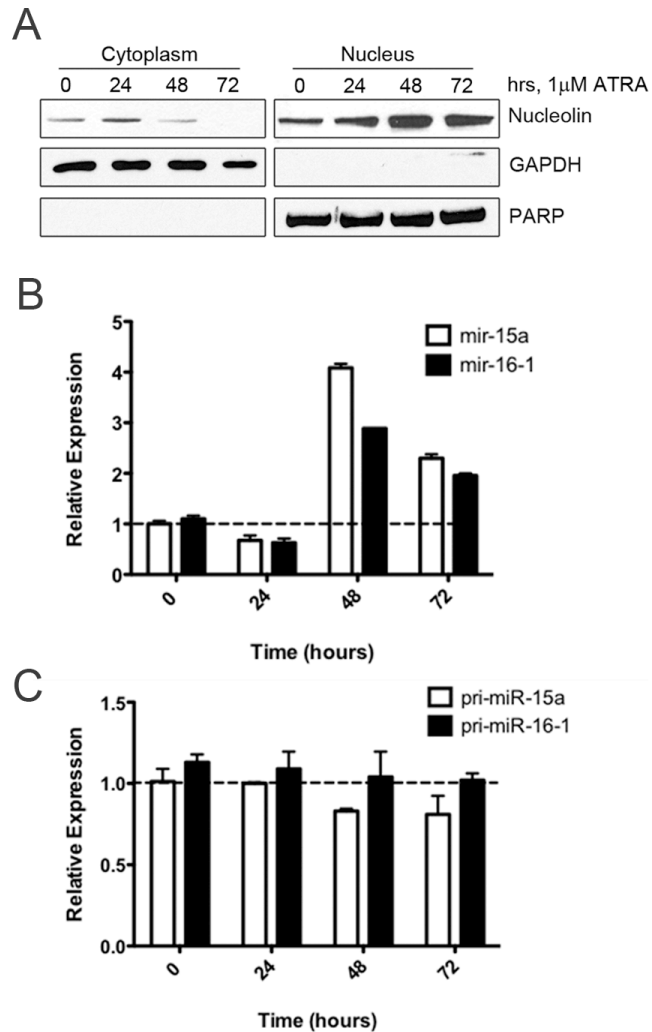


Figure 7. Treatment with all-*trans* retinoic acid (ATRA) induces nuclear localization of nucleolin and increased miRNA expression.

A) HL-60 acute promyelocytic leukemia cells were treated with 1 μ M ATRA to decrease cytoplasmic localization of nucleolin and increase nuclear localization as described previously (25). B) Expression of mature miR-15a/16 in cells treated with ATRA closely correlates nucleolin localization. All points are normalized to DMSO-treated cells (dashed line). C) Primary miRNA expression shows no significant change in expression over time as determined by qRT-PCR normalized to DMSO-treated cells (dashed line).

3.2.3. Knockdown of nucleolin ablates processing of primary miRNA

To further validate that nucleolin is involved in the processing of primary miRNA, nuclear-localized nucleolin was induced in MCF-7 cells. This was achieved through treatment of MCF-7 cells with parthenolide. Interestingly, in MCF-7 cells parthenolide induced nuclear-localized nucleolin, whereas in MOLM-13 AML cells parthenolide increased cytoplasmic levels of nucleolin (Fig 6A and 8C). This differential effect was independent of parthenolide's capacity as a specific HDAC 1 inhibitor, which is the same in both cell lines (165). Upon analyzing the miRNA expression in parthenolide-treated and DMSO-treated control cells, there was a substantial (>12-fold) increase in mature miR-15a in parthenolide-treated cells. MiR-16 expression also significantly increased in parthenolide-treated cells, albeit to a lesser extent (~2.5 fold). This could be due to the fact that the steady-state levels of mature miR-16 are over 50-fold higher under normal conditions than miR-15a and may not be as easily increased as miR-15a. To rule out that all miRNA are altered upon PN treatment we also analyzed let-7a expression, which was not altered following changes in nucleolin expression (Fig. 4B and 4D). Let-7a mature miRNA remain unchanged. To determine whether the large increases observed were truly due to nucleolin and not the effects of parthenolide, nucleolin or RISC-free control siRNA were transfected into MCF-7 cells and 72 hours later treated with parthenolide. Incredibly, when nucleolin is dramatically knocked down (Fig. 8A inset) the increase in miR-15a is almost completely ablated, as the resulting miRNA levels were close to that of the DMSO-treated cells while the RISC-free control remained comparable to untransfected cells. Similarly, miR-16 in nucleolin

knockdown cells decreased significantly from the RISC-free control group following parthenolide treatment (Fig 8A).

We next sought to determine how the primary miRNA precursors of miR-15a and miR-16 were affected by the induced nuclear localization of nucleolin. From the data shown in figure 2 we concluded that cytoplasmic nucleolin inhibited the processing of pri-miRNA species as determined by their increase. Upon analyzing the pri-miRNA following parthenolide treatment in either the untransfected or RISC-free control groups we observed an absence of pri-miR-15a and pri-miR-16. These data indicate that in the presence of increased nuclear nucleolin the primary miRNA are efficiently processed into precursor and ultimately mature miRNA resulting in exhaustion of the pool of primary species in the cell. However, after knocking down nucleolin a significant portion of the primary species persists, comparable to the levels observed in the DMSO-treated controls (Fig. 8B). The levels of pri-let-7a, like mature let-7a, were unaltered in all conditions. From these data we conclude that it is likely not off-target effects from parthenolide that induces the biogenesis of pri-miR-15a/16 but rather the increased nuclear localization of nucleolin. In the absence of nucleolin, the microprocessor complex appears unable to efficiently upregulate the processing of the pri-miRNA, resulting in no increase of mature miR-15a and miR-16 species.

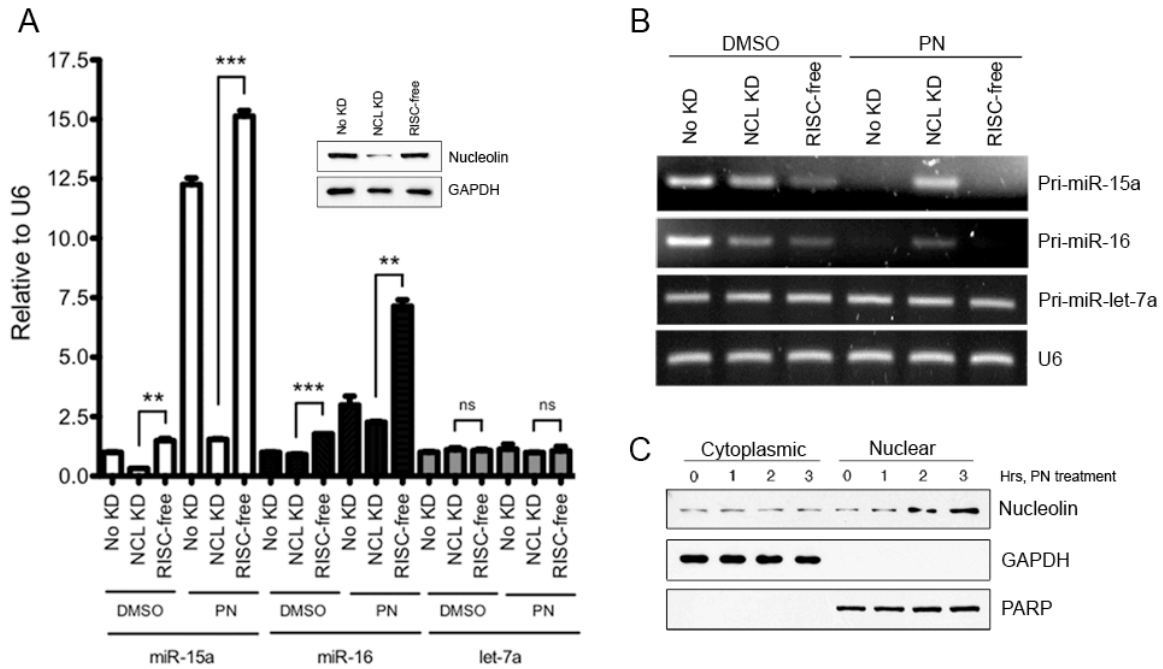


Figure 8. Primary miRNA processing is inhibited in the absence of nucleolin.
 A) MCF-7 cells were treated with 25 μ M parthenolide (PN) or DMSO for 3 hours before RNA extraction and qRT-PCR of mature miRNA. Nucleolin knockdown and RISC-free siRNA control cells were transfected 72 hours prior to parthenolide treatment. B) PCR amplification of primary miRNA from RNA extracted in (A). C) Cellular fractionation of MCF-7 cells following treatment with PN demonstrating the increased nuclear nucleolin levels at the 3 hour time point used in (A and B).

Nucleolin interacts with the components of the microprocessor independent of RNA

The data generated from the altered localization of nucleolin demonstrate that nucleolin is only able to exert an effect on miR-15a/16 expression while in the nucleus and that it is the primary miRNA that are affected, indicating nucleolin may interact with the microprocessor complex. To determine if it affects processing by directly binding to the proteins in the microprocessor complex composed of Drosha and DGCR8 an immunoprecipitation experiment was conducted. HEK293 cells stably expressing tandem affinity purification (TAP) FLAG and HA tags at the N-terminus of DGCR8 were used. Lysates were immunoprecipitated with either FLAG or HA antibody to bring down DGCR8 and western blot was used to determine if nucleolin was present in the pulldown. HEK293 cells not transfected with the expression plasmid were used as a control for non-specific binding of FLAG or HA. Nucleolin was not present in the IgG isotype control pulldown or in the lysates not expressing DGCR8 with FLAG or HA but strongly came down with both FLAG and HA in FLAG/HA-DGCR8 expressing cells (Fig 9A). Nucleolin is a well-known RNA binding protein and to rule out the possibility that nucleolin came down as a result of tethering to a common RNA the lysates were exhaustively treated with RNase A. The interaction between DGCR8 and nucleolin persisted even after complete digestion with RNase A indicating a protein-protein interaction.

Nucleolin has been shown to co-localize with Drosha to affect the processing of a long non-coding RNA *mrhl* in the nucleolus (156). However, in that study a direct interaction was never investigated. FLAG-tagged nucleolin was immunoprecipitated in HEK293 lysates and probed for Drosha binding. No interaction was found when FLAG-

nucleolin alone was used in the immunoprecipitation (Fig. 8B). When lysates were treated with RNase A, a weak band appeared, which could be the result of freeing Drosha from other complexes dependant on RNA. We consistently found that Drosha was decreased in the supernatant and yet failed to appear in the immunoprecipitation. We surmised that it was in fact binding to nucleolin but was lost during the washes due to a weak interaction or unstable complex. To overcome this issue 5% polyethylene glycol with molecular weight 8000 Da was used in the wash buffer to reduce the void space during the washes. The addition of PEG to the wash buffer reduced the loss of Drosha and revealed that Drosha also interacts with nucleolin.

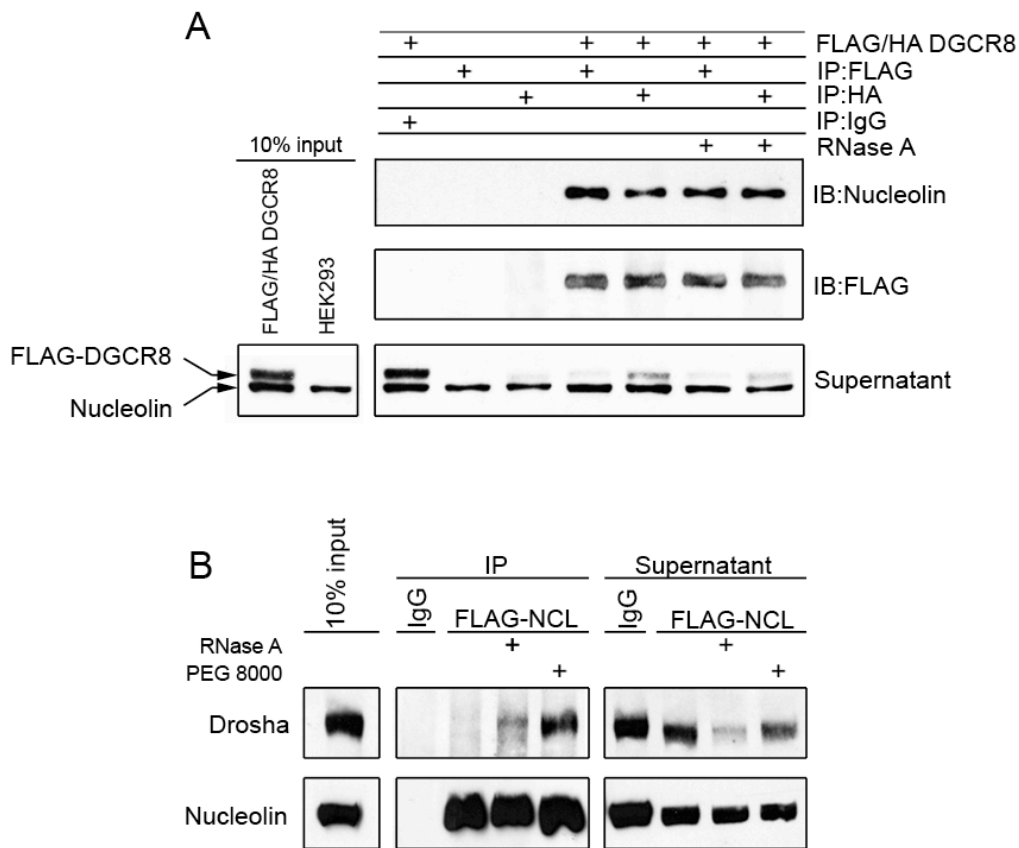


Figure 9. Nucleolin interacts with the microprocessor complex.

A) Immunoprecipitation of DGCR8 from whole cell extracts of HEK293 expressing FLAG/HA-DGCR8. IgG isotype control in DGCR8-expressing cells and FLAG or HA in cells not expressing tagged DGCR8 served as controls for non-specific interactions. RNase A treatment indicates incubation with 20 μ g/ml overnight. Supernatant represents 10% of total supernatant. B) Immunoprecipitation of FLAG-nucleolin from HEK293 cells whole cell extracts and immunoblotting for Drosha. PEG 8000 indicates that polyethylene glycol m.w. 8000 was added to the wash buffer to a final concentration of 5% (w/v).

3.2.5. Nucleolin binds to primary miR-15a and miR-16

Nucleolin is a well-known RNA binding protein. It has no known catalytic function in RNA cleavage but it necessary for rRNA cleavage (157). The proposed mechanism is that nucleolin holds the RNA in proper conformation to be cleaved by other components of rRNA biogenesis. Furthermore, nucleolin has been shown to co-localize with Drosha to affect the biogenesis of a long non-coding RNA but cannot itself cleave the RNA (156). We determined that nucleolin binds to the components of the microprocessor but sought to determine if it also binds to the primary miRNA, perhaps to stabilize its conformation for cleavage. An RNA immunoprecipitation experiment was conducted with HEK293 cells overexpressing either nucleolin or DGCR8, as a positive control. After crosslinking and sonication, nucleolin or DGCR8 were immunoprecipitated with FLAG antibody or IgG control and the presence of primary miR-15a, miR-16, or let-7a was determined by PCR. DGCR8 bound to pri-miR-15a and -16, as expected (Fig 10). When primary miR-15a and miR-16 were amplified from nucleolin immunoprecipitates we found that nucleolin bound them to a level equal to that of DGCR8 indicating that nearly the entire pool of pri-miR-15a and -16 in the cell that is bound by DGCR8 also contains nucleolin. To determine if binding of nucleolin is specific, we also amplified pri-let-7a from both pools of extracted RNA and found it was only bound by DGCR8 but not by nucleolin (Fig. 10). The background contamination from genomic DNA was minimal as PCR amplification of extracted RNA without reverse transcription (No RT) revealed no amplification of primary miRNA (Fig. 9). It also appears that a large pool of primary miR-15a and miR-16 exists in the cell that is poised to be processed but is not actively engaged with DGCR8 or nucleolin since the bound

RNA was less than 1% of the total pool. This seems plausible since both miRNA are implicated in controlling the apoptotic response of a cell in addition to controlling the cell cycle, both of which require a rapid response to stimuli best provided from an inactive pool of unprocessed miRNA.

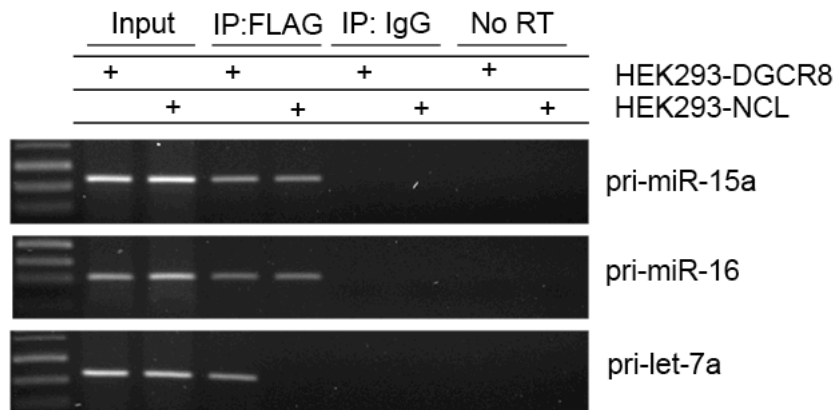


Fig. 10. Nucleolin binds to pri-miR-15/16.

HEK293 cells expressing either FLAG-nucleolin or FLAG/HA-DGCR8 were immunoprecipitated with either IgG or FLAG and the bound primary miRNA amplified by PCR. No RT indicates purified RNA from immunoprecipitates that was not reverse transcribed before PCR analysis. Input represents 0.1% of total RNA.

3.2.6. Nucleolin affects the processing of primary miRNA *in vitro*

To confirm that nucleolin can indeed facilitate the processing of primary miRNA we conducted an *in vitro* microRNA processing assay. Whole cell extracts were generated from HEK293 cells with nucleolin knocked down or Drosha knocked down as a positive control for defective processing (Fig 11A). In extracts with nucleolin knocked down, nucleolin was reconstituted by the addition of immunoprecipitated FLAG-tagged nucleolin (Fig 11B). Both control extracts (no transfection and control siRNA) were able to process the radiolabeled pri-miRNA to generate the precursor species for miR-15a/16 and let-7a (Fig. 11C). When Drosha was knocked down, the extracts were unable to generate the predicted precursors for both miRNA. Extracts lacking nucleolin were unable to process miR-15a/16 but could still generate the precursor for let-7a. The addition of immunoprecipitated nucleolin could rescue the processing in nucleolin deficient cells indicating it can directly affect miRNA processing. There was no affect on let-7a processing with nucleolin rescue. Taken together, these data indicate nucleolin directly and specifically affects the processing of primary miR-15a and miR-16.

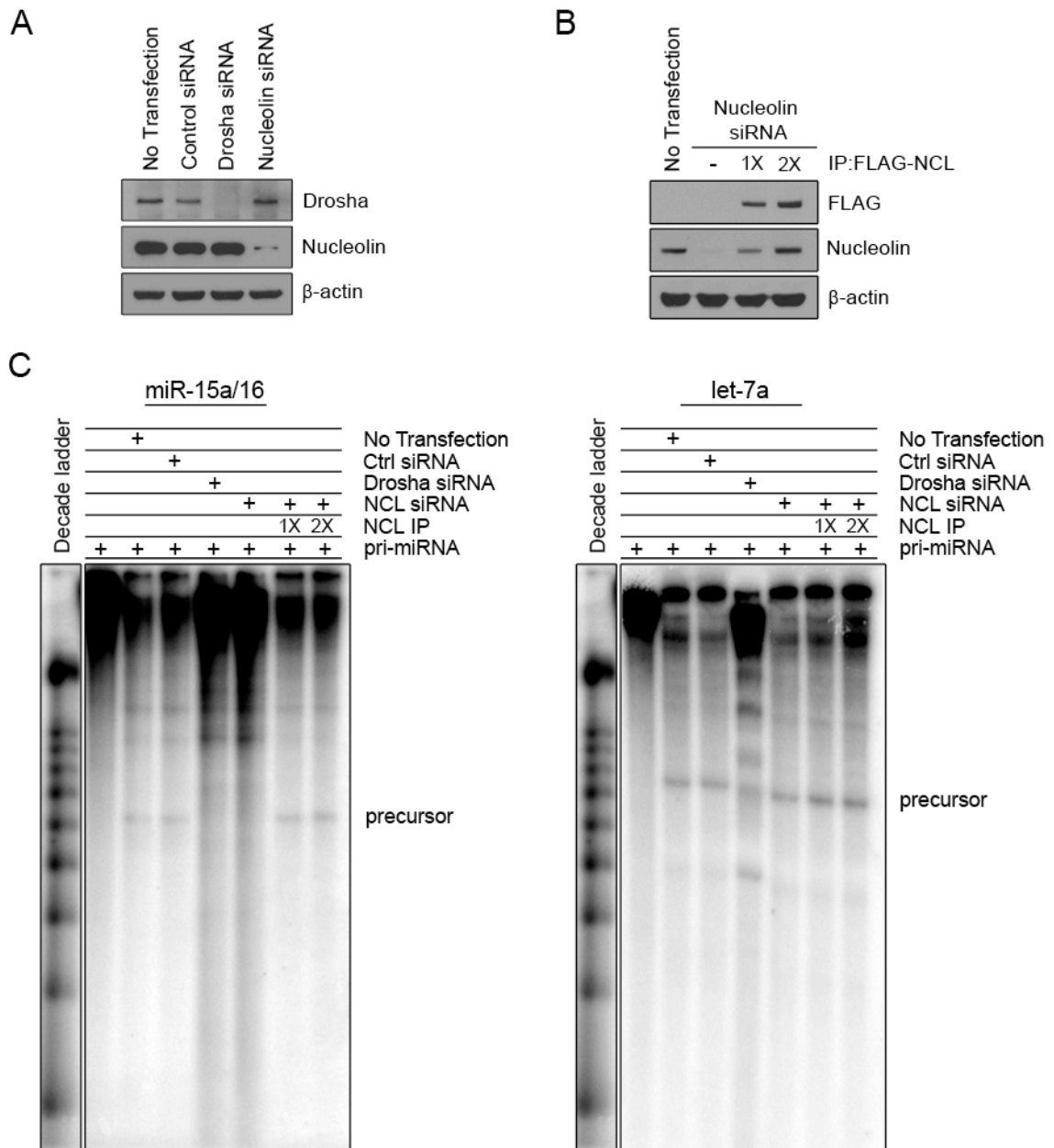


Figure 11. Nucleolin directly affects processing of primary miR-15a and miR-16.

A) HEK293 cells treated with either Drosha or nucleolin siRNA. B) Reconstituted nucleolin in nucleolin knockdown extracts. FLAG-nucleolin was immunoprecipitated from HEK293 stable cells and mixed at either 1 or 2 concentrations. 2 reconstitution restores nucleolin to levels equivalent in untransfected extracts. C) *In vitro* processing of primary miRNA. Gel purified *in vitro* transcribed RNA was incubated with 15 μ l of cell extracts from (A) for 90 minutes at 37C and analyzed on a 12.5% denaturing gel. Precursors of the predicted size are indicated.

3.3. Discussion

In this study, we demonstrate that nucleolin affects the expression of miR-15a/16. We also found that cellular localization of nucleolin is important for its function and concluded that this is most likely because of its interaction with the microprocessor complex in the nucleus. When nucleolin is knocked down or is altered in its localization the processing of primary miRNA is significantly decreased indicating it is necessary for proper expression of miR-15a/16. In addition, we found that nucleolin can bind directly to the primary miRNA species for miR-15a/16 and facilitate their processing in vitro. Taken together, these data suggest that nucleolin acts as an accessory protein to the microprocessor complex to facilitate miRNA biogenesis. As is the case with other accessory proteins involved in miRNA biogenesis nucleolin does not globally regulate miRNA processing like Drosha or DGCR8.

We initially identified a correlation between nucleolin localization and miR-15a/16 expression before exploring how nucleolin may affect their expression. Nucleolin has been characterized as an AU-rich binding protein that stabilizes the 3'UTR of bcl-2 mRNA upon cytoplasmic localization (158). The result of this is increased bcl-2 protein expression and inhibition of apoptosis – one of the hallmarks of cancer. MiR-15a/16 have been well-characterized as negative regulators of bcl-2 mRNA and decreased expression of these miRNA is noted in numerous cancers. In some instances decreased miR-15a/16 expression is due to chromosomal deletions; however, this only accounts for about half the patients with increased bcl-2 indicating other mechanisms must be present (119). Our data indicates that increased cytoplasmic localization of nucleolin in cancer may be partially responsible for reduced miR-15a/16 expression. We propose that nucleolin plays a critical role in the

balance between miR-15a/16 and bcl-2 mRNA to control the induction of apoptosis. Under normal conditions, nucleolin is localized in the nucleus of cells, specifically in the nucleolus, where it associates with the microprocessor complex. This results in an increase in expression of mature miR-15a/16, which then downregulates bcl-2 mRNA (Fig. 11). After induction of cellular stress, nucleolin leaves the nucleus to stabilize the 3'UTR of bcl-2 while simultaneously decreasing the expression of miR-15a/16 thereby further stabilizing bcl-2 mRNA.

A number of proteins involved in miRNA processing are also essential for ribosomal RNA biogenesis including Drosha, one of the core proteins in the microprocessor complex (146). It is tempting to speculate that miRNA processing evolved from the existing machinery required for rRNA. Indeed a number of miRNA have been shown to localize to the nucleolus, a region long-believed to be exclusive to rRNA biogenesis (166, 167). Moreover, nucleolin co-localizes with Drosha in the nucleolus to facilitate the processing of *mrhl*, a long non-coding RNA in mice. The transcript of this lncRNA is 2.8 kilobases, which gets cleaved by the cooperative actions of nucleolin and Drosha to an 80 nucleotide precursor reminiscent of precursor miRNA (156). This product can be further processed by Dicer into a 22 nucleotide species, analogous to miRNA. DGCR8 localizes primarily to the nucleolus and the dsRNA binding domains appear to be necessary for this since a truncation mutant lacking these domains is retained in the nucleus but fails to enter the nucleolus (81). Similarly, if the RNA recognition motifs (RRM) of nucleolin are deleted it fails to enter the nucleolus (168). Nucleolar retention of nucleolin requires a minimum of two of the four RRM domains to be present. It is possible that cytoplasmic localization of nucleolin does not

account for the disruption of miRNA processing we observed in Fig. 5 but instead is the result of nucleolin leaving the nucleolus because of the induction of stress on the cell, which has been previously reported (164).

The domain structure of nucleolin includes an acidic N-terminal region followed by a NLS, four RNA recognition motifs, and an arginine-glycine rich repeat domain with putative RNA helicase activity (169). The four RNA recognition motifs bind to rRNA in a stem-loop conformation stabilizing it for cleavage (169). While the four RRM domains are sufficient for RNA binding, the acidic N-terminal domain is required for cleavage of the precursor rRNA *in vitro* indicating it may be necessary for interactions with other proteins in the complex (157). Our data demonstrates that nucleolin interacts with DGCR8 and Drosha in an RNA-independent manner and yet also binds to the pri-miRNA. Based on this, we propose that while nucleolin may not possess any RNase III domains characteristic of the core proteins in the miRNA biogenesis pathway (13, 170), it instead facilitates cleavage of the primary miRNA by maintaining proper conformation of the pri-miRNA while simultaneously positioning Drosha and DGCR8 for binding and cleavage.

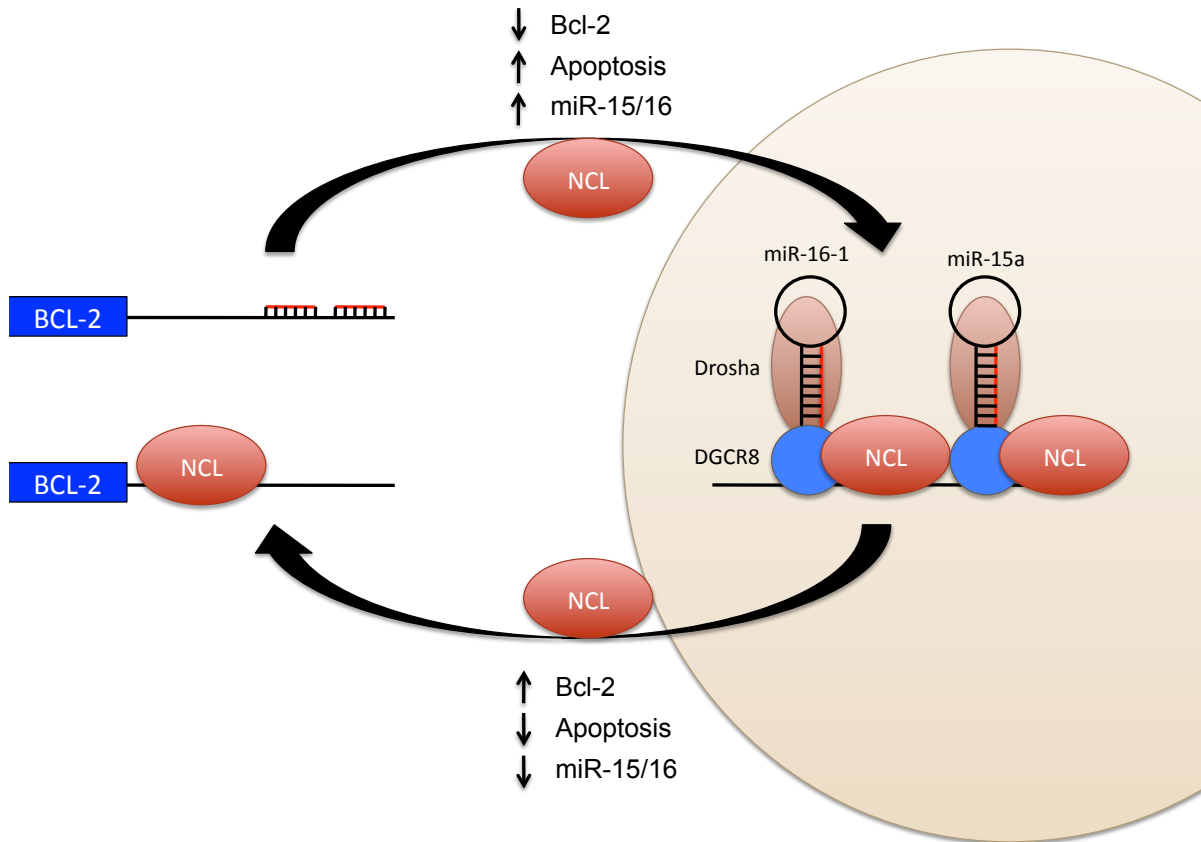


Fig 12. Model of the bipartite regulation of bcl-2 by nucleolin.

Under normal conditions nucleolin resides in the nucleus where it can bind with Drosha and DGCR8 to increase the processing of miR-15a and miR-16-1, which target BCL-2 mRNA for degradation. However, upon induction of cellular stress, nucleolin moves from the nucleus to the cytoplasm where it binds to and stabilizes BCL-2 mRNA. Simultaneously, there is less miR-15a and miR-16-1 due to reduced biogenesis in the absence of nuclear nucleolin. This provides cells with multiple levels of control in their reaction to cellular stress.

Chapter 4: Identification of RRBP1 as a repressor of miR-200 biogenesis and a novel miRNA-mediated coherent feedforward loop.

4.1. Introduction

Zinc-finger enhancer binding (ZEB) transcription factors (ZEB1 and ZEB2) are critical mediators in the acquisition of stem-like characteristics of cancers. Recently it was found that the histone methylation of H3K4 in the promoter region of ZEB1 is be found in a bivalent in plastic cancer cell populations allowing the conversion of non-stem like cells to a stem-like population thereby increasing tumorigenic and malignant potential (171). The ZEB1/2 transcriptional repressors form a well-established feedback loop that inhibits the transcription of the miR-200 family (miR-200a/b/c, miR-141, and miR-429), which in turn inhibit the mRNA of ZEB1/2 (110, 111, 172).

4.2. Results

4.2.1. TCGA analysis of miRNA in patients stratified by ZEB1/2 expression

We screened the TCGA breast cancer dataset using samples that had both RNAseq and miRNAseq (n=509) and separated stratified samples having high and low ZEB1/ZEB2 expression. There was a good correlation of ZEB1 and ZEB2 expression (Pearson correlation $r=0.84$), suggesting the expression of these molecules are under similar regulation (Fig. 13). Therefore expression data from both molecules were used to separate samples into ZEB1/2 high and low groups. There was no particular association of ZEB1/2 to any breast cancer subtypes.

We identified the top differentially expressed miRNAs between the ZEB high/low groups and found 145 altered miRNA (Appendix table 1). The expression of mature miRNA in the miR-200 family (miR-200a/b/c, miR-141, miR-429) was inversely correlated with ZEB1/2 as is expected due to the reciprocal feedback between the two (Fig. 13). Since the regulation of ZEB1/2, and indeed all known mechanisms of miR-200 regulation are transcriptional in nature, we evaluated the expression of the primary miRNA and surprisingly saw that it did not correlate with mature miR-200 expression (Fig 14). The levels of primary miR-200 family members remained constant between ZEB1/2 low compared to ZEB1/2 high samples.

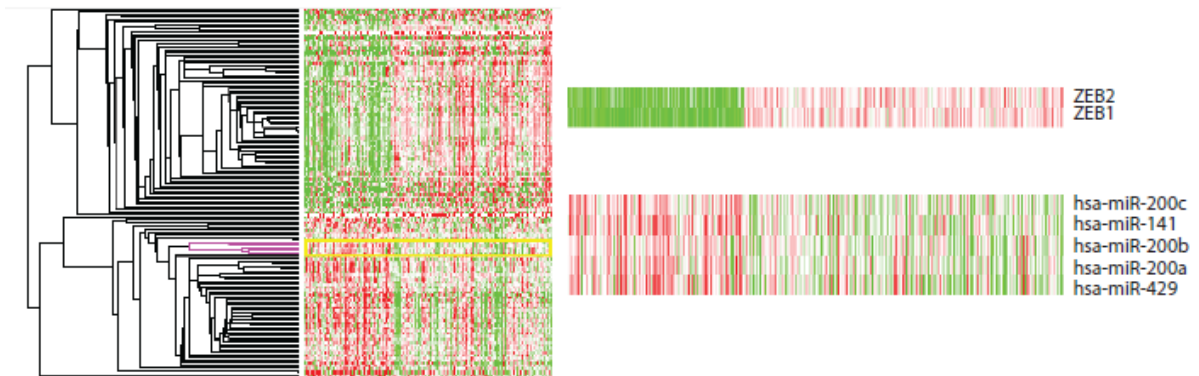


Fig. 13. Correlation between miRNA in ZEB1/2 high and low patient samples

145 differentially expressed miRNAs were found in ZEB1/2 high vs low expressing samples that are shown on the heat map on the left (see Appendix for list of miRNAs). The miR-200 family (highlighted in yellow in heat map on the left) were compared to ZEB1/2 expression and found to be inversely proportional as existing models of ZEB1/2-miR-200 axis predict.

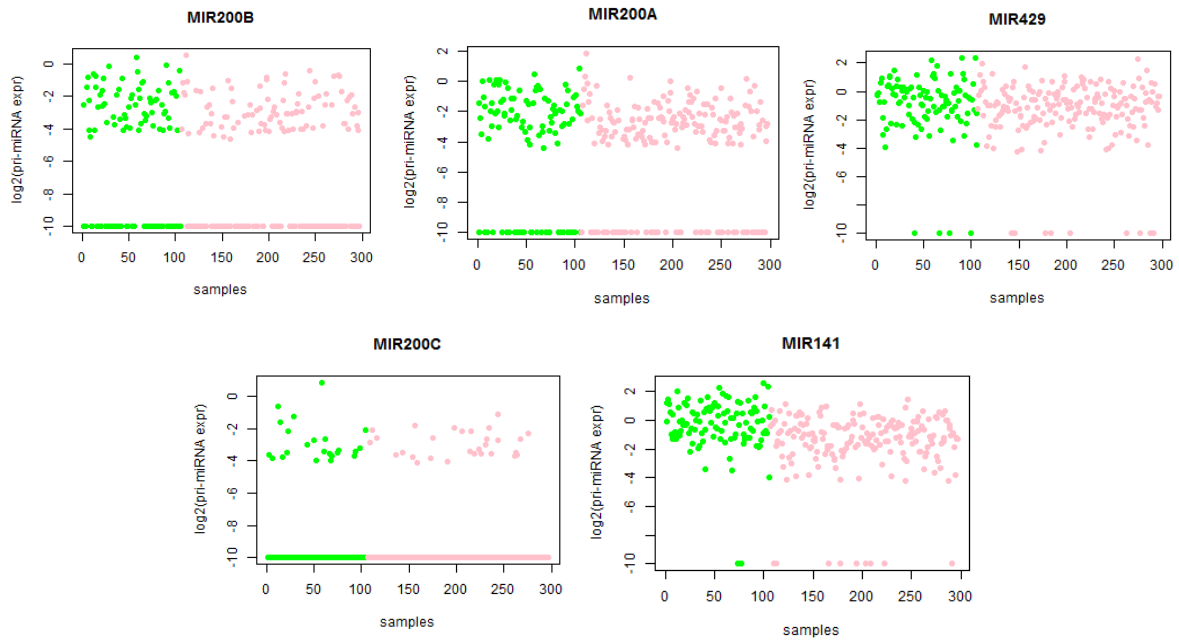


Fig. 14. Expression of pri-miR-200 vs. ZEB1/2 high and low patient datasets

Sequencing reads were mapped back to pri-miRNA sequences to quantify pri-miR-200 family expression. Some samples could not be mapped back (plotted along x-axis). For all samples with pri-miR-200 reads, no significant correlation was found between ZEB1/2 expression (low= green, high= pink) suggesting in patient samples the expression of pri-miR-200 family is independent of ZEB1/2 expression.

4.2.2. Analysis of pri- and mature miR-200 family in breast cancer cell lines

We screened a panel of breast cancer cell lines for mature and primary miR-200 in an attempt to validate the TCGA data. Consistent with the TCGA data, breast cancer cell lines separated by their miR-200 family expression showed an inverse correlation with ZEB1/2 expression (Fig. 15A,B) and yet the primary species of the miR-200 family did not recapitulate the mature miR-200 expression (Fig. 15C). We also found no association with p53 expression, another established transcriptional regulator of miR-200 (173). Included in the cell line panel are MCF-10A non-transformed mammary epithelial cells and MCF-10A.zeta cells overexpressing the protein 14-3-3 ζ that we have previously to have high levels of ZEB1/2 due to activation of the TGF- β pathway (174).

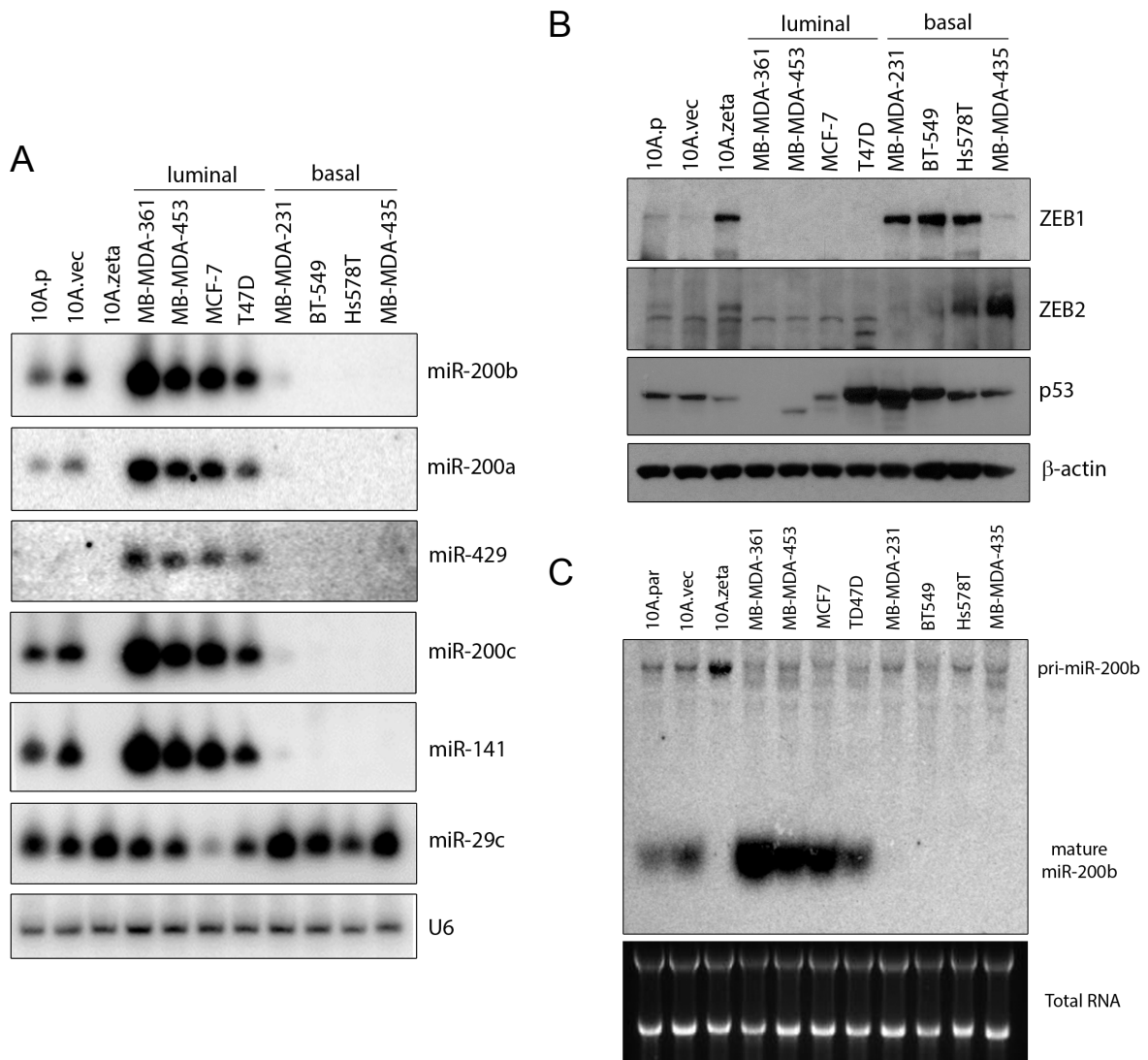


Fig. 15. MiRNA and protein expression in breast cancer cell lines.

A) Breast cancer cell lines were separated by decreased mature miRNA expression. MCF-10A non-transformed cells used as a normal control while MCF-10A.zeta cells as a positive control for ZEB1/2 expression. MiR-29c and U6 are controls for miRNA expression and loading, respectively. B) ZEB1 and ZEB2 expression is found only in mesenchymal breast cancer cell lines and correlations with mature miR-200 expression. There is no correlation between p53 expression and mature miR-200. C) Pri-miR-200b remains largely unchanged regardless of ZEB1/2 or p53 expression in breast cancer cell lines.

We used the MCF-10A and MCF-12A cell line models with or without 14-3-3 ζ overexpression to interrogate possible mechanisms by which the miR-200 family may be post-transcriptionally regulated because 1) these cells displayed the largest difference between primary and mature miR-200 expression, and 2) to minimize the variability between cancer cell lines. When examining the miR-200 family by northern blot we found there was no change in a precursor species despite loss of mature miRNA and simultaneously there was an excess of primary miR-200b in the cells with decreased mature miR-200b (Fig. 16). The inverse correlation between primary miRNA and mature miRNA is indicative of processing defects while the unchanging levels of the precursor species suggested that pre- to mature miRNA processing may be the biogenesis stage being affected.

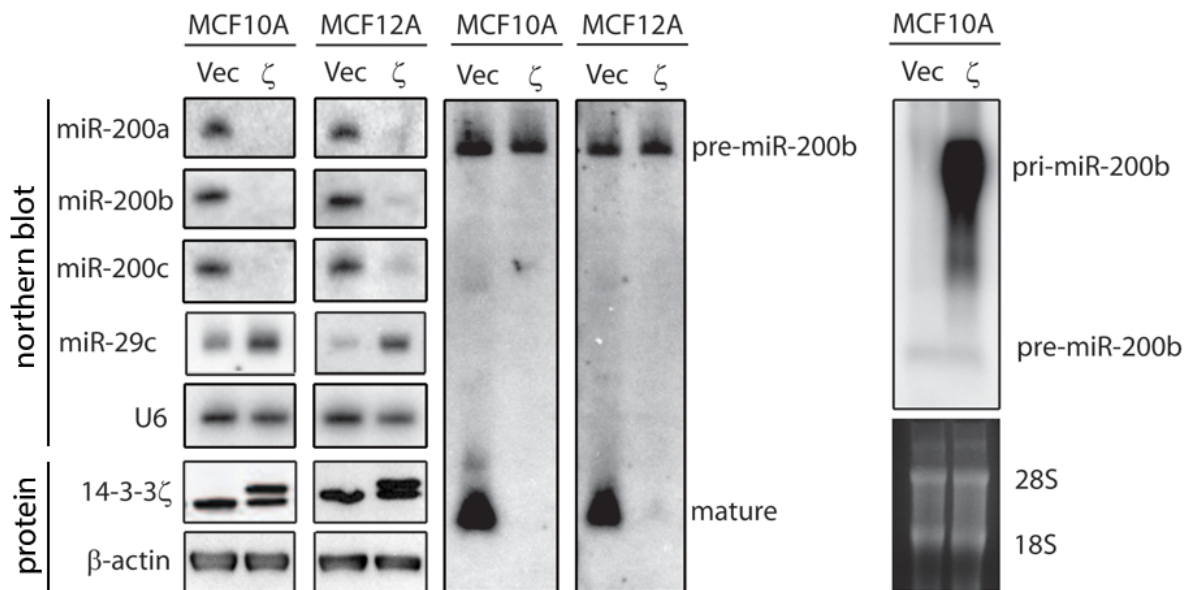


Fig 16. Loss of mature miR-200 expression does not alter pre-miR-200 levels and increases pri-miR-200.

The overexpression of 14-3-3 ζ significantly reduces mature miR-200 expression in both MCF-10A and MCF-12A non-transformed cell lines. The level of pre-miR-200b is indicated in the northern blot remains unaltered between high and low miR-200 expression. The pri-miR-200 levels significantly increase in cells with low expression of mature miR-200.

4.2.3. ZEB1/2 maintain transcriptional repression of the miR-200 family

We sought to determine if the transcriptional repressors ZEB1/2 might fail to repress the miR-200b/a/429 cluster in the 10A.ζ overexpressing cells despite ZEB1/2 being expressed at high levels compared to vector control cells. To test this we conducted a dual luciferase assay with the promoter region of the miR-200b/a/429 cluster containing the two E-boxes upstream of the transcriptional start site cloned upstream of firefly luciferase (Fig. 17A). As a control, an E-box mutant was included which was previously characterized as failing to be recognized by ZEB1/2 (111). MCF-10A or MCF-12A vector control cells or 14-3-3ζ overexpressing cells were co-transfected with either the wild type or mutant promoter constructs along with Renilla luciferase. As expected, we found the MCF-10A vector control cells had equal levels of expression between wild type and mutant constructs while the 14-3-3ζ overexpressing cells had a relative luminosity nearly equal to the empty luciferase plasmids due to repression from ZEB1/2 (Fig. 17B). A similar case was found in the MCF-12A cells; however, the vector control cells with the E-box mutants exhibited higher relative luminosity compared to the wild type luciferase transfected cells. This is likely because MCF-12A cells exhibit slightly more basal-like morphology due to higher ZEB1/2 levels. When examining the luciferase signal from the E-box mutants in either the MCF-10A or 12A 14-3-3ζ overexpressing cells we found even the mutants were unable to restore the luciferase signal to that of their respective vector control cells. We postulated this may be due to the fact 14-3-3ζ overexpressing cells have reduced p53 expression and since p53 is a positive regulator of miR-200 transcription the cells were unable to express an equal level of luciferase compared to vector controls. To test this, we overexpressed p53 in the

14-3-3 ζ overexpressing cells; however, we found this had no effect on luciferase expression. Nor did it have any impact on miR-200 expression, indicating loss of p53 was not responsible for low miR-200 expression in 14-3-3 ζ overexpressing cells (Fig. 17D). It is possible that another transcription factor is responsible for the failure of the E-box mutants to return to vector control cell luciferase levels.

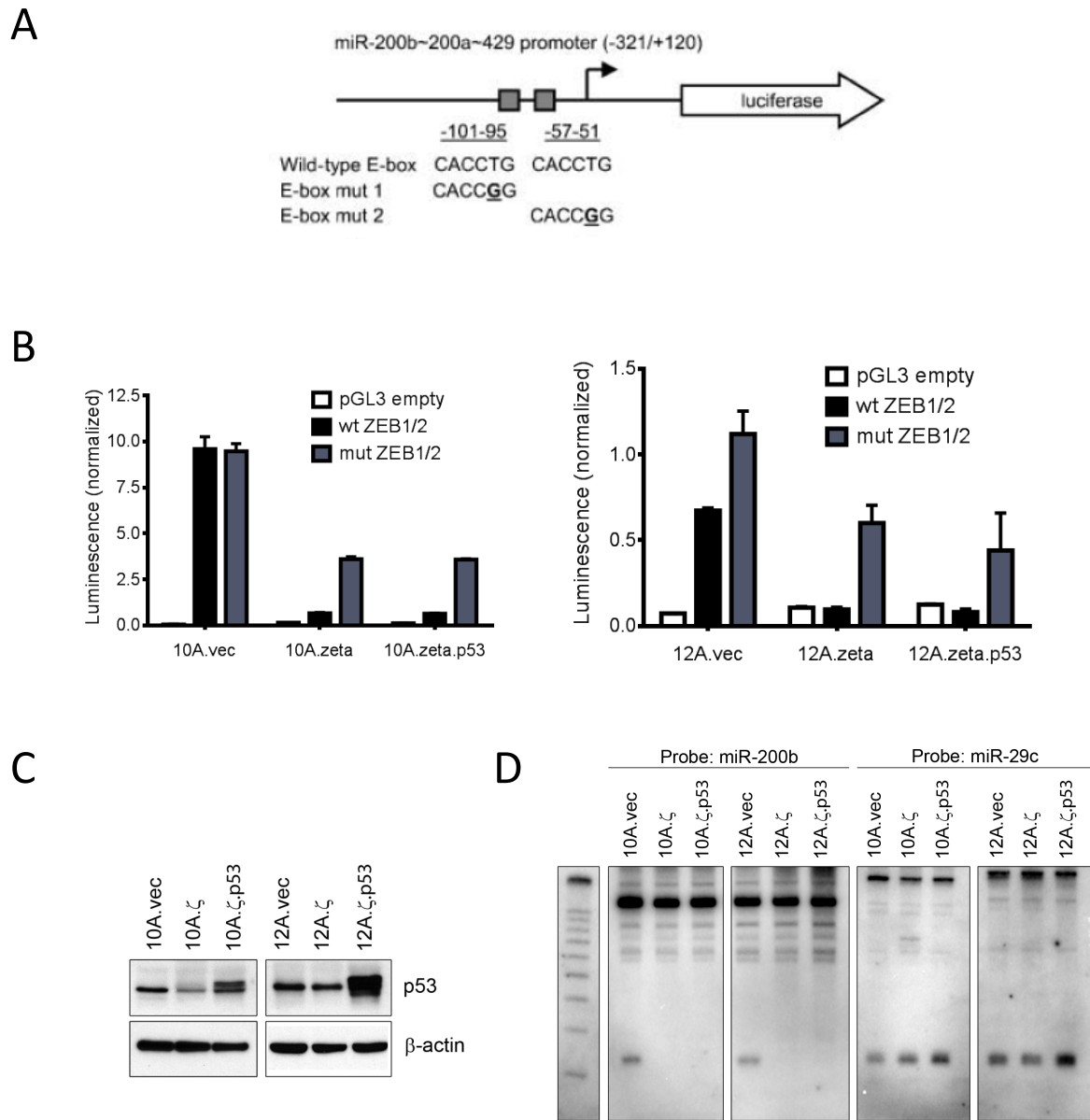


Fig 17. ZEB1 and ZEB2 transcriptionally repress the miR-200b/a/429 promoter

A) Diagram of luciferase constructs with miR-200b/a/429 ZEB1/2 WT and mutant E-box binding sites listed. B) Luminescence readings (normalized to Renilla) of 10A (left) and 12A (right) cells with low or high 14-3-3 zeta. The luciferase readings in zeta high cells are nearly the same as the empty vector indicating significant repression from ZEB1/2. C) Western blot demonstrating the exogenous rescue of p53 expression in 10A or 12A zeta. D) Northern blot of miR-200b and miR-29c in p53 rescued cells shows no change in expression of mir-200b.

4.2.4. TGF- β stimulation or p53 loss do not alter pri- or pre-miR-200 expression

14-3-3 ζ is a known activator of the TGF- β pathway and inhibitor of p53 expression via Akt phosphorylation of MDM2 (174, 175). We sought to separate these pathways and examine their affect on miR-200 expression in the absence of 14-3-3 ζ overexpression to determine if 14-3-3 ζ may be playing a direct role in miR-200 regulation. We treated MCF-12A cells with 5 ng/ml of TGF- β for two weeks, which was sufficient to induce an epithelial-to-mesenchymal transition (Fig. 18A). After two weeks samples were either maintained in TGF- β or allowed to grow in its absence for an additional two weeks. Additionally, we generated MCF-12A cells stably expressing an p53-specific shRNA or a control shRNA to GFP (Fig. 18A). The knockdown efficiency was greater than 90%, which reduced the cell levels of p53 to below that of 14-3-3 ζ overexpressing cells. We observed reduced miR-200 expression in the TGF- β -treated cells and the loss of expression was maintained following removal of TGF- β . Loss of p53 had a similar level of decreased miR-200 (Fig. 18B). MiR-29c was used as a control as it is known to increase in expression following EMT. Consistent with previous observations, the precursor levels of the miR-200 family were unaltered in the TGF- β -treated or p53 knockdown cells indicating the miR-200 expression patterns associated with 14-3-3 ζ overexpression were not due to 14-3-3 ζ directly affecting miR-200 regulation. More likely, the effects observed in 14-3-3 ζ overexpressing cells are due to a combined effect from both the TGF- β pathways and loss of p53. This also indicates that the post-transcriptional regulation of the miR-200 family is a common phenomenon and not specific to any particular stimulus.

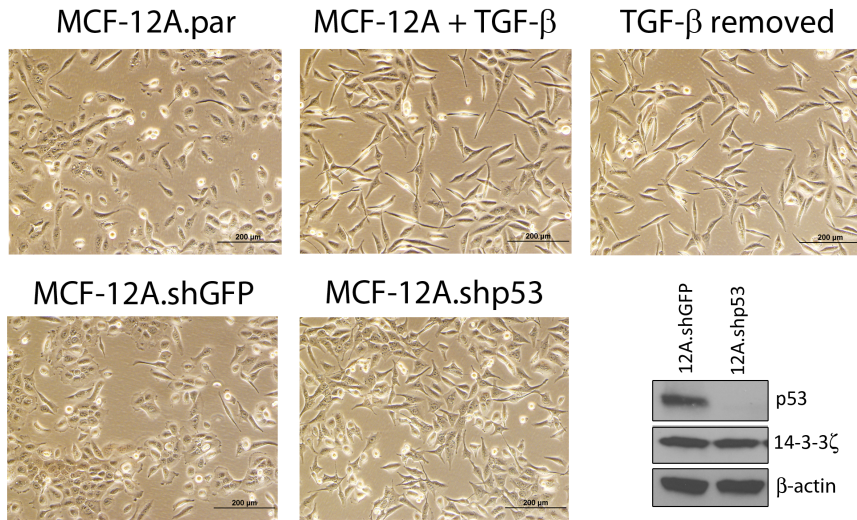
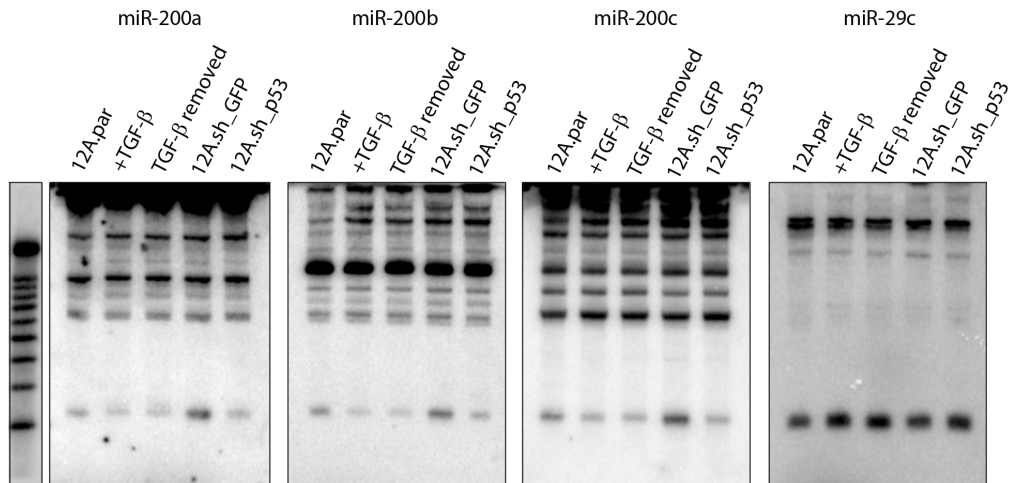
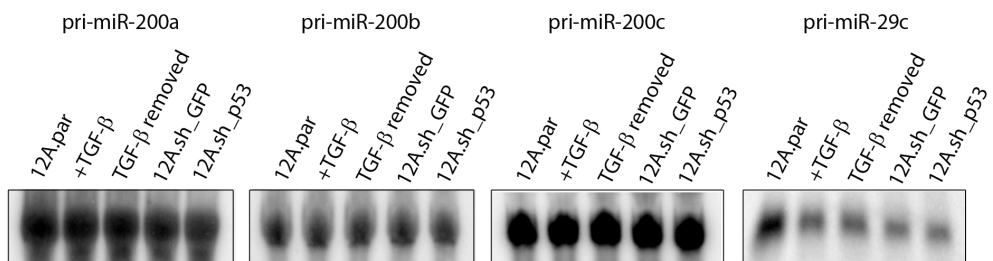
A**B****C**

Fig 18. TGF-beta treatment or p53 loss downregulate miR-200 post-transcriptionally

A) Bright field microscopy of MCF-12A cells with TGF-beta treatment or p53 loss (inset) that appear more spindle-shaped indicative of an EMT. B) Northern analysis of miR-200 family expression. Neither TGF-beta treatment nor p53 loss affects pre-miR-200 expression or pri-miR-200 expression (C).

4.2.5. Knockdown of ZEB1/2 in 14-3-3 ζ overexpressing cells

We sought to determine if loss of ZEB1/2 in 14-3-3 ζ cells would restore miR-200 expression. ZEB1 or ZEB2 were knocked down with siRNA either individually or simultaneously for 96 hours and miR-200 expression assessed by northern blot and qRT-PCR. In MCF-10A. ζ cells, siRNA treatment had no effect on miR-200b levels whatsoever (Fig. 19A,B). Loss of either ZEB1 or ZEB2 in MCF-12A. ζ cells did not alter miR-200 expression compared to a non-targeting control siRNA; however, the combined loss of both transcriptional repressors was able to slightly increase miR-200b expression. Yet, the increase was unable to restore miR-200b levels of the vector control levels despite ZEB1 and ZEB2 being reduced to nearly equal levels (Fig. 19C).

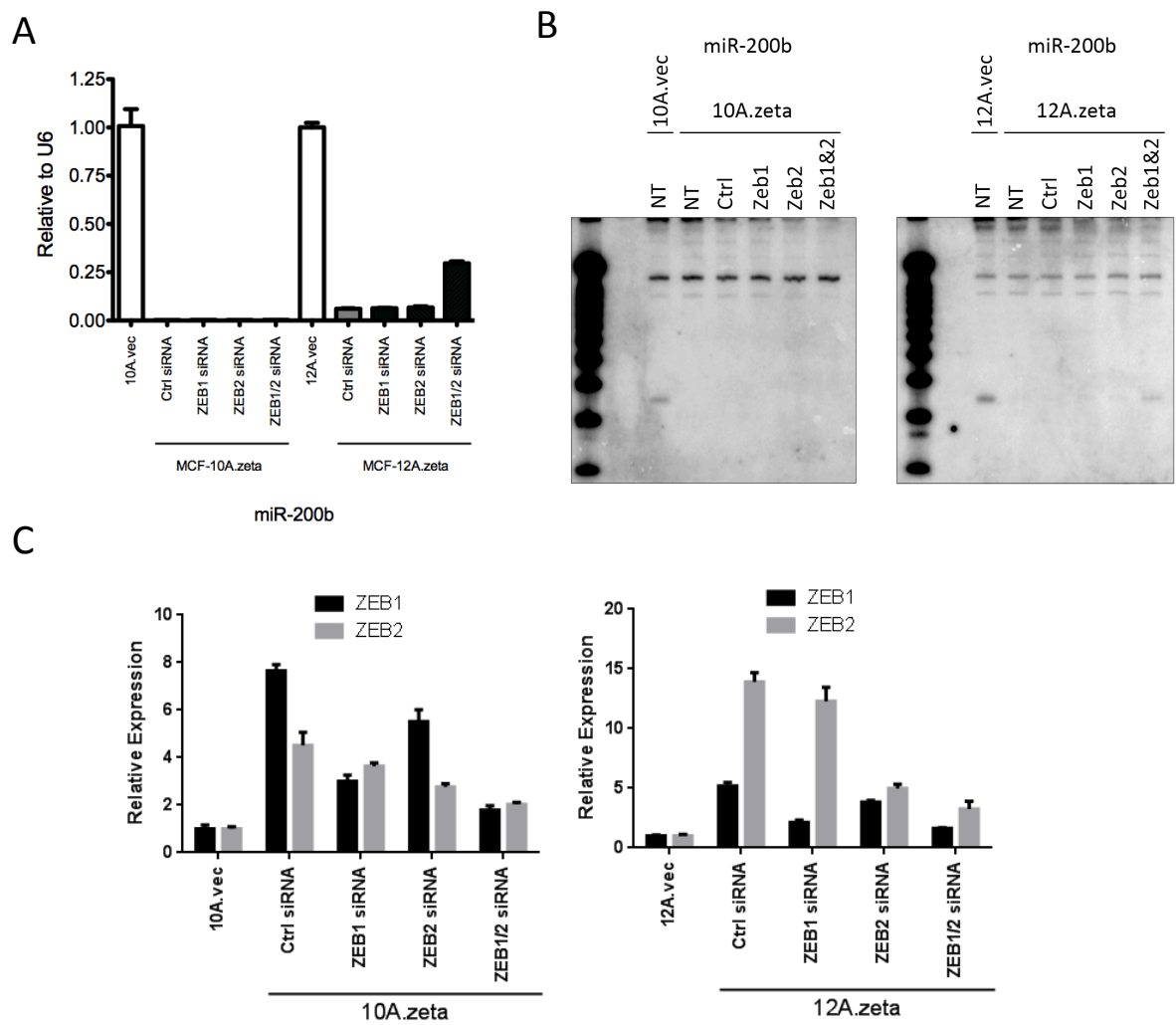


Fig. 19. Knockdown of ZEB1 and ZEB2 fails to restore miR-200 expression

A) qRT-PCR of miR-200 in MCF-10A (left) and MCF-12A (right) cells. B) Northern analysis of miR-200b in knockdown cells. C) qRT-PCR of ZEB1/2 mRNA expression between 10A and 12A cells 96 hours after siRNA treatment.

4.2.6. Pre-miRNA levels remain unchanged in miR-200 low cells

To this point we have demonstrated through patient data analysis, cell line studies, and genetic approaches that the miR-200 family exhibits a high degree of post-transcriptional control despite ZEB1/2 functioning to repress their transcription. These claims are largely based on northern blot data, which shows the presence of distinct precursor bands corresponding to the individual miR-200 family members. In an effort to rule out non-specific hybridization, we fractionated the RNA from 10A.vec and 10A.ζ cells to isolate species less than 200 nucleotides using RNazol. This fraction should contain the precursor miRNA but exclude the much larger primary miRNA. Successful fractionation was determined by northern blotting for miR-200b as shown in Fig. 20A. The fractionated RNA, along with total RNA, was subjected to reverse transcription by random hexamers and pri and pre-miR-200b were quantified with specific primers to the stem-loop structure, which detects both pri and pre-miR-200b species. In complete consistency with northern blot data, the small RNA fraction containing only the pre-miRNA showed no altered expression between 10A.vec and 10A.ζ cells while the total RNA fraction (containing both pri- and pre-miRNA species) showed a significant increase of approximately 6 fold in 10A.zeta cells (Fig. 20B). To further assess if the LNA probes are detecting non-specific bands we synthesized an antisense RNA probe specific to the loop of miR-200b. This region is distinct from the hybridization site of the LNA probe. The cells express an inducible miR-200b lentiviral construct that rapidly increase miR-200 levels in response to doxycycline to generate an otherwise hard to detect 60 nt Dicer substrate along with mature miR-200b expression. The northern blots for the RNA loop probe and LNA probe are taken from the exact same

membrane. The membrane was hybridized using the RNA loop probe first, then stripped and re-exposed for 4 days to ensure that no residual signal remained, and then re-probed with the LNA to miR-200b (Fig. 20C). These data indicated the precursor species detected by northern blot were real and not due to non-specific hybridization of the LNA probes.

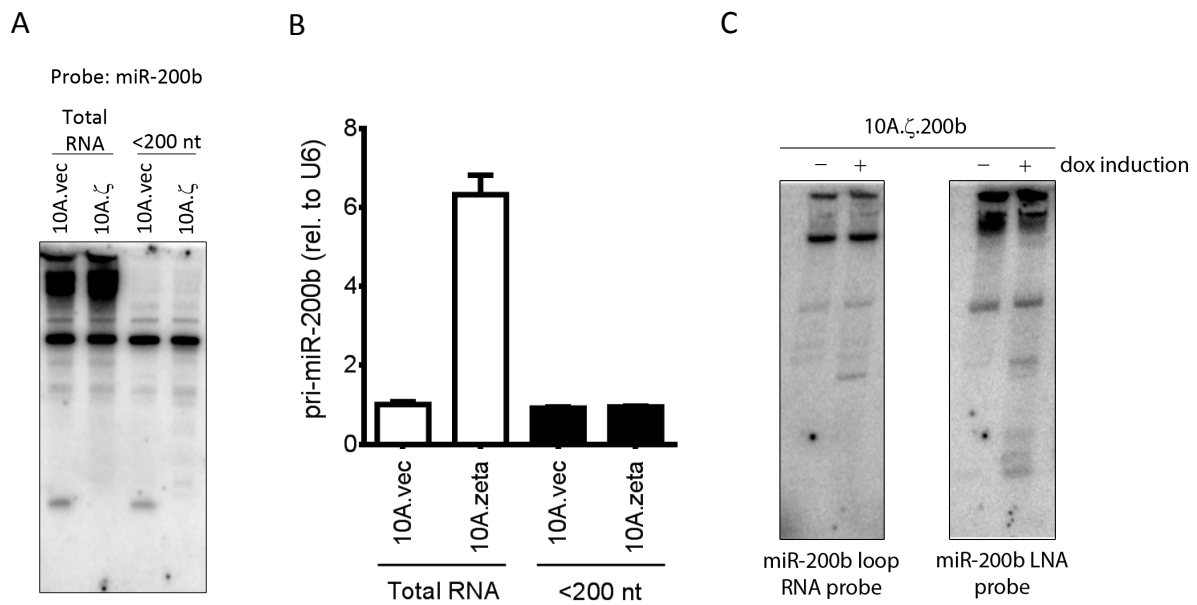
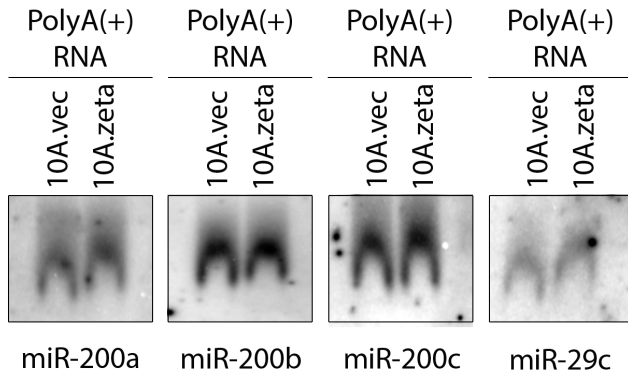
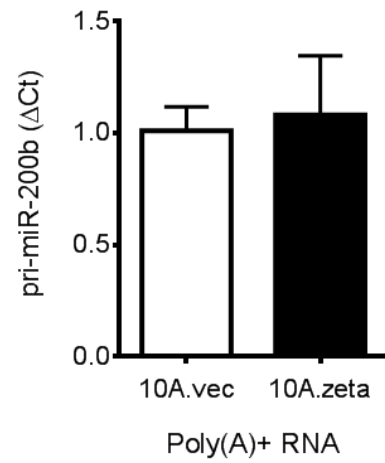


Fig. 20. Validation of miR-200 precursor

A) Validation of low molecular weight RNA fractionation by northern blot. B) qRT-PCR using either total RNA (white bars) or small RNA fraction (black bars) for pre-miR-200b. C) Northern blot for pre-miR-200b using an anti-sense RNA to the loop region (left) that binds a different region from the LNA probe (right). The loop RNA probe fails to detect mature miR-200 but detects pre-miR-200b exactly as the LNA probe demonstrating the pre-miR-200b signal is not an artifact of hybridization

We went on to assess the validity of the pri-miRNA northern blot signal for possible non-specific hybridization. As described in **section 1.1** pri-miRNA are transcribed by RNA pol II that results in the addition of a poly(A) tail. We isolated poly(A)+ RNA by oligo-dT bead capture and analyzed the expression of pri-miR-200 by northern blot and qRT-PCR. Interestingly, northern blot analysis of poly(A)+ RNA showed no significant differences between 10A.vec and 10A.ζ cells (Fig. 21A). These results were also confirmed by qRT-PCR for pri-miR-200b, yet total RNA showed increased pri-miR-200b (Fig. 21B, Fig 20B). This indicates the poly-adenylated pri-miRNA is likely rapidly cleaved by Drosha, at which point the poly(A)+ tail is cleaved. The overall abundance of poly(A)+ pri-miRNA was also significantly lower in its northern blot signal suggesting the cleavage occurs quickly and the poly(A)+ pri-miR-200 family represents only a small minority of the total pri-miRNA signal detected from total RNA. These findings are consistent with the observation that Drosha cleavage occurs co-transcriptionally (23).

A**B****Fig. 21. Poly-(A)+ selected RNA northern blot and qRT-PCR**

A) Pri-miR-200 family expression was analyzed in poly-(A)+ selected RNA and showed no difference in expression. B) Confirmation of northern data by qRT-PCR of pri-miR-200b.

4.2.7. Re-expression of miR-200 clusters

We have demonstrated through multiple independent assays that the miR-200 family is under negative post-transcriptional control and this is a common feature amongst various methods known to induce loss of miR-200.

To ascertain if the loss of miR-200 is due to the loss of an activator of miRNA processing or the gain of an inhibitor, we transduced MCF-10A.vec and MCF-10A.ζ cells with two lentiviruses expressing either the miR-200b/200a/429 cluster or the miR-200c/141 cluster as they exist in their respective genomic context. We postulated that if there were a loss of an activator of miR-200 processing then regardless of the amount of upstream miRNA put into the cells, the mature miRNA would fail to be generated in the 14-3-3ζ overexpressing cells. We observed that the miRNA were readily processed in both the vector and the zeta overexpressing cells (Fig. 22C). This implied that 14-3-3ζ cells possessed a repressor of biogenesis that could be titrated away with sufficient quantities of primary miRNA allowing the remaining, uninhibited miRNAs to be recognized by the biogenesis machinery and generate the mature species. In addition to this; however, we found when one cluster was overexpressed (*e.g.* miR-200b/a/429), the miRNA from the other cluster (*i.e.* miR-200c/141) also increased to an equal level. This could be explained with the feedback between miR-200 and ZEB1/2 where high levels of miR-200b/a/429 inhibit ZEB1/2, which de-represses the endogenous promoter for miR-200c/141. However, after examining the ZEB1/2 levels by western blot and qRT-PCR we found the levels of ZEB1/2 are not restored to the levels of the 10A.vec cells (Fig. 22D,E). The lack of full ZEB1/2 restoration is also exemplified by E-cadherin expression, which is directly transcriptionally inhibited by

ZEB1/2. E-cadherin the 10A.ζ cells overexpressing either cluster is not fully restored to the level of 10A.vec cells. Additionally, the increase between the exogenous and endogenous cluster expression was equal. The only exception to this was miR-429, which was only increased in cells expressing the exogenous miR-200b/a/429 cluster but not the miR-200c/141 cluster (Fig. 22C).

Another possible explanation lies in the sequence similarity between the various mature species. MiR-200b and miR-200c are identical except for two residues as are miR-200a and miR-141. Highly similar mature miRNA (Fig. 22A) with the potential to cross react to the northern probes exist on either cluster, despite locked nucleic acids being exquisitely specific. To rule out cross reactivity of probes we synthesized a series of spike-in miRNAs to specific to miR-200a, b, or c along with 8 nucleotides of their flanking nucleotides. The amount of spike-in RNA roughly equivalent to twice that of the levels present in 10A.vec cells and optimized hybridization and washing conditions were determined by titrating the spike-in RNAs with and comparing to the expression in 10A.vec cells (Fig. 22B). When these same conditions were applied to the northern blots of the miR-200 cluster expressing clones it is clear that the increase of non-cluster expressed miRNA is not due to cross reactivity.

Taken together, this suggests that miR-200 repression is due to the presence of an inhibitor and not the absence of an activator of miRNA biogenesis. More importantly, our data suggests that the individual miR-200 family members may be able to ‘communicate’ with one another as to their expression levels through titrating away the repressor protein(s). However, this may not be the case for miR-429 since overexpression of the miR-200c/141

cluster did not upregulate its expression beyond that of the 10A.vec cells, which is expected due to the loss of ZEB1/2.

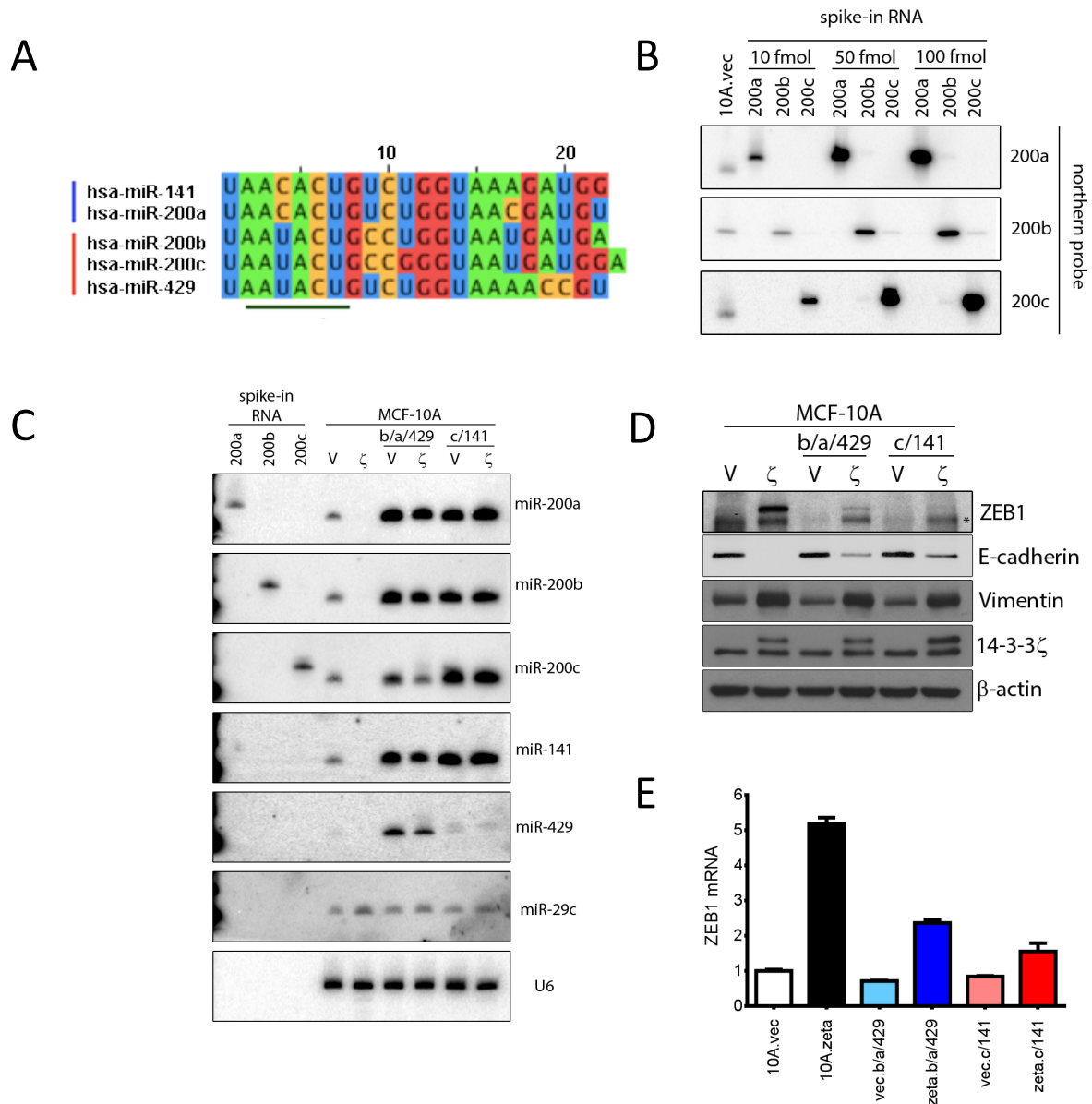


Fig. 22. Re-expression of miR-200 clusters induces upregulation endogenous cluster independent of transcription.

A) Sequence similarity between the miR-200 family members. MiR-200a and miR-141 differ in two nucleotides, as do mir-200b and mir-200c, while mir-429 is the most divergent from the others. B) Optimization of northern stringency to distinguish closely related miR-200 family members. Synthetic RNAs were spiked-in at varying concentration to detect cross-hybridization. C) Re-expression of miR-200 family clusters as they exist in a genomic context with spike-in RNAs to rule determine specificity. D) Western blot analysis of miR-200 cluster re-expressed cells. E-cadherin is a direct target of ZEB1 while vimentin is not but remains a marker of mesenchymal cells. E) qRT-PCR analysis of ZEB1 expression in cluster re-expressed cells.

4.2.8. Coherent feedforward regulation of miR-200 biogenesis

The results of the miR-200 cluster expression indicate that a level of crosstalk exists between the miR-200 species. However, accurate dissection of this is complicated by the fact these miRNAs are stably expressed for an extended period of time before analyzing expression patterns and the contribution of individual miR-200 species cannot be separated from the others in the cluster. In an effort to obtain more specific details of the timing and contribution of individual miR-200 family members we cloned individual pri-miR-200 members into the pTRIPz doxycycline-inducible lentiviral plasmid. Each pri-miRNA was cloned with 50 nucleotides of flanking regions to the hairpin to include any *cis* acting sequences (10). MCF-10A.ζ cells were transduced with lentiviruses expressing the inducible constructs because they contain very low levels of endogenous miR-200 allowing accurate quantification and visualization by northern blot of the miRNA increase as a result of doxycycline induction. Following a timecourse induction with pri-miR-200b over 24 hours, qRT-PCR analysis showed a nice correlation between the expression of pri-miR-200b and mature miR-200b (Fig 23A). There is a slight delay in the mature species from the primary, which is likely due time necessary for processing by the microprocessor and Dicer.

When MCF-10Aζ cells with inducible miR-200c were induced over a 24 hour timecourse an ~25-fold increase in mature miR-200c was detected at 4 hours increasing to an 80-fold increase by 24 hours (Fig 23B). An analysis of mature miR-200b along the same timecourse revealed an ~20-fold increase by 4 hours, which plateaued at 8 hours after induction. This indicated that upregulation of miR-200c alone can induce the post-transcriptional upregulation of miR-200b at time points too early for a feedback inhibition to

occur with ZEB1/2. Indeed, when ZEB1/2 mRNA was analyzed along the same timecourse there was no significant change in expression (Fig. 23C).

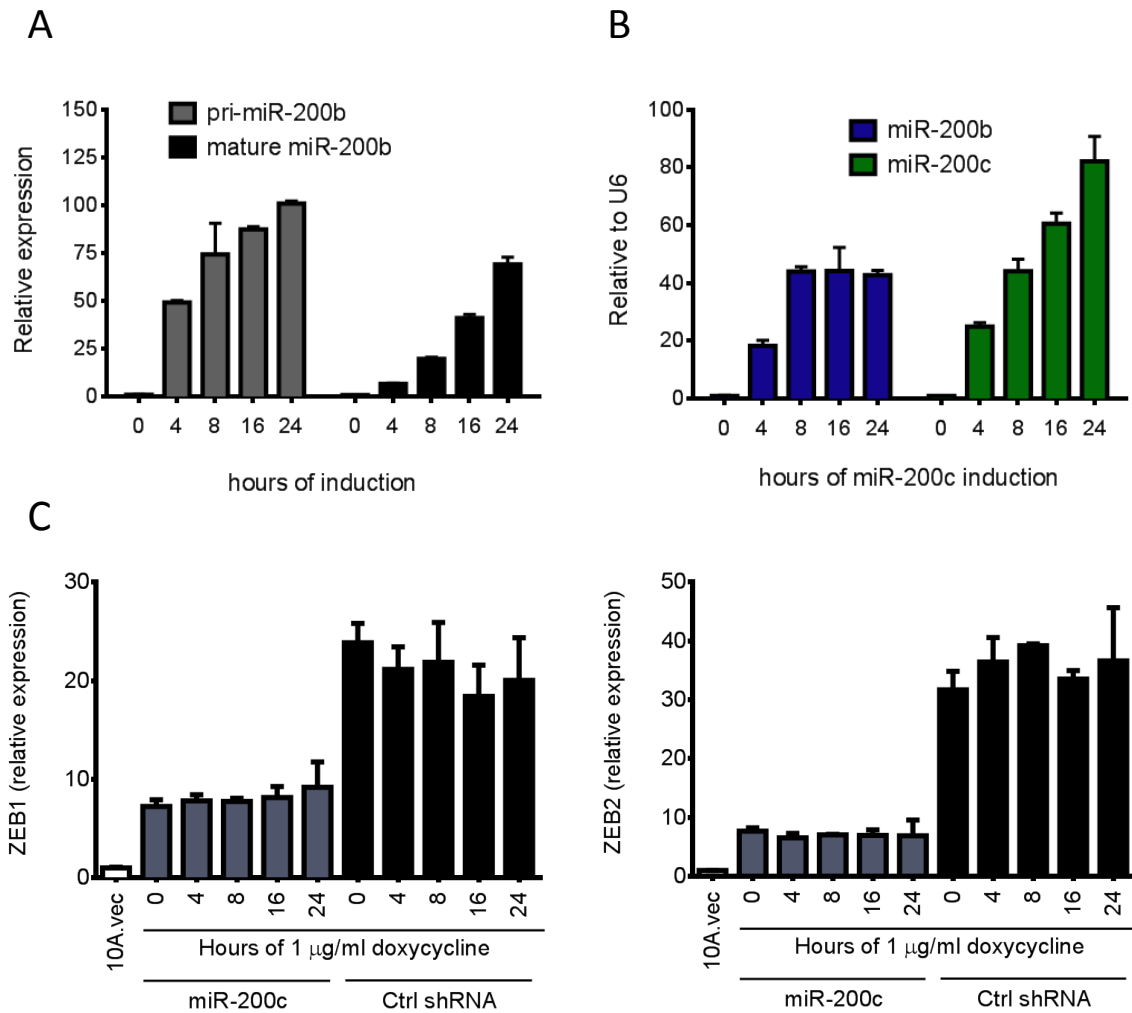


Fig. 23. Time course dependent induction of individual miR-200 members upregulates other members independent of transcription.

A) Timecourse of miR-200b induction determined by qRT-PCR. Mature miR-200b induction (black bars) lags slightly behind pri-mir-200b induction (grey bars). B) Induction of mir-200c (green bars) induces the expression of mature miR-200b (blue bars). C) ZEB1 (left) and ZEB2 (right) mRNA expression comparing 10A.vec cells with miR-200c induction and a control shRNA induction timecourse.

To evaluate this effect under the most stringent conditions we decreased the time of induction to time points at 1, 2, 4, 6, and 8 hours and analyzed the increased expression by high stringency northern blotting with miR-200 spike-in RNAs to rule out cross reactivity. In addition to the inducible pri-miR-200 members, we also included a non-targeting inducible shRNA, which still requires processing by Drosha and Dicer to rule out the effects of doxycycline or increased processing load on the biogenesis machinery. We ruled out feedback from ZEB1 by evaluating its expression via western blot at each time point and for each individual miR-200-inducible clone (Fig. 24). MCF-10A.vec cells were included as a control to determine physiological levels of miR-200 family members. MiR-29c was included as a control to rule out the possibility that miRNA expression is being globally regulated. Lastly, whenever possible, the same membrane was used to probe all miRNAs to reduce any variability in loading or transferring. MiR-429 is not included in the analysis because its expression was undetectable in all cases due to extremely low expression.

Induction of miR-200a caused the coordinated upregulation of both miR-200b and miR-141 but failed to induce miR-200c (Fig. 25). Evidence of post-transcriptional biogenesis of miR-200b and miR-141 is additionally evident due to the appearance of a 60 nt band corresponding to the Dicer substrate precursor. MiR-200b induction only caused the upregulation of miR-200c (Fig. 26) and, conversely, the induction of miR-200c only upregulated miR-200b (Fig. 27). As expected, inducing the control shRNA failed to induce the expression of any of the miR-200 family members (Fig. 28).

The data presented from the miR-200 clusters and inducible systems clearly demonstrates a post-transcriptional upregulation of miR-200 biogenesis wherein individual

species crosstalk with one another to titrate away the effects of a repressor. This represents the first time miRNAs have been shown to regulate one another through a mechanism independent feedback involving proteins.

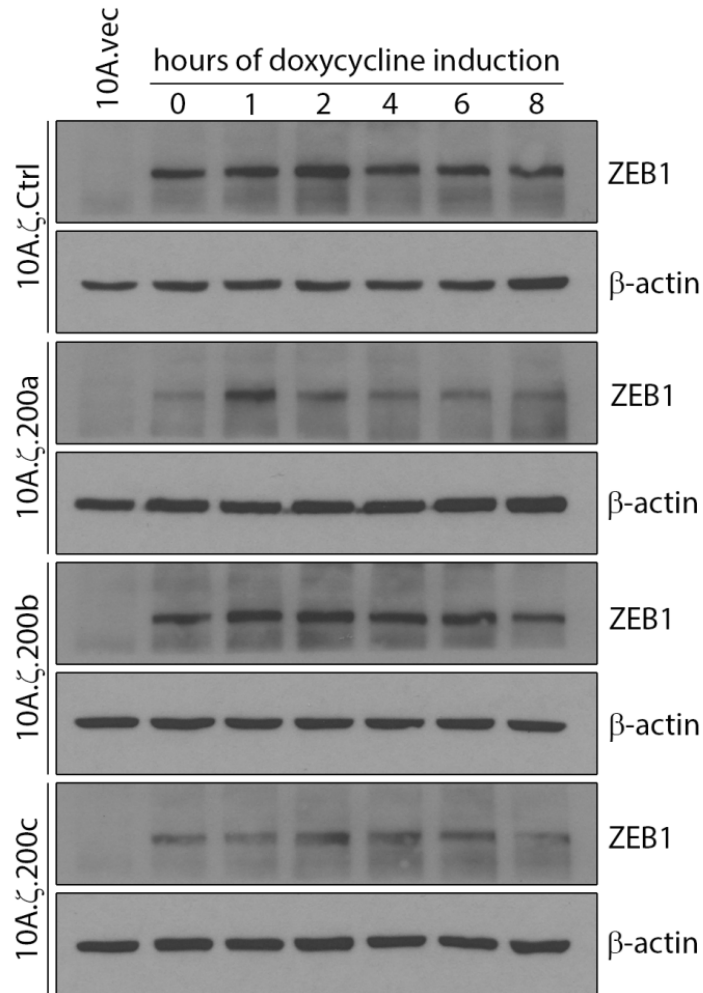


Fig. 24. ZEB1 expression in each of the miR-200 expressing clones during induction timecourse.

Each of the miR-200 expressing clones were induced with doxycycline over an 8 hour timecourse to evaluate the expression of ZEB1 expression. Samples are compared to 10A.vec with low ZEB1 expression and high mir-200 expression.

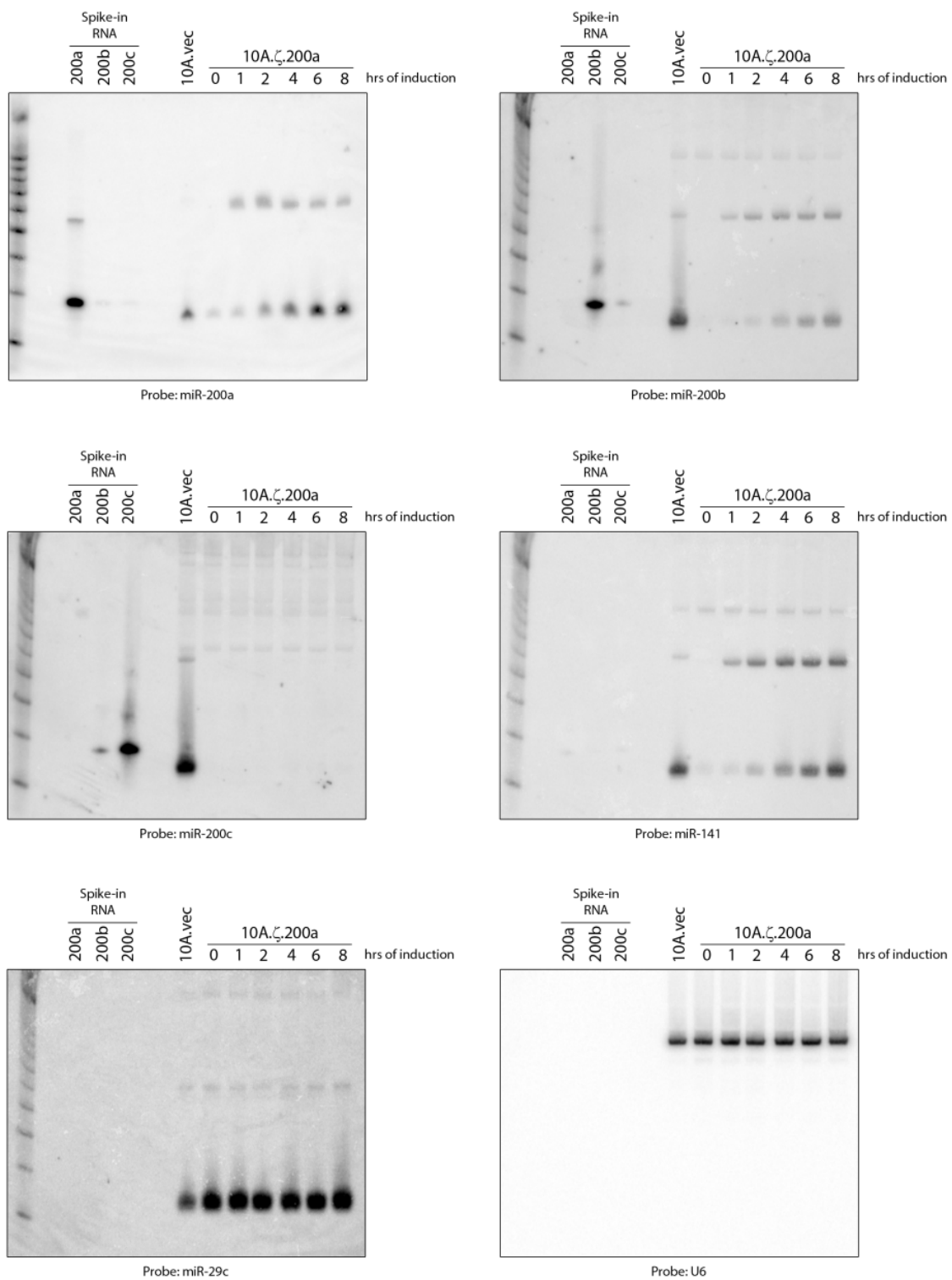


Fig. 25. Co-upregulation of miRNA following miR-200a induction

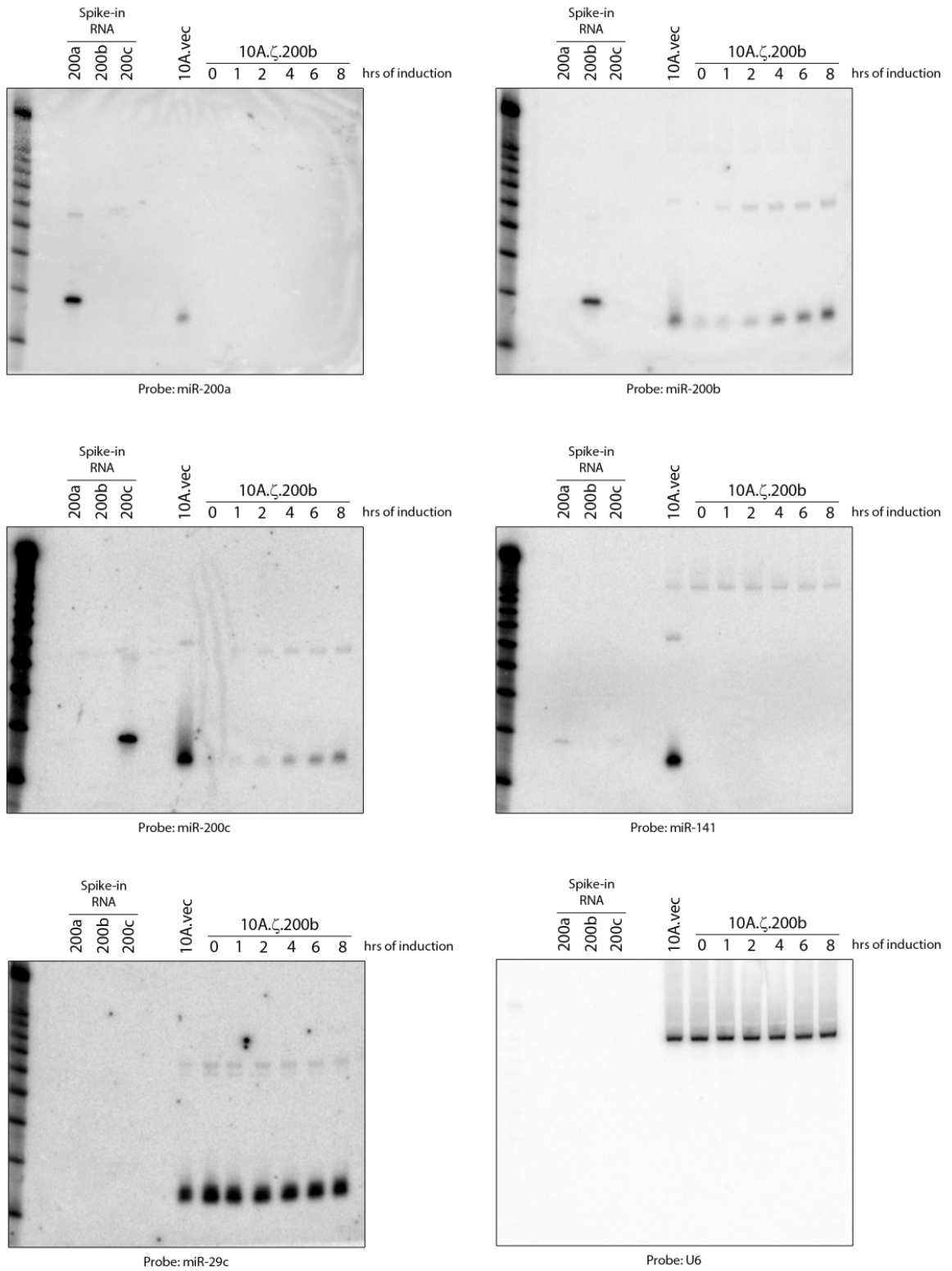


Fig. 26. Co-upregulation of miRNA following miR-200b induction

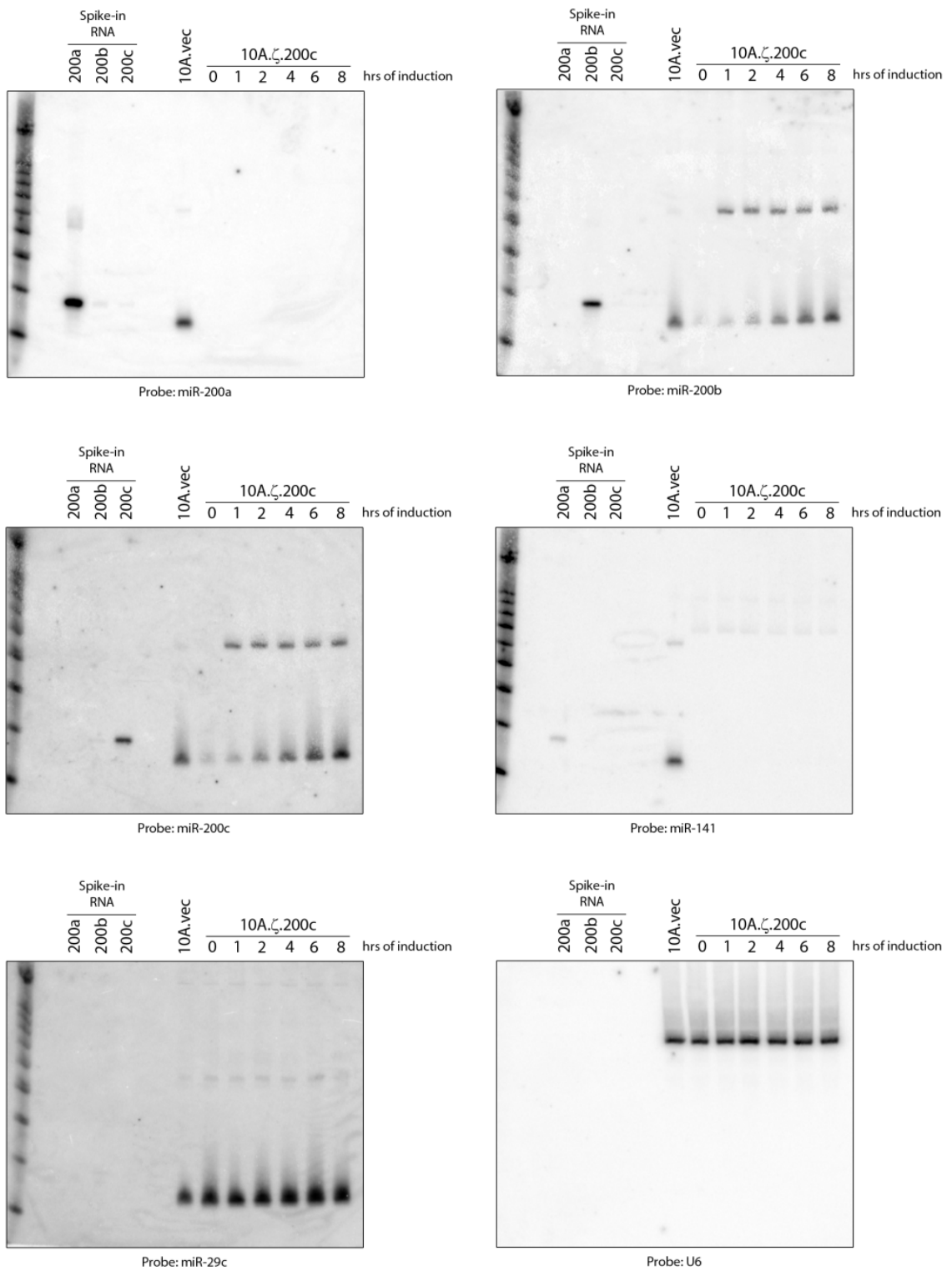


Fig. 27. Co-upregulation of miRNA following miR-200c induction

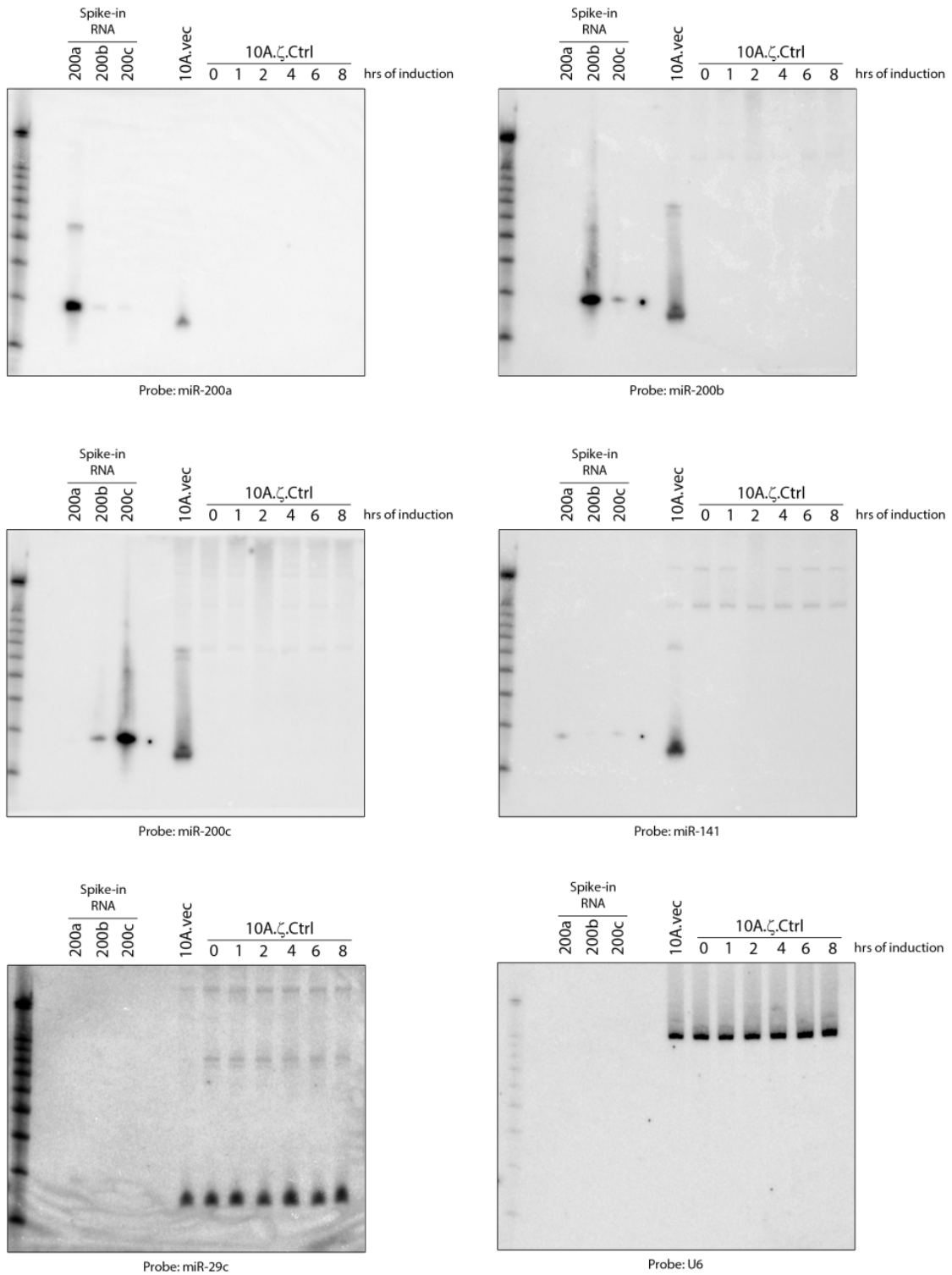


Fig. 28. Co-upregulation of miRNA following induction of a non-targeting shRNA

4.2.9. Development of Cross-linking and PNA Pulldown (CLaPP) assay

To identify what protein(s) may be responsible for inhibition we first attempted a standard RNA pulldown assay with *in vitro* transcribed biotinylated precursor miRNAs and identified many known RNA binding proteins by mass spectrometry yet functional analysis revealed these were all non-specific binders. Therefore, we sought to develop a new technique in which we could specifically capture the endogenous precursor miRNA in a cell after photocrosslinking to create a covalent bond between protein and RNA. Similar approaches have been taken to capture proteins bound to all polyadenylated RNAs using an Oligo-dT capture probe (139, 140, 176) but this lacks specificity and precursor miRNA do not possess a poly(A) tail. Specific capture of nucleic acids has been performed using biotinylated antisense RNA probes but to achieve the necessary specificity the antisense probes must be at least 150 nucleotides in length, which is longer than the length of the entire precursor (143). Instead we chose to design antisense peptide nucleic acid (PNA) probes because of their strand invasive potential to disrupt the precursor miRNA stem-loop structure and because of a high level of specificity achieved with only 15 nucleotides (144, 177–181). Furthermore, since PNAs contain an amino acid backbone and not a negatively charged sugar phosphate backbone their hybridization efficiency is independent of the ionic strength of the hybridization buffer. We designed 15-mer antisense PNAs to the 3' tail of the miR-200 precursor, which were long enough to specifically recognize individual miRNA precursors but short enough to minimally disrupt the endogenous protein-RNA interactions (Table 1). Importantly, their hybridization temperatures (T_m) were approximately 30°C above that for RNAs with the same sequences under the same conditions (Table 2).

Table 1. Antisense PNA sequences used in CLaPP assay

PNA name	Sequence
AS-miR-200a	Biotin-O-gcg ggt cac ctt tga
AS-miR-200b	Biotin-O-cgt gca ggg ctc cgc
AS-miR-200c	Biotin-O-cct cca tca tta ccc
AS-miR-29c	Biotin-O-tcc ccc tac atc ata

* -O- = acetyl-ethyleneglycol-ethyl-amine (AEEA)

Table 2. Comparison of hybridization temperatures for PNAs and RNAs with the same base sequence.

	Target miRNA for capture			
	miR-200a	miR-200b	miR-200c	miR-29c
PNA T _m (°C)	69.2	76.3	64.6	64.4
RNA T _m (°C)	37.2	45.4	34.4	31.9

We first sought to determine the sensitivity and specificity with which we can capture the precursor miRNAs. *In vitro* transcribed precursor miRNAs (miR-200a, b, c, and 29c) corresponding to the sequences in miRbase were PAGE purified and mixed. The mixed oligo pool was divided equally six ways. One sample was used as an input control, aliquot for each of the four PNAs, and one aliquot was mixed with magnetic streptavidin beads only (Fig 29). For binding and washing conditions see materials and methods. 100 pmol of PNA was used per reaction and ~20 pmol of each pre-miRNA was present in the reaction giving a 5-fold excess of PNA. After hybridization, streptavidin capture, and washing, the RNA was eluted in formamide loading buffer by heating to 80°C for 5 minutes. The supernatants after the initial capture were ethanol precipitated to determine sensitivity. Input RNA, eluted RNA, and precipitated supernatants were analyzed by staining with SYBR gold II and by northern blotting. Interestingly, in each of the PNA capture lanes a doublet band appears where the lower band represents free RNA and the upper band is the PNA-RNA hybrid indicating the PNA-RNA interaction remains so tightly bound that even under denaturing conditions the two remain hybridized. Additionally, the PNA was able to specifically distinguish between miR-200b and miR-200c while the LNA probe was unable to do so under the most stringency of hybridization conditions, again validating the specificity of PNAs over other nucleic acid capture techniques.

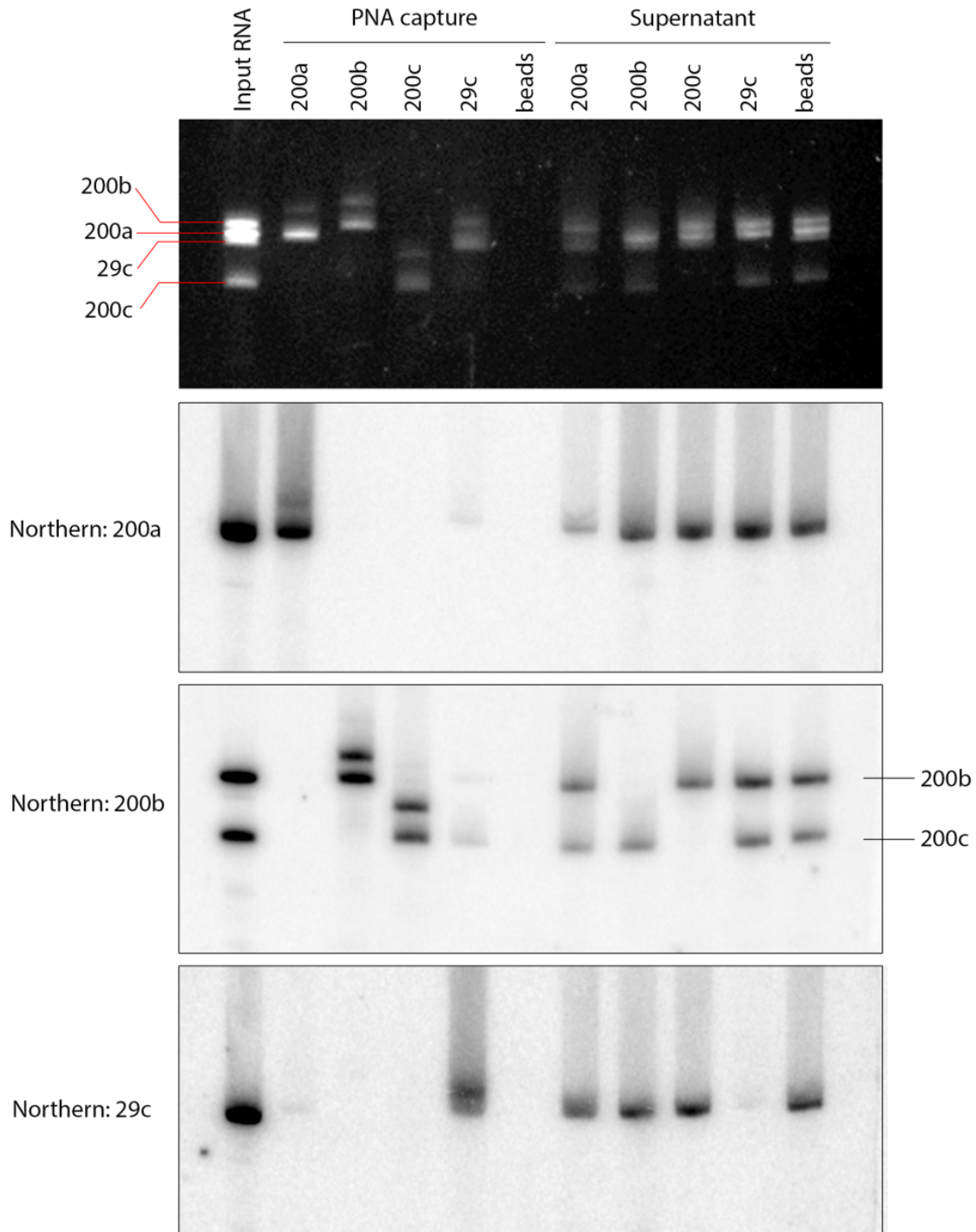


Fig. 29. Specific capture and detection of pre-miR-200 sequences with antisense PNAs
 The top panel is SYBR gold II staining of RNA. Northern analysis was performed to specifically detect captured probes and supernatant as labeled. MiR-200b and miR-200c were unable to be distinguished by the LNA probe due to the high concentration of present in each lane.

4.2.10. Identification of RRBP1 by CLaPP

To identify differential proteins bound to the miR-200 precursors we incubated MCF-12A.vec or MCF-12A.ζ cells in the presence of 100 μM 4-thiouridine for 24 hours followed by crosslinking RNAs to proteins by UVC (see methods). Cell lysates were incubated with antisense PNAs to specific miR-200 precursors, extensively washed, and proteins were eluted by RNase treatment (Fig. 30).

We found one protein band in MCF-12A.ζ samples that was only identified in miR-200a/b/c antisense PNAs but not miR-29c antisense PNA (Fig. 31). The band in question was identified by mass spectrometry to be Receptor of Ribosome Binding Protein 1 (RRBP1).

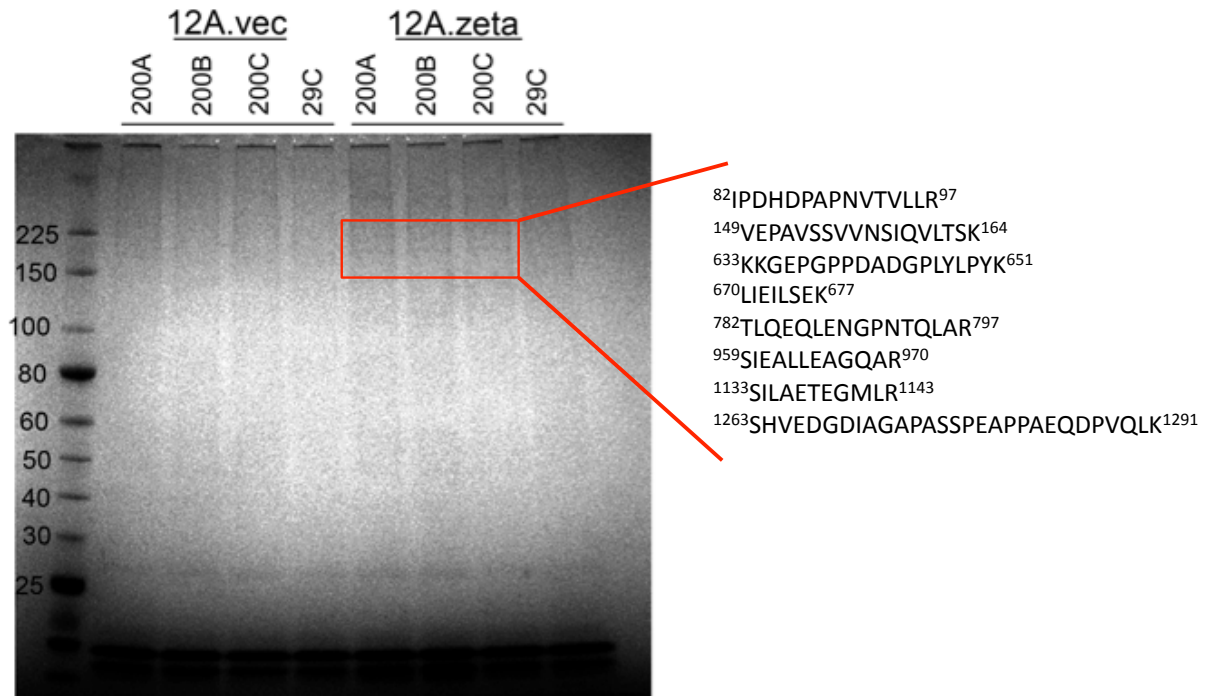


Fig. 31. Coomassie stain of gel after PNA capture

Lanes are marked with the specific antisense PNA used in the capture. Highlighted region indicates bands identified by mass spectrometry as RRBP1

RRBP1 was originally identified as ES/130 for the polyclonal antibody used to detect it (ES) and its molecular weight in chicken embryonic cardiocytes (130 kDa) (182). Interestingly, it was found to be necessary for transitioning the cells from epithelial to mesenchymal during heart development. Later studies established that RRBP1 expression is not limited to cardiac development but also necessary for development of the limb bud ectoderm, gut, and notochord suggesting widespread importance for embryogenesis (183). The first evidence of RRBP1 existing in human cells mapped its chromosomal location to 20p12 (184). The human homologue contains two distinct isoforms, a 180 kDa isoform which contains a decapeptide repeat of NQGKKAEGAQ repeated 54 times at its C-terminus and a 130 kDa isoform lacking the repeat region. The decapeptide repeat region was found to be responsible for binding to ribosomes in the endoplasmic reticulum (185, 186) and RRBP1 assembles polysomes in the ER via its coiled-coil domain (187). Overexpression of RRBP1 induces an elongated spindle shape in HeLa cells due to a microtubule binding region that functions to connect the endoplasmic reticulum to the microtubule network (151). Intestinal crypt stem cells were recently found to contain high levels of RRBP1 compared to the differentiated villus cells suggesting a role of RRBP1 in maintaining stemness in adult tissues (188). Staining of breast cancer patients' tissue samples revealed an extremely high number of samples (84%, 177/219) had overexpression of RRBP1 (189). Additionally, RRBP1 was found to be overexpressed in lung cancer patients where it serves to protect the cancer cells from apoptosis induced by the unfolded protein response (UPR). Induction of the UPR in mammary tissues was recently found to promote a stem-like population of CD44^{high}/CD24^{low} cells, which are known to have low levels of miR-200 (190, 191).

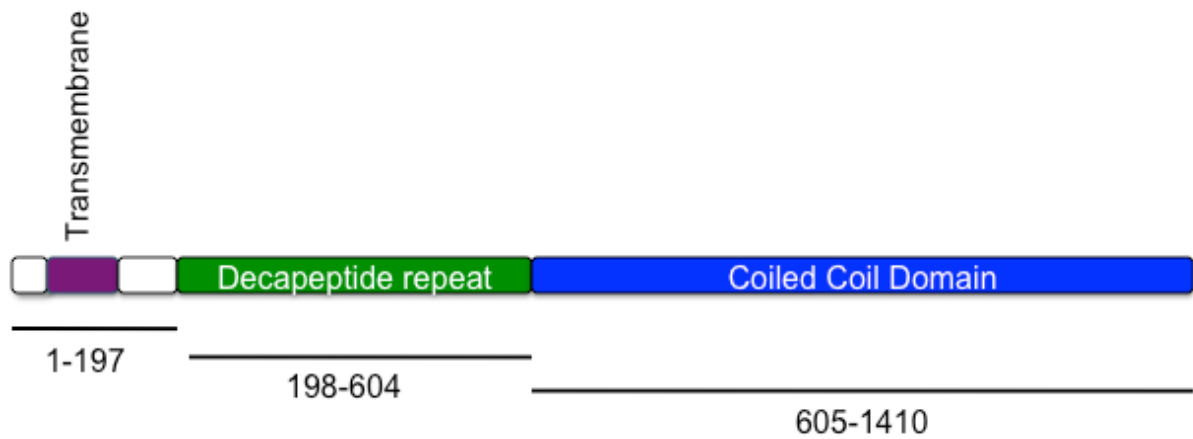


Fig. 32. Overview of RRBP1 domain structure.

RRBP1 consists of a transmembrane domain at the N-terminus (purple) a decapeptide repeat necessary for binding to ribosomes, and a coiled coil domain that interacts with microtubules. RRBP1 is expressed as two isoforms, a p180 isoform as drawn and a p130 isoform that lacks the decapeptide repeat region

4.2.11. Characterization of RRBP1 as a repressor of miR-200 biogenesis

In our CLaPP assay RRBP1 was associated only with pre-miR-200 family members and only in cells with low levels of mature miR-200 suggesting it may be necessary for repressing their biogenesis. We first evaluated RRBP1 expression in the breast cancer cell lines described in Fig. 15. There was a nearly perfect inverse correlation between RRBP1 expression and mature miR-200 expression in these cells (Fig. 33). This was excellent correlative data; however, to establish a causal role for RRBP1 in miR-200 repression we exogenously expressed either the p130 or p180 isoforms in MCF-10A cells. Expression levels were within physiological levels observed in basal-like breast cancer cells (Fig. 34A). Expression of both isoforms induced an EMT in the MCF-10A cells. Northern blot and qRT-PCR analysis of miR-200 levels revealed exogenous expression reduced mature levels to approximately 20% the levels of vector control cells (Fig. 34B,C). The most striking evidence that RRBP1 overexpression is the cause of miR-200 biogenesis defects was in analyzing the pri-miR-200 levels. Exogenously expressed RRBP1 isoforms induced an upregulation of pri-miR-200b and -200c while pri-miR-200a remained unchanged, exactly recapitulated the alterations in pri-miRNA observed with overexpression of 14-3-3 ζ (Fig. 34D). RRBP1 shRNA loss-of-function studies revealed a slight, but consistent increase in miR-200 expression in both the MCF-10A and MCF-12A cell lines (Fig. 35C,D).

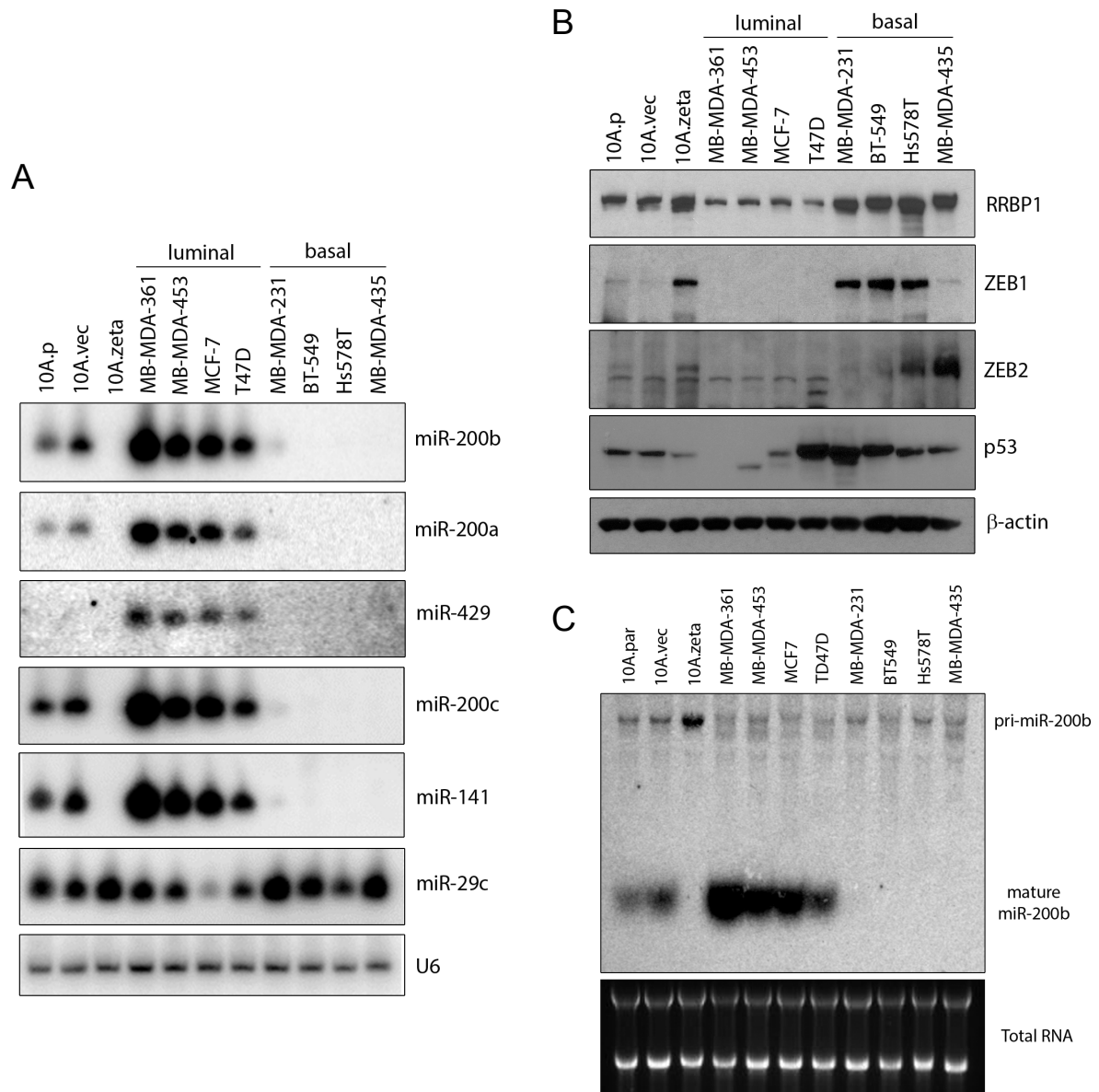


Fig. 33. RRBP1 expression in breast cancer cell line panel

RRBP1 expression was analyzed in the context of the breast cancer cell line panel as before (Fig 14). A strong inverse correlation exists between mature mir-200 family members and RRBP1.

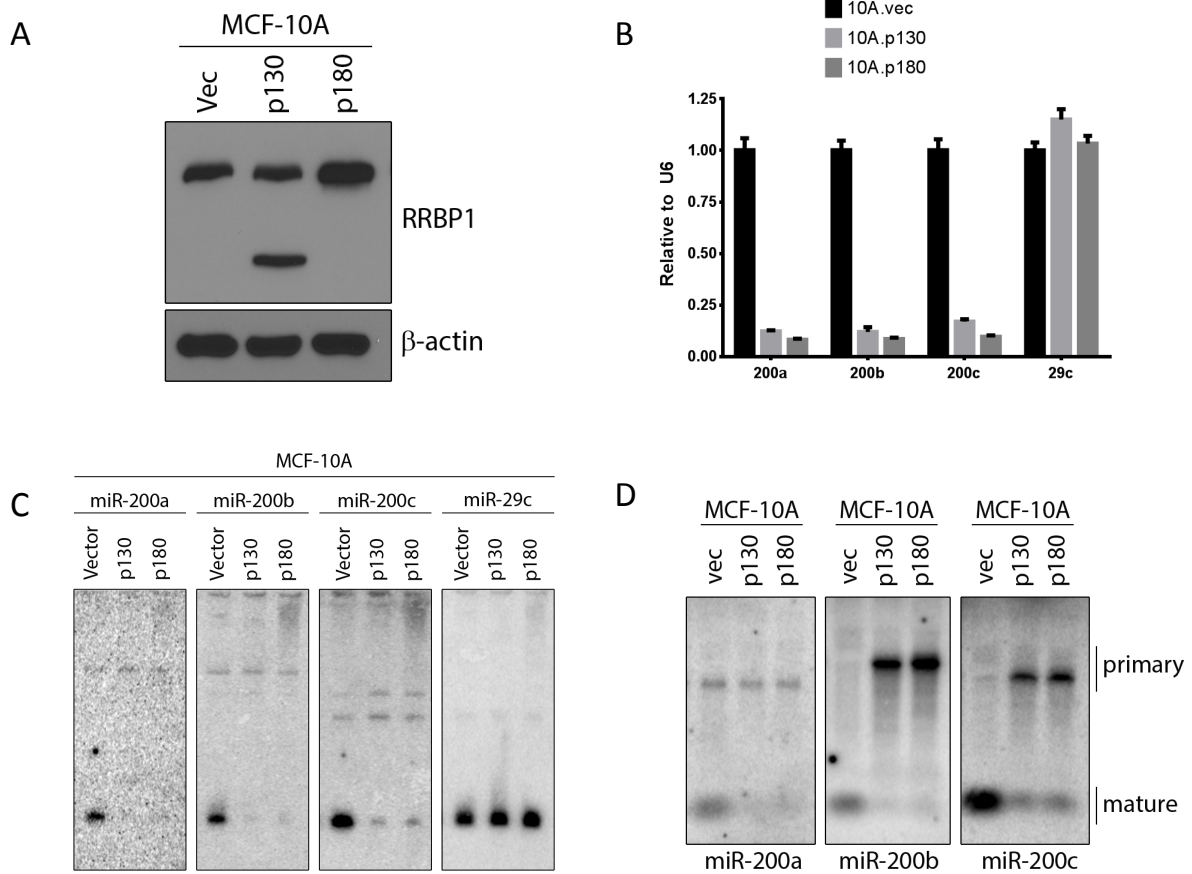


Fig. 34. Gain-of-function analysis of RRBBP1 on miR-200 expression

A) RRBBP1 was expressed as two different isoforms, p130 or p180. B) qRT-PCR analysis of miR-200 mature expression in RRBBP1 overexpressing cells. C) Northern analysis of miR-200 in RRBBP1 overexpressing cells. D) Pri-miR-200a, 200b, and 200c expression.

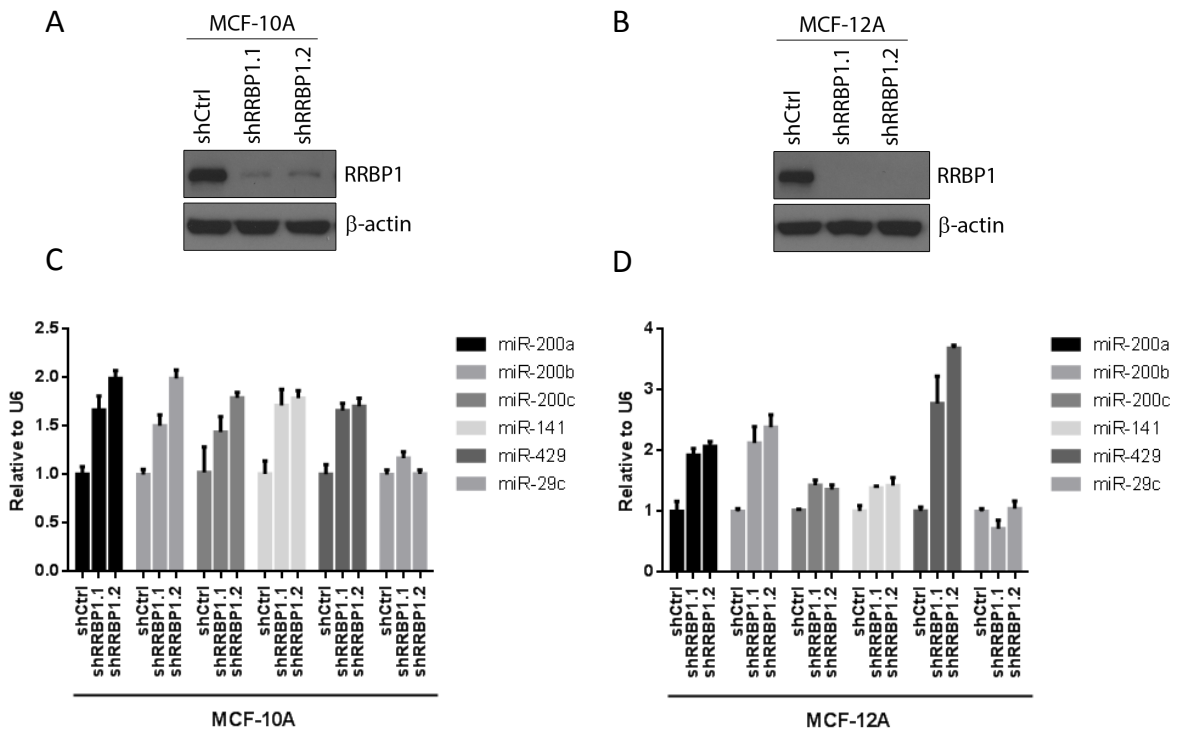


Fig. 35. Knockdown of RRBP1 increases miR-200 expression

A) Knockdown of RRBP1 using two different shRNA clones in MCF-10A cells. B) Knockdown efficiency in MCF-12A cells. C) qRT-PCR analysis of mature miR-200 in MCF-10A knockdown cells. D) qRT-PCR analysis of mature miR-200 in MCF-12A knockdown cells.

4.2.12. TGF- β induces expression of RRBP1

TGF- β is one of the best-characterized inducers of mir-200 loss (110). We asked whether TGF- β has any effect on RRBP1 expression. To test this, we treated MCF-10A cells with 5 ng/ml TGF- β and monitored RRBP1 expression by both western blot and qRT-PCR (Fig. 36A,B). Protein levels of RRBP1 significantly increased at 24 and 48 hours following treatment with TGF- β in addition to the appearance of the p130 isoform, which is undetectable in unstimulated cells. RRBP1 mRNA levels also increase ~4-fold suggesting transcriptional activation may be responsible for the activation (Fig. 36B). As expected, there was a decrease in the expression of miR-200b, which was inversely proportional to the level of RRBP1 (Fig. 36C).

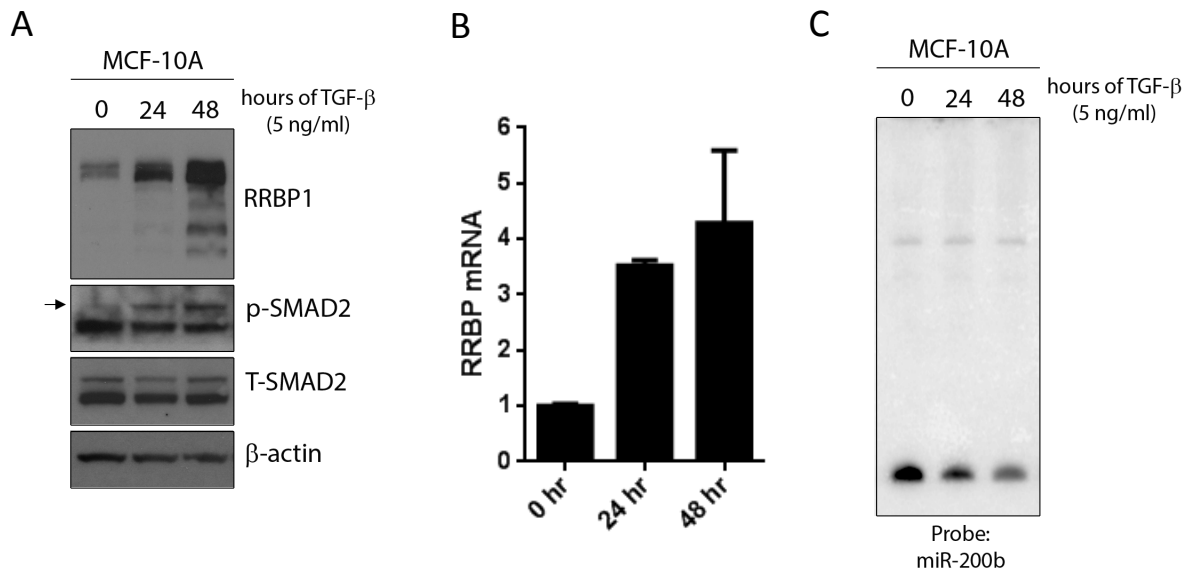


Fig. 36. TGF-beta treatment induces RRB1 expression

A) MCF-10A cells were treated with 5 ng/ml of TGF-beta for 24 or 48 hours and protein expression determined by western blot. B) mRNA expression of RRB1 following TGF-beta treatment C) Northern analysis confirming the loss of miR-200b with the increase in RRB1.

4.2.13. Characterizing RRBP1 binding to miR-200 by iCLIP

RRBP1 consistently displayed an inverse correlation with miR-200 in cell lines, exogenous expression, and knockdown cells. Additionally, we identified RRBP1 by capturing the precursor miR-200 family members via CLaPP assay under highly stringent conditions implicating its direct binding to the miR-200 precursors. To exhaustively link RRBP1 as a direct repressor of miR-200 biogenesis we sought to characterize its binding by conducting an individual nucleotide Crosslinking and Immunoprecipitation assay (iCLIP). We first optimized crosslinking conditions for p130 and p180 isoforms after incubating with 4-thiouridine and crosslinking with UV₃₆₅. FLAG-tagged DGCR8 was included as a control during optimization steps. Crosslinking of RRBP1 to RNA was apparent even by western blotting, which caused a shifted species to be detected (Fig. 37). We also observed that high levels of p180 get post-translationally cleaved into p130. To assess specificity of binding, samples were treated with a low dilution of RNase I (1:50), in which the crosslinked protein-RNA hybrids migrate at approximately 5 kDa above the non-crosslinked protein instead of forming a diffuse slow migrating band (192). We found the p130 isoform was the dominant isoform responsible for RNA-binding as most of the RNA from the p180-expressing cells migrated with that isoform (Fig. 38A). RRBP1 also appears to be a robust RNA-binding protein since RNA remained bound to RRBP1 in the presence of 1 molar NaCl while no RNA was detected in the uncrosslinked DGCR8 lane. This was overcome by treating immunoprecipitated RRBP1 with a 7M urea solution, diluting the eluate, and immunoprecipitating again. Optimal RNase concentrations were determined by a dilution series of RNase I on the crosslinked p130 isoform (Fig. 38B). A dilution of 1:250 of RNase I

was found to be optimal. Each isoform of RRBP1 was immunoprecipitated in triplicate as well as three negative controls of untransfected cells and uncrosslinked p130 and p180 (Fig. 39). Each replicate, including negative controls was individually barcoded to trace back sequences to individual replicates following next generation sequencing.

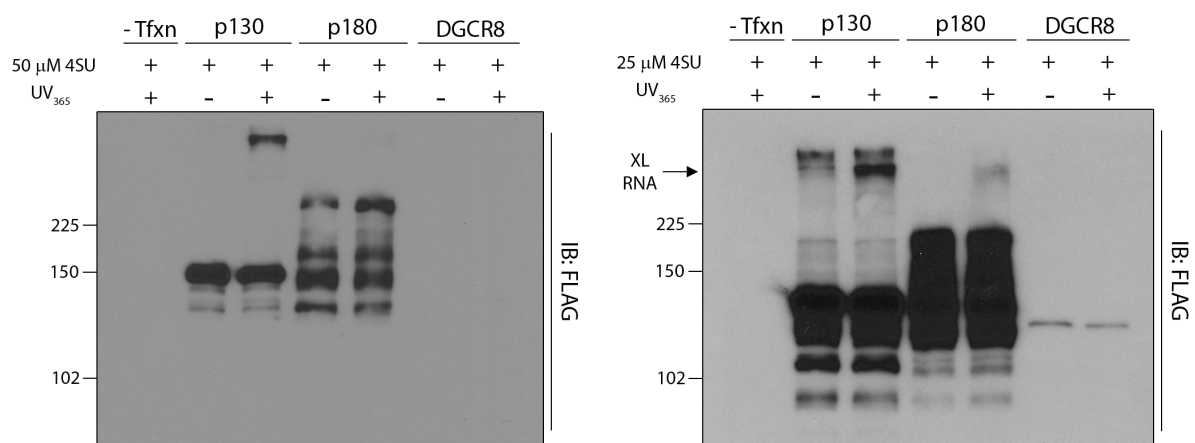


Fig. 37. Expression validation of RRBP1 clones for iCLIP

Western blot analysis of FLAG in cells without transfection (first lane), and with p130 and p180 expression plus or minus UV crosslinking (lanes 2-5) and DGCR8 serving as a positive control (last two lanes). The two images are the same membrane at different exposures.

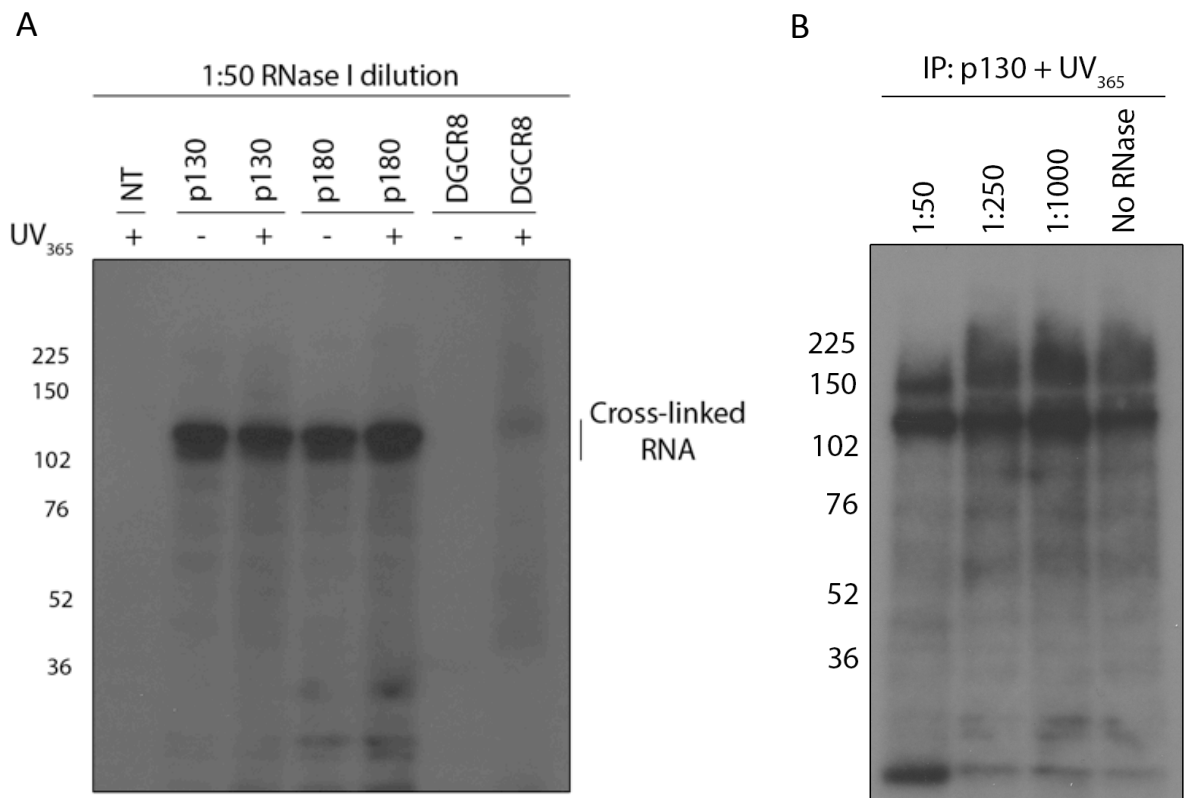


Fig. 38. Optimization of crosslinking conditions for RRBP1

A) FLAG-tagged RRBP1 or DGCR8 was immunoprecipitated following extensive RNase I digestion to determine specificity of the crosslink. B) Dilution series of RNase I on the p130 isoform to obtain optimal RNA fragmentation.

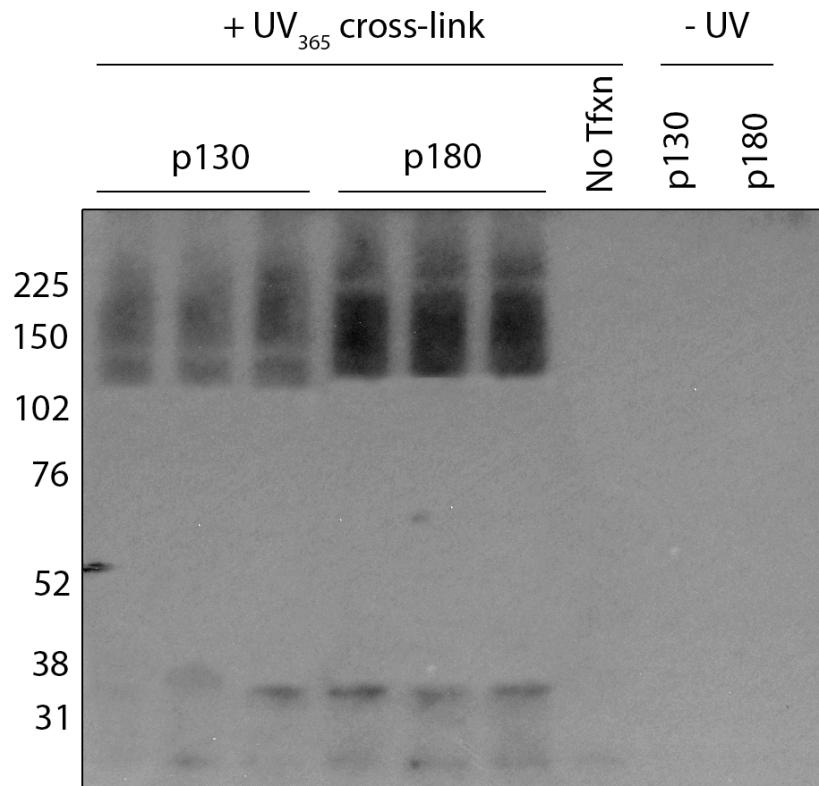


Fig 39. Triplicate iCLIP analysis of p130 and p180 isoforms

Using the optimized conditions determined in Fig 36, the p130 and p180 isoforms were immunoprecipitated in triplicate along with three negative control experiments.

Library preparation optimization was done with low, medium, and high eluates (see methods) to determine the optimal cycle numbers to amplify libraries without inducing non-specific amplification. There was no detectable signal in the non-transfected negative control library, as expected, while the p130 and p180 uncrosslinked samples had a minimal detectable signal (Fig. 40). This is likely due to residual RNA binding given the aforementioned robustness of RRBP1. Specific crosslinked immunoprecipitations of both p130 and p180 isoforms resulted in strong signals compared to negative controls. The optimal cycle numbers were used for preparative scale library amplification. The individual libraries were pooled, gel-purified, and precipitated for next-gen sequencing by Illumina HiSeq 2500 50-nt single read sequencing.

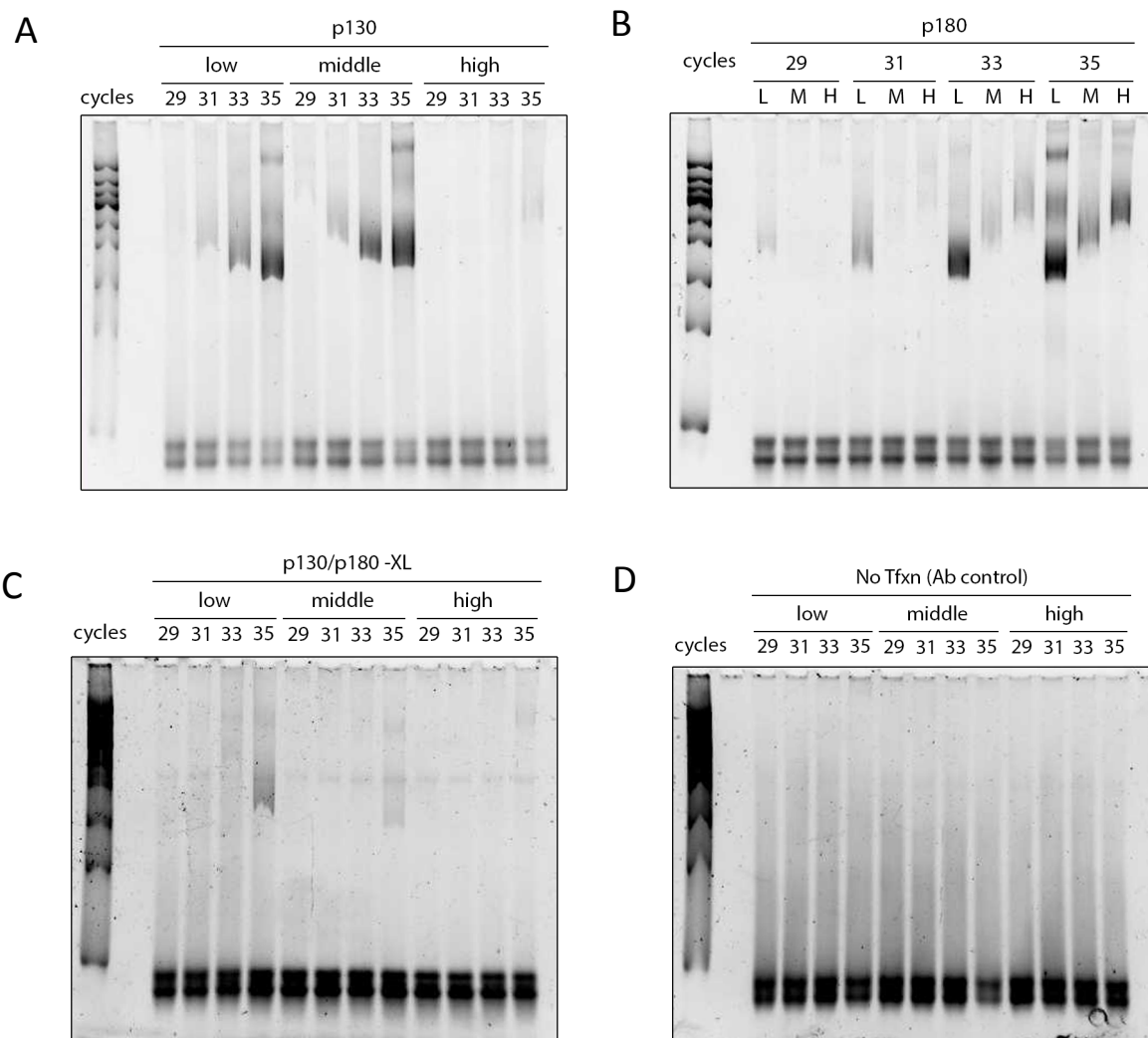


Fig. 40. Library amplification of RRBP1-bound RNA
 cDNAs were gel extracted in low, middle, and high sizes (see methods) and optimal amplification conditions for each was determined A) p130, B) p180, C) uncrosslinked pooled p130 and p180, D) No transfection of RRBP1

4.2.14. Detection of pre-miRNA sequences in iCLIP libraries by PCR

Before samples were pooled for next-gen sequencing, aliquots were analyzed by endpoint PCR to detect the presence or absence of precursor miRNA species. Primers specific for the precursors of miR-200a, miR-200b, and miR-29c were used and a plasmid containing miR-200a and -200b sequences (b/a/429+Ctrl) or a PCR amplicon of pri-miR-29c from genomic DNA were used for specificity (Fig. 41). The precursor for miR-200b was detected in high abundance in the p130-low library while it was detected in the p180-low/med/high libraries but in lower abundance than the p130-low library. No detection of pre-miR-200b was observed in the negative control libraries. Additionally, there was no signal detected for pre-miR-200a in any of the libraries while the positive control gave a clear signal. This may indicate that RRBP1 does not bind to the precursor of miR-200a or may simply be that the region in which it binds is outside of the primers used to detect pre-miR-200a. Ultimately, the next-gen sequencing results will determine exactly what sequences are bound by RRBP1. Similar to pre-miR-200a, we observed no signal in the libraries when pre-mir-29c was amplified. This result is expected since capture of pre-miR-29c by CLaPP assay did not return peptides to corresponding to RRBP1.

When the analysis of the iCLIP data and the CLaPP data are taken together, we can conclude that RRBP1 does directly bind to at least a portion of the miR-200 family members. Capture of pre-miR-200a by CLaPP did return RRBP1 peptides by mass spectrometry; however, it is possible that RRBP1 does not bind near the miR-200a stem-loop but rather binds to the pri-miR-200b/a/429 transcript and the anti-sense PNA captured the entire pri-miRNA thus returning peptide hits by mass spectrometry.

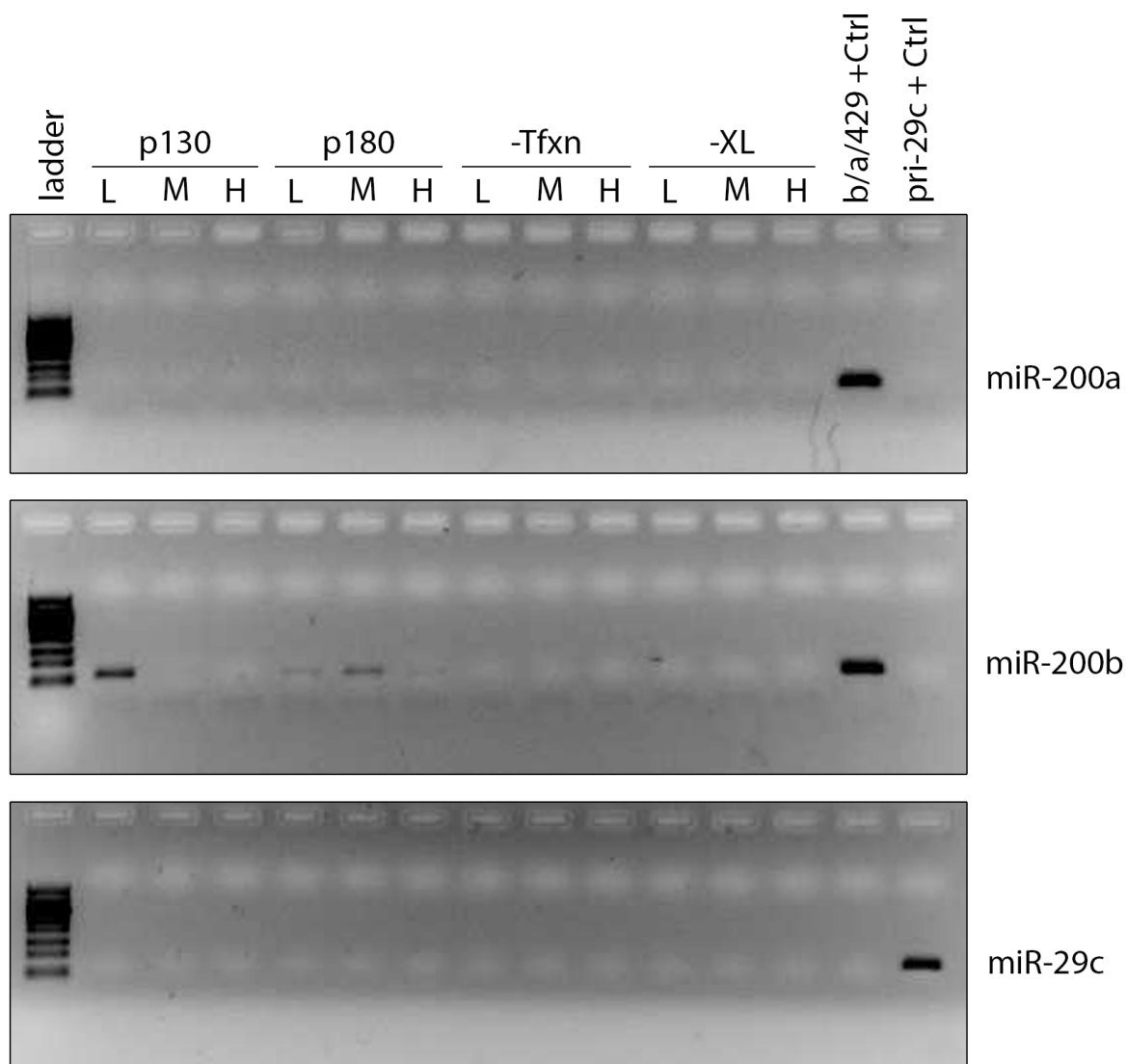


Fig. 41. Detection of pre-miR-200 family members from iCLIP library
 Amplified iCLIP libraries were subjected to endpoint PCR analysis using primers specific to the precursors of miR-200a (top), miR-200b (middle), or miR-29c (bottom). Plasmids and PCR products for miR-200b/a/429 and pri-miR-29c, respectively were used as positive controls.

4.3. Discussion

There are many molecular events that can independently lead to EMT in cells, yet all result in the loss of miR-200 (172, 193). The ZEB1/2-miR-200 double negative feedback loop has been extensively described in the literature (110, 111, 194–198) yet analysis of patient data from TCGA indicates the a stronger correlation between miR-200 repressing ZEB1/2 than the inverse. We validated this phenomenon in breast cancer cell lines and found it to support the TCGA data. Our analysis, as well as others, of ZEB1/2 inhibition on the miR-200b/a/429 promoter by dual luciferase assay does support the repressive role of ZEB1/2; however, we found blockage of downstream processing of the miR-200 family resulted in large pools of unprocessed primary miRNA. To reconcile these differences we propose that transcription of the miR-200 family may be greatly reduced in cells expressing high levels of ZEB1/2 but the inability of the cell to process existing pri-miR-200 pools, in addition to transcriptional ‘leakiness’ results in the observed counter-intuitive increased expression.

We uncovered a novel feedforward mechanism that exists between the different species of the miR-200 family. In principle it is very similar to the ceRNA hypothesis, which postulates that upregulates of a mRNA targeted by a particular miRNA will ‘sponge’ away that miRNA resulting in increased expression of other mRNAs targeted by the same miRNA (113). The difference in this instance is that one miRNA within the family can upregulate the other miRNAs in the family by titrating away a common repressor in RRBP1 (Fig. 42). In this way, cells are able to insure the expression of all miR-200 family members equally. We propose this miRNA-mediated miRNA upregulation may not be unique to the miR-200

cluster and may exist for other clusters containing miRNAs with highly similar sequences. Additionally, RRBP1 may not function solely as a repressor of the miR-200 family and may, in fact, exert broad influences on other miRNA species. RRBP1 may also recruit specific mRNAs to the ER to activate or inhibit their translation, which is a known function of RRBP1. If this is true, it would be interesting to see if the mRNAs and miRNAs bound by RRBP1 can be functionally classified into distinct classes such as a ‘pro-EMT’ or ‘pro-MET’ signature. These hypotheses are testable from the data retrieved from the iCLIP of RRBP1.

In this study we developed a novel technique for capturing endogenous protein-RNA interactions using peptide nucleic acids. Our technique, termed CLaPP, offer significant advantages to existing methods of identifying proteins bound to specific RNA species. First, our technique targets specific RNA species instead of relying on global analyses from poly-(A)⁺ selection. Second, the uncharged peptide backbone of the PNA facilitates strand invasion and displacement of highly structured RNAs under low salt condition. Others have avoided this problem by generating tiling arrays to different parts of the target mRNA to avoid failed detection in structured region (142, 143). However, this is often not possible in the case of miRNA given their short length. Third, while not employed in this study, PNAs can be easily modified to cross the cell membrane in a transfection-free system. It is possible that one could capture target RNAs before cellular lysis or even inject into an animal to capture the repertoire of RNA-binding proteins in tumor models or during different developmental stages.

In conclusion, we developed a highly sensitive assay to capture endogenous protein-RNA interactions to identify RRBP1 as a novel repressor of miRNA synthesis, which

allowed characterization for the first time of a miRNA-mediated post-transcriptional feedforward loop.

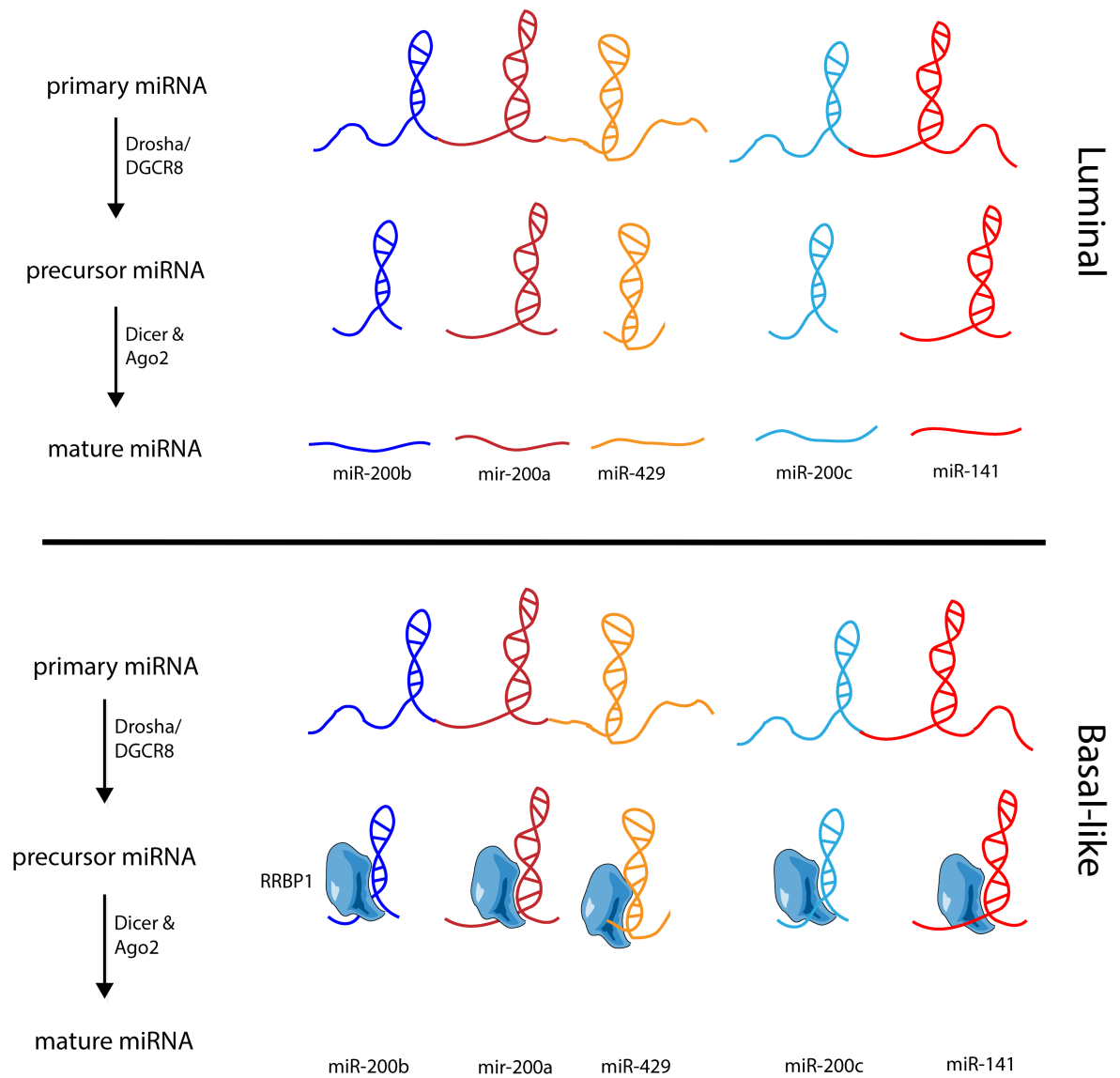


Fig. 42. Model of RRBP1 regulation of miR-200 in luminal and basal-like breast cancers. In luminal breast cancers RRBP1 expression remains low facilitating the biogenesis of the miR-200 family to maintain a more epithelial phenotype. RRBP1 expression in basal-like breast cancers is increased resulting in reduced conversion of pre-miRNA to mature miRNA and a more mesenchymal phenotype.

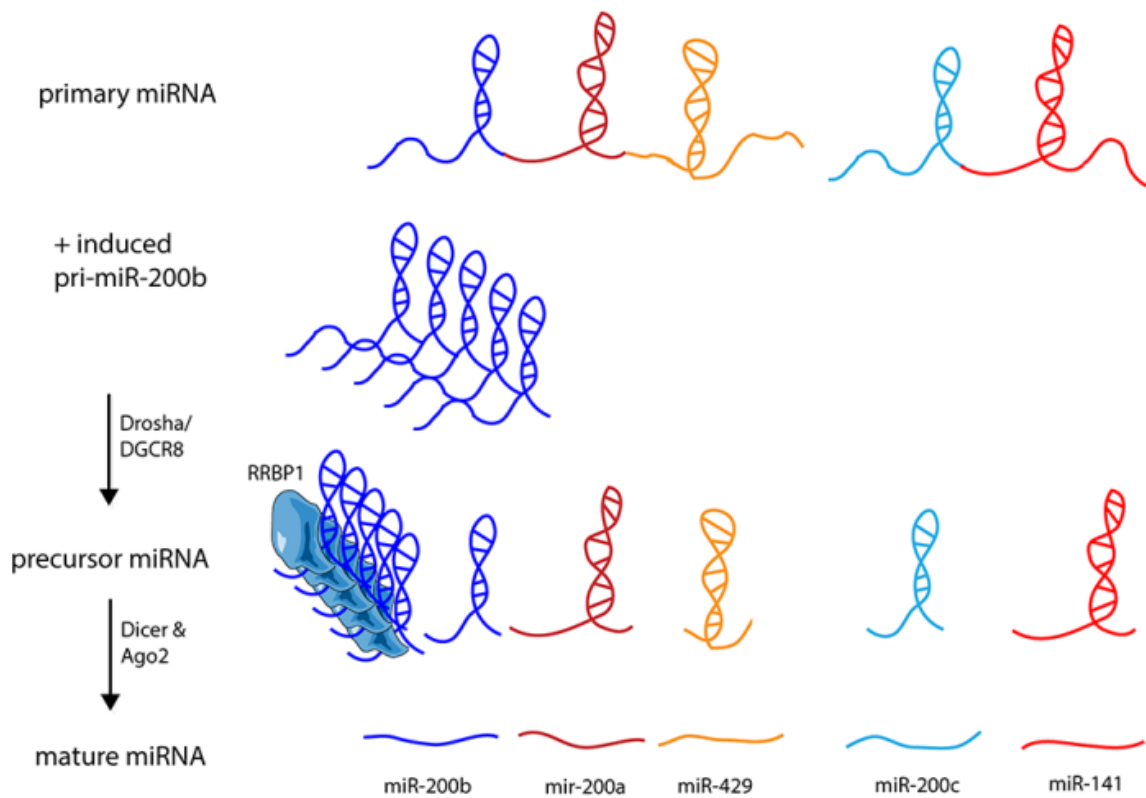


Fig. 43. Model of repressor titrating miRNA upregulation. Under conditions where RRBP1 expression is high, processing of the miR-200 family is repressed. However, upregulation of any one member or cluster results in saturation of the repressing ability of RRBP1 and allows the expression of the mature form of all miR-200 members to increase.

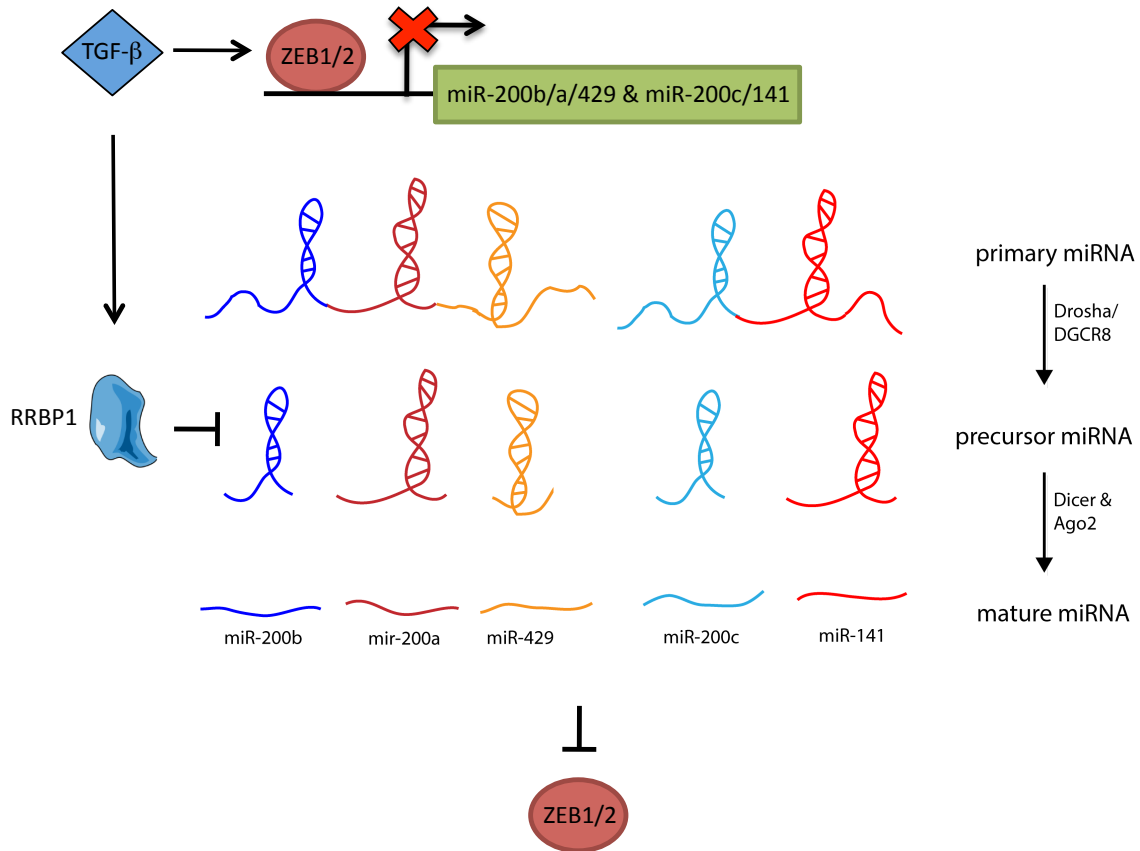


Fig. 44. TGF-beta-induced loss of miR-200 expression via multiple mechanisms.

Established models of TGF-beta treatment involve the upregulation of ZEB1/2 following TGF-beta treatment via transcriptional activation by SMAD2/3. ZEB1/2 transcriptionally repress the miR-200b/a/429 and miR-200c/141 clusters. Simultaneously, TGF-beta treatment induces the expression of RRBP1 at the mRNA and protein level, which binds to the miR-200 precursors to prevent their processing to mature miRNA. The reduced levels of mature miR-200 can no longer repress the mRNA of ZEB1/2 resulting in further transcriptional repression of the miR-200 clusters.

Chapter 5: Summary and Future Directions

5.1. Summary

The research presented herein identifies and characterizes two ribosome interacting proteins in nucleolin and RRP1 as key accessory proteins for microRNA biogenesis. Each forms unique feedback mechanisms via regulating miRNA. Nucleolin is a protein able to shuttle in and out of the nucleus. While in the nucleus it interacts with the microprocessor complex and directs the biogenesis of miR-15a/16-1 that downregulates the mRNA of bcl-2. When nucleolin shuttles to the cytoplasm upon induction of cellular stress, it stabilizes the mRNA of bcl-2 by binding the 3'UTR while simultaneously reducing the abundance of miR-15a/16-1, further increasing bcl-2 mRNA stability. When considered in the context of cancer, in which nucleolin is often found in the cytoplasm (158), cancer cells are able to inhibit apoptosis efficiently by compartmentalizing the various functions of nucleolin. While not analyzed in this study, previous reports of the binding sites for nucleolin and miR-15a/16-1 do not overlap indicating that nucleolin is not stabilizing bcl-2 by occupying miRNA binding sites.

Nucleolin has garnered attention from drug developers because it is often found on the surface of cancer cells, as a result of phosphorylation by Akt, and surface localization correlates with metastatic potential (199, 200). One unique function of nucleolin is an ability to tightly bind G-quadruplex DNA structures, which are formed by repetitive sequences of guanosines forming a planar surface (162, 201). A G-quadruplex forming oligonucleotide called AS1411 was specifically designed to bind surface expressed nucleolin causing its internalization (202). Indeed, targeting nucleolin in breast cancer using AS1411 was shown

to inhibit tumor proliferation *in vivo* (203). Since G-quadruplexes are extraordinarily stable and cheap to produce, drugs like AS1411 represent an alternative to small molecule therapies and may have reduced chances for drug resistance due to the wide net of genes targeted by altering miRNA biogenesis.

Through mining TCGA data, we observed a disconnect between what is known regarding the regulation of the miR-200 family and their expression patterns in patient data. After extensively validating the presence of primary and precursor miR-200 in cells failing to express the mature species we concluded a repressor complex must be present. Re-expressing the miRNA-200 clusters revealed they possess the ability to upregulate one another in a manner independent of known feedback transcriptional loops. This observation is similar in principle to a proposed model of sponging RNAs also called competing endogenous RNAs (113). This hypothesis states that two different RNAs targeted by the same miRNAs can coherently alter the expression of each other through up- or down-regulation of one of the RNA species. For example, upregulation of one species would be bound by a greater proportion of the miRNA pool resulting in depression of the second mRNA, thus as mRNA X increases so does mRNA Y and vice versa. The hypothesis proposed in this study is similar except that the miRNA is not the repressor; rather it is the repressed RNA species with a protein component as a repressor. We demonstrated that miR-200b can post-transcriptionally upregulate the expression of miR-200c through titrating away RRBP1 as a repressor. Similarly, miR-200a can post-transcriptionally upregulate miR-141 and miR-200b. This effect is specific for the miRNA repressed by RRBP1 and do not globally alter miRNA expression since miR-29c was unaltered during these experiments.

We speculate that sequence homology may play a part in the co-upregulation since miR-200b and miR-200c rapidly upregulated one another within one hour inducing either but miR-200a and miR-141 upregulation was not increased until several hours later. The same is true where induction of miR-200a rapidly upregulated miR-141 but miR-200b and miR-200c to a lesser extent. Interestingly, miR-200b and miR-200c show the greatest sequence similarity to one another amongst the miR-200 family and miR-200a and miR-141 are also highly similar to each other and less to the family. We found miR-429, having the more sequence divergence from any other miR-200 member, showed no detectable induction in any of the experiments. From a biological standpoint it is understandable why a cell would devise such a mechanism of regulation since the miR-200 family function in parallel with one another to regulate stemness. The miR-200 family often target the same mRNAs (*e.g.* ZEB1/2) but they can have individual effects on mRNAs regulating a particular process such as the regulation of miR-200c in the regulation of BMI1 (204). Since these miRNAs are expressed from two different genomic clusters the cell upregulation of one cluster but not the other could cause faulty instructions to the cells as to whether or not to differentiate. Therefore, maintaining a pool of pri-miRNA that can be post-transcriptionally upregulated in response to a single cluster being expressed would offer a buffer to this system. It is possible RRBPI functions as a repressor for other miRNA families in a similar mechanism and also that other undiscovered repressors function similarly for entirely different families of miRNAs.

The exact feedforward details were uncovered by utilizing an inducible system under highly stringent conditions to demonstrate for the first time miRNA species that regulate each other's expression post-transcriptionally. This observation led us to postulate the presence of

a yet undiscovered repressor complex, which we identified as the protein RRBP1. To identify RRBP1, we developed a unique assay to capture short, non-polyadenylated, highly structured RNAs we call CLaPP. The necessity of developing this assay stemmed from the need to overcome pitfalls of other similar approaches. Castello and coworkers pioneered this technology to identify the *in vivo* complexes of RNA binding proteins on the entirety of the poly-(A)+ transcriptome; however, this method fails to identify RBPs on individual RNAs. Methods such as ChIRP and RAP added a level of specificity by using biotinylated antisense RNA oligos in a tiling array to capture the endogenous RNA species. Yet these methods require long capture sequences (generally 150 nt) and fail to displace highly structured sequences, instead relying on redundancy in probes to capture the specific RNA. When identifying proteins bound to precursor miRNAs these methods are incompatible because the precursors are shorter than the minimum capture probe length required and are almost entirely structured leaving no accessible areas for capture probe hybridization. In using peptide nucleic acids we were able to overcome these shortcomings. The use of our technique is applicable to identify RBPs bound to any RNA but is particularly useful for short, highly structured RNAs. An additional benefit of the unique chemistry of PNAs comes with modifications to the PNAs allowing them to easily cross a cell membrane in the absence of a transfection reagent or delivery vehicle such as liposomes. Conjugating a cell penetrating peptide sequence to the PNA allows them to readily cross the cell membrane *in vitro* and *in vivo*. Future advances of the CLaPP technique described in this study could involve delivery of the PNA into live cells before crosslinking to allow hybridization to its target before cell lysis, thus reducing the degradation of the target mRNA following lysis but

before capture by the PNA. A more exciting prospect lies in identifying protein-RNA complexes directly animals. While the application of other methods to do this is technically feasible it becomes challenging when confronted with RNA degradation during extensive handling of tissues before RNA capture. For example, to identify the proteins bound to mRNAs in particular tumors a tumor would need to be surgically extracted, dissociated to form a monolayer for crosslinking, and finally lysis before capture probes can be added. Using PNAs with cell penetrating peptides, one could simply inject the PNAs into the tumor mass to allow hybridization *in vivo* and depending on tumor size, can be directly crosslinked in the animal before extraction. This technique could also be useful for identifying protein-RNA interactions during the course of development in normal tissues. For example, *in utero* injections of PNAs could identify key proteins interacting with RNAs during the development of the mouse embryo. PNAs, not having a standard sugar phosphate backbone, are stable in the bloodstream since they are resistant to nucleases as well as proteases. The only limitation to such a technique would be the necessity to rapidly recover the tissues since PNA-RNA interactions in a live cell can induce cleavage by the RNAi machinery so extended incubations would result in loss of the target rather than recovery.

We identified RRBP1 as inversely correlating to miR-200 expression by analyzing breast cancer cell lines as well as using genetic approaches for gain- and loss-of-function. Furthermore, we presented a complimentary mechanism by which TGF- β may regulate the miR-200 through upregulating RRBP1 expression. Finally, we confirmed RRBP1 binds to precursor miR-200 members by conducting an iCLIP analysis. Our proposed model of miR-200 regulation begins with RRBP1 upregulation by extracellular cues or ER stress

where it binds to the pre-miR-200 family members preventing their processing into the mature form. This results in an epithelial-to-mesenchymal transition, an important developmental function of RRBP1, and the maintenance of stem-like characteristics. This function is consistent with previous observations of RRBP1 function in both the induction of EMT in a chick embryo heart and elevated expression of RRBP1 in the stem cells residing in the colon (183, 205, 206). Recently, a spliced form of the RNA for XBP1, a readout of endoplasmic reticulum stress, was found to correlate to basal-like breast cancer cells whereas luminal cells possessed no signs of ER stress (190). Spliced XBP1 was found at increased levels in the stem cell population characterized as CD44^{high}/CD24^{low} suggesting a role in ER stress in maintaining a stem cell state. We found RRBP1 expression closely follows this pattern in breast cancer cell lines in that basal-like cells possessed high levels of RRBP1. RRBP1 is a known regulator of ER stress by binding to GRP78 (also known as BiP) (207). It will be interesting to uncover whether increased RRBP1 in breast stem cells is the cause or consequence of ER stress.

The endoplasmic reticulum plays a key role in protein secretion through its connection to the golgi apparatus that glycosylates proteins and ultimately releases them extracellularly through exocytosis. Cells with specialized function for secretion often have an extended endoplasmic reticulum network to facilitate this process. For example, B-cells, which secrete large quantities of antibodies, have ER networks that take up nearly the entire volume of the cytoplasm (208). Other such organs specialized for secretion include the pancreas and mammary glands. The massive quantities of proteins produced and secreted by these cells inevitably induces an ER stress response leading to the activation of XBP1.

RRBP1 is a critical factor in protein secretion and its function in this process is conserved down through yeast (209, 210). If indeed RRBP1 and XBP1 expression is connected as seen in breast cancer cell lines, it may suggest that RRBP1 may also be important in the formation of cancers in these cell types. Furthermore, exosomes, lipid enclosed secretions from cells, have been found in elevated levels in cancers. They may play a role in optimizing the 'soil' environment at the metastatic site in preparation for cancer cells to metastasize (211). While the exact mechanisms responsible for exosome secretion are poorly characterized currently, it is possible that RRBP1 plays a role in this process given its known role in exocytosis. Additionally, metastatic cells often undergo an EMT before entering the circulatory system suggesting RRBP1 may regulate both the secretion of exosomes to prepare the metastatic site and inducing an EMT in the cells that are to metastasize.

It has become relatively accepted in the field that miRNA evolved as a primitive immune defense against viruses (212). While plants and metazoans have similar biogenesis pathways, they share enough distinctions to suggest that miRNA evolved independently between plants and metazoans in an example of convergent evolution. This study, as well as many others, has characterized multiple proteins involved in miRNA biogenesis as regulators of rRNA biogenesis. We propose that in a necessity to defend themselves against viruses, early cells took advantage of the existing protein machinery for generating rRNA and redirected its purpose towards viral defense. The cells that were able to do this survived viral infections and became generally more fit to their environment. Over time cells repurposed RNAi against viruses and began finely tuning their own gene expression in what we currently recognize as miRNA. Cells with more precise control of critical cellular functions such as

differentiation, apoptosis, cell cycle regulation, and more, provided a selective advantage over cells only able to defend against exogenous RNA. We still have much to learn about miRNA biogenesis and future data may refute these claims; however, this seems a plausible explanation for the origin of miRNA biogenesis and the differences between animals and plants.

5.2. Future studies

In this study we identified a novel miRNA-media post-transcriptional feed forward loop between miRNA within closely related clusters. This represents the first time such a loop has been characterized yet many other miRNA clusters exist with closely related miRNA (*e.g.* the miR-34a/b/c cluster). This area is ripe for exploration.

The development of the CLaPP assay was instrumental in identifying RRBPI as a repressor of miRNA biogenesis. The principles outlined in this study lay the groundwork for other studies where capturing a target RNA may prove troublesome by other techniques (*i.e.* highly structured RNAs, small RNAs, distinguishing RNAs from closely related homologues, etc...). Furthermore, modification to the PNA allows them to easily cross the cell membrane, which opens the possibility to study protein-RNA interaction in animal models with a high degree of sensitivity and specificity.

The functional role of RRBPI has been understudied in the literature. We characterized it as a key regulator in miRNA biogenesis. It is possible that RRBPI functions to regulate other miRNAs in a similar fashion. Moreover, iCLIP sequencing data should reveal additional RNAs bound by RRBPI that may serve to reinforce the phenotypes associated with miR-200 expression to generate an RRBPI 'signature'. The fate of the

precursor miRNA bound by RRBP1 still remains unclear. It is possible they persist for long periods of time but it is equally likely that they get funneled into a degradation pathway to maintain constant levels similar to let-7 following uridylation.

Appendix

Table A1: Top differentially expressed miRNA between ZEB1/2 low and high breast cancers						
miRNA	logFC	AveExpr	t	P.Value	adj.P.Val	B
hsa-mir-21	0.447	17.718	5.799	1.71E-08	2.42E-07	8.762
hsa-mir-22	0.435	16.115	7.014	1.58E-11	4.46E-10	15.564
hsa-mir-10b	0.909	15.981	9.817	7.13E-20	5.33E-18	34.425
hsa-mir-148a	-0.512	15.453	-4.122	4.89E-05	0.0003758	1.127
hsa-mir-143	0.741	15.209	7.154	6.67E-12	2.12E-10	16.405
hsa-mir-183	-0.611	13.739	-4.818	2.32E-06	2.21E-05	4.029
hsa-mir-200c	-0.774	13.241	-7.944	4.13E-14	1.73E-12	21.384
hsa-mir-25	-0.322	12.977	-3.875	0.0001313	0.0009475	0.194
hsa-mir-92a-2	-0.601	12.728	-5.527	7.15E-08	9.46E-07	7.380
hsa-mir-199b	1.041	12.098	9.743	1.24E-19	8.64E-18	33.881
hsa-mir-93	-0.689	11.878	-6.908	3.03E-11	8.12E-10	14.929
hsa-mir-199a-2	1.074	11.749	10.370	1.09E-21	1.14E-19	38.547
hsa-mir-100	1.141	11.458	10.025	1.50E-20	1.31E-18	35.961
hsa-let-7c	1.189	11.055	9.525	6.25E-19	3.63E-17	32.288
hsa-mir-199a-1	1.102	10.988	10.830	3.07E-23	4.01E-21	42.063
hsa-mir-141	-0.952	10.597	-8.609	4.47E-16	2.12E-14	25.826
hsa-mir-1307	-0.706	10.280	-5.836	1.40E-08	2.07E-07	8.954
hsa-mir-145	0.618	10.249	5.243	3.02E-07	3.51E-06	5.989
hsa-mir-191	-0.553	9.840	-4.397	1.54E-05	0.0001295	2.225
hsa-mir-127	1.273	9.714	12.670	1.13E-29	5.89E-27	56.682

hsa-mir-200a	-0.534	9.658	-4.029	7.14E-05	0.00053	0.768
hsa-mir-125b-1	0.977	9.558	9.058	1.87E-17	9.77E-16	28.946
hsa-mir-99a	1.270	9.385	9.961	2.42E-20	1.95E-18	35.489
hsa-mir-379	1.521	9.246	13.418	2.22E-32	2.32E-29	62.832
hsa-mir-140	0.485	9.121	5.220	3.37E-07	3.88E-06	5.883
hsa-mir-150	1.103	9.091	4.896	1.61E-06	1.59E-05	4.377
hsa-mir-16-1	-0.470	9.067	-5.167	4.40E-07	4.69E-06	5.628
hsa-mir-106b	-0.577	9.033	-5.824	1.50E-08	2.17E-07	8.893
hsa-mir-200b	-0.643	9.008	-4.922	1.43E-06	1.44E-05	4.496
hsa-mir-17	-0.897	8.790	-7.068	1.14E-11	3.31E-10	15.883
hsa-mir-192	-0.633	8.713	-5.428	1.19E-07	1.53E-06	6.888
hsa-mir-9-1	-1.309	8.679	-5.214	3.49E-07	3.96E-06	5.851
hsa-mir-9-2	-1.327	8.667	-5.268	2.66E-07	3.20E-06	6.111
hsa-mir-134	1.161	8.572	11.122	3.10E-24	5.40E-22	44.324
hsa-mir-30b	-0.540	8.548	-4.331	2.04E-05	0.0001665	1.956
hsa-mir-210	-1.522	8.498	-6.302	1.07E-09	1.96E-08	11.458
hsa-mir-92a-1	-0.759	8.426	-6.115	3.06E-09	5.08E-08	10.434
hsa-mir-29b-2	-0.542	8.230	-4.645	5.12E-06	4.66E-05	3.272
hsa-mir-186	-0.441	8.093	-4.134	4.65E-05	0.00036	1.174
hsa-mir-152	0.630	7.980	7.192	5.28E-12	1.73E-10	16.634
hsa-mir-29b-1	-0.565	7.949	-4.697	4.04E-06	3.74E-05	3.498
hsa-mir-338	-0.543	7.800	-4.010	7.70E-05	0.0005675	0.697
hsa-mir-542	0.729	7.707	6.179	2.14E-09	3.66E-08	10.782
hsa-mir-148b	-0.493	7.515	-6.077	3.77E-09	6.17E-08	10.229

hsa-mir-423	-0.431	7.220	-5.209	3.56E-07	4.00E-06	5.831
hsa-mir-20a	-0.825	7.160	-6.620	1.69E-10	3.76E-09	13.253
hsa-mir-708	0.685	6.827	6.521	3.02E-10	6.38E-09	12.685
hsa-mir-15a	-0.308	6.807	-4.043	6.75E-05	0.0005079	0.822
hsa-mir-19b-2	-0.834	6.532	-6.121	2.96E-09	4.99E-08	10.467
hsa-mir-484	-0.566	6.490	-5.098	6.14E-07	6.37E-06	5.305
hsa-mir-429	-0.899	6.323	-5.260	2.77E-07	3.29E-06	6.071
hsa-mir-98	-0.376	5.810	-3.977	8.78E-05	0.0006421	0.573
hsa-mir-339	-0.563	5.697	-5.186	4.00E-07	4.36E-06	5.718
hsa-mir-328	-0.677	5.564	-4.913	1.49E-06	1.49E-05	4.454
hsa-mir-324	-0.814	5.455	-7.277	3.10E-12	1.08E-10	17.155
hsa-mir-744	-0.807	5.420	-6.693	1.10E-10	2.62E-09	13.670
hsa-mir-331	-0.488	5.303	-4.272	2.62E-05	0.0002057	1.719
hsa-mir-139	0.747	5.261	5.801	1.70E-08	2.42E-07	8.771
hsa-mir-505	-0.613	5.136	-4.369	1.73E-05	0.0001438	2.111
hsa-mir-136	0.803	5.124	6.467	4.12E-10	8.29E-09	12.383
hsa-mir-409	1.114	5.087	10.260	2.53E-21	2.40E-19	37.715
hsa-mir-337	1.374	5.068	9.680	1.99E-19	1.30E-17	33.416
hsa-mir-218-2	0.736	4.992	7.114	8.55E-12	2.63E-10	16.164
hsa-mir-214	1.134	4.971	9.354	2.19E-18	1.21E-16	31.054
hsa-mir-96	-1.021	4.803	-5.608	4.69E-08	6.29E-07	7.787
hsa-mir-769	-0.497	4.769	-5.940	8.00E-09	1.27E-07	9.500
hsa-mir-32	-0.502	4.679	-4.567	7.28E-06	6.51E-05	2.936
hsa-mir-382	1.259	4.487	11.855	8.82E-27	2.31E-24	50.105

hsa-mir-381	1.276	4.484	10.904	1.72E-23	2.57E-21	42.631
hsa-mir-130b	-0.631	4.433	-4.975	1.11E-06	1.14E-05	4.739
hsa-mir-181d	-0.556	4.246	-4.316	2.17E-05	0.0001731	1.898
hsa-mir-1247	1.398	4.228	6.519	3.05E-10	6.38E-09	12.675
hsa-mir-345	-0.846	4.214	-5.199	3.75E-07	4.13E-06	5.781
hsa-mir-654	1.274	4.153	9.671	2.12E-19	1.30E-17	33.353
hsa-mir-125b-2	1.112	4.073	8.381	2.17E-15	9.86E-14	24.275
hsa-mir-758	1.538	4.041	12.434	7.84E-29	2.73E-26	54.767
hsa-mir-450b	0.513	4.025	4.302	2.30E-05	0.0001823	1.841
hsa-mir-19a	-0.996	3.977	-6.459	4.34E-10	8.56E-09	12.333
hsa-mir-590	-0.873	3.932	-5.203	3.67E-07	4.08E-06	5.802
hsa-mir-1301	-0.796	3.777	-5.946	7.74E-09	1.25E-07	9.532
hsa-mir-33a	-1.191	3.729	-5.933	8.31E-09	1.30E-07	9.464
hsa-mir-1180	-0.862	3.562	-5.874	1.15E-08	1.71E-07	9.152
hsa-mir-493	1.170	3.511	7.008	1.64E-11	4.51E-10	15.528
hsa-mir-301a	-1.199	3.501	-5.740	2.34E-08	3.22E-07	8.459
hsa-mir-3074	-0.674	3.491	-4.369	1.73E-05	0.0001438	2.111
hsa-mir-370	1.297	3.188	11.695	3.21E-26	6.71E-24	48.832
hsa-mir-1306	-0.647	3.173	-4.675	4.48E-06	4.11E-05	3.400
hsa-mir-34c	0.744	3.152	4.754	3.12E-06	2.94E-05	3.748
hsa-mir-431	1.315	3.134	10.806	3.71E-23	4.31E-21	41.875
hsa-mir-454	-0.798	3.127	-5.768	2.02E-08	2.82E-07	8.601
hsa-mir-103-2	-0.554	3.111	-5.142	4.97E-07	5.25E-06	5.511
hsa-mir-671	-0.626	3.092	-6.362	7.58E-10	1.42E-08	11.789

hsa-mir-889	1.289	2.955	6.400	6.08E-10	1.16E-08	12.005
hsa-mir-362	-0.649	2.929	-4.937	1.33E-06	1.35E-05	4.563
hsa-mir-369	1.161	2.927	7.098	9.42E-12	2.82E-10	16.069
hsa-mir-539	0.958	2.915	4.032	7.05E-05	0.0005268	0.780
hsa-mir-16-2	-0.824	2.907	-5.169	4.33E-07	4.67E-06	5.641
hsa-mir-18a	-1.137	2.667	-5.495	8.45E-08	1.10E-06	7.218
hsa-mir-154	1.164	2.568	7.358	1.86E-12	6.71E-11	17.655
hsa-mir-184	2.249	2.507	4.362	1.78E-05	0.0001466	2.084
hsa-mir-19b-1	-0.772	2.388	-4.443	1.25E-05	0.0001084	2.418
hsa-mir-410	1.916	2.357	6.768	7.02E-11	1.79E-09	14.107
hsa-mir-495	1.406	2.258	7.403	1.40E-12	5.23E-11	17.933
hsa-mir-411	1.918	2.214	8.053	2.01E-14	8.75E-13	22.091
hsa-mir-432	1.631	2.205	8.677	2.77E-16	1.38E-14	26.296
hsa-mir-33b	-1.589	2.202	-5.098	6.15E-07	6.37E-06	5.304
hsa-mir-940	-1.094	1.912	-3.964	9.26E-05	0.0006727	0.523
hsa-mir-487b	1.810	1.808	7.448	1.05E-12	4.07E-11	18.213
hsa-mir-376c	1.118	1.665	4.590	6.55E-06	5.91E-05	3.037
hsa-mir-483	2.016	1.645	5.417	1.26E-07	1.57E-06	6.834
hsa-mir-485	1.706	1.641	6.577	2.18E-10	4.74E-09	13.005
hsa-mir-412	2.142	1.423	6.297	1.10E-09	1.98E-08	11.431
hsa-mir-323	1.436	1.214	4.697	4.05E-06	3.74E-05	3.498
hsa-mir-377	1.686	1.120	6.622	1.67E-10	3.76E-09	13.260
hsa-mir-299	1.836	1.117	6.728	8.91E-11	2.17E-09	13.876
hsa-mir-760	-1.465	1.046	-4.523	8.82E-06	7.69E-05	2.753

hsa-mir-1245	2.185	0.953	7.197	5.11E-12	1.72E-10	16.666
hsa-mir-496	2.109	0.466	6.426	5.25E-10	1.02E-08	12.148
hsa-mir-655	2.460	-0.010	5.906	9.65E-09	1.48E-07	9.318
hsa-mir-3926-1	2.011	-0.291	5.427	1.20E-07	1.53E-06	6.882
hsa-mir-487a	2.741	-0.663	6.285	1.18E-09	2.08E-08	11.363
hsa-mir-204	3.660	-0.687	6.511	3.20E-10	6.56E-09	12.629
hsa-mir-1277	-2.162	-0.983	-4.536	8.36E-06	7.35E-05	2.804
hsa-mir-543	3.333	-0.983	7.813	9.83E-14	3.95E-12	20.534
hsa-mir-376b	2.191	-1.035	4.545	8.02E-06	7.11E-05	2.843
hsa-mir-494	2.724	-1.040	5.344	1.82E-07	2.21E-06	6.478
hsa-mir-218-1	2.648	-1.798	4.879	1.74E-06	1.70E-05	4.305
hsa-mir-1295	2.785	-1.871	5.422	1.23E-07	1.55E-06	6.857
hsa-mir-433	3.051	-1.878	5.710	2.75E-08	3.73E-07	8.304
hsa-mir-1258	4.038	-2.458	6.778	6.61E-11	1.73E-09	14.166
hsa-mir-656	2.299	-2.856	4.070	6.04E-05	0.0004574	0.927
hsa-mir-380	3.444	-3.077	5.898	1.01E-08	1.53E-07	9.277
hsa-mir-3129	2.616	-3.682	4.322	2.12E-05	0.0001716	1.920
hsa-mir-1262	2.748	-3.745	4.404	1.49E-05	0.0001265	2.255
hsa-mir-202	3.583	-3.746	5.361	1.67E-07	2.05E-06	6.562
hsa-mir-541	4.149	-4.333	6.679	1.19E-10	2.78E-09	13.589
hsa-mir-665	3.923	-4.586	6.214	1.75E-09	3.05E-08	10.976
hsa-mir-376a-2	3.105	-4.669	4.817	2.33E-06	2.21E-05	4.027
hsa-mir-605	2.668	-4.781	4.107	5.20E-05	0.0003974	1.067
hsa-mir-329-2	3.343	-4.920	5.258	2.80E-07	3.29E-06	6.063

hsa-mir-329-1	3.122	-5.293	4.853	1.97E-06	1.91E-05	4.187
hsa-mir-1185-1	4.247	-5.900	6.745	8.04E-11	2.00E-09	13.976
hsa-mir-3926-2	2.902	-6.194	4.427	1.35E-05	0.0001156	2.349
hsa-mir-346	2.616	-8.355	4.218	3.29E-05	0.0002566	1.502
hsa-mir-1185-2	2.621	-8.501	4.318	2.15E-05	0.0001731	1.903

Bibliography

1. Kim, V. N., Han, J., and Siomi, M. C. (2009) Biogenesis of small RNAs in animals. *Nat. Rev. Mol. Cell Biol.* **10**, 126–139
2. Moss, E. G., Lee, R. C., and Ambros, V. (1997) The cold shock domain protein LIN-28 controls developmental timing in *C. elegans* and is regulated by the *lin-4* RNA. *Cell* **88**, 637–646
3. Lewis, B. P., Burge, C. B., and Bartel, D. P. (2005) Conserved seed pairing, often flanked by adenosines, indicates that thousands of human genes are microRNA targets. *Cell* **120**, 15–20
4. Lee, Y., Kim, M., Han, J., Yeom, K.-H., Lee, S., Baek, S. H., and Kim, V. N. (2004) MicroRNA genes are transcribed by RNA polymerase II. *EMBO J.* **23**, 4051–4060
5. Cai, X., Hagedorn, C. H., and Cullen, B. R. (2004) Human microRNAs are processed from capped, polyadenylated transcripts that can also function as mRNAs. *RNA N. Y. N* **10**, 1957–1966
6. Borchert, G. M., Lanier, W., and Davidson, B. L. (2006) RNA polymerase III transcribes human microRNAs. *Nat. Struct. Mol. Biol.* **13**, 1097–1101
7. Monteys, A. M., Spengler, R. M., Wan, J., Tecedor, L., Lennox, K. A., Xing, Y., and Davidson, B. L. (2010) Structure and activity of putative intronic miRNA promoters. *RNA* **16**, 495–505
8. Gregory, R. I., Yan, K., Amuthan, G., Chendrimada, T., Doratotaj, B., Cooch, N., and Shiekhattar, R. (2004) The Microprocessor complex mediates the genesis of microRNAs. *Nature* **432**, 235–240
9. Zeng, Y., Yi, R., and Cullen, B. R. (2005) Recognition and cleavage of primary microRNA precursors by the nuclear processing enzyme Drosha. *EMBO J.* **24**, 138–148
10. Han, J., Lee, Y., Yeom, K.-H., Nam, J.-W., Heo, I., Rhee, J.-K., Sohn, S. Y., Cho, Y., Zhang, B.-T., and Kim, V. N. (2006) Molecular basis for the recognition of primary microRNAs by the Drosha-DGCR8 complex. *Cell* **125**, 887–901

11. Zeng, Y., and Cullen, B. R. (2005) Efficient processing of primary microRNA hairpins by Drosha requires flanking nonstructured RNA sequences. *J. Biol. Chem.* **280**, 27595–27603
12. Lund, E., Güttinger, S., Calado, A., Dahlberg, J. E., and Kutay, U. (2004) Nuclear Export of MicroRNA Precursors. *Science* **303**, 95–98
13. Provost, P., Dishart, D., Doucet, J., Frendewey, D., Samuelsson, B., and Rådmark, O. (2002) Ribonuclease activity and RNA binding of recombinant human Dicer. *EMBO J.* **21**, 5864–5874
14. Meister, G., Landthaler, M., Patkaniowska, A., Dorsett, Y., Teng, G., and Tuschl, T. (2004) Human Argonaute2 Mediates RNA Cleavage Targeted by miRNAs and siRNAs. *Mol. Cell* **15**, 185–197
15. Grimson, A., Farh, K. K.-H., Johnston, W. K., Garrett-Engele, P., Lim, L. P., and Bartel, D. P. (2007) MicroRNA targeting specificity in mammals: determinants beyond seed pairing. *Mol. Cell* **27**, 91–105
16. Ozsolak, F., Poling, L. L., Wang, Z., Liu, H., Liu, X. S., Roeder, R. G., Zhang, X., Song, J. S., and Fisher, D. E. (2008) Chromatin structure analyses identify miRNA promoters. *Genes Dev.* **22**, 3172–3183
17. Han, J., Pedersen, J. S., Kwon, S. C., Belair, C. D., Kim, Y.-K., Yeom, K.-H., Yang, W.-Y., Haussler, D., Billech, R., and Kim, V. N. (2009) Posttranscriptional Crossregulation between Drosha and DGCR8. *Cell* **136**, 75–84
18. Wang, Z., Yao, H., Lin, S., Zhu, X., Shen, Z., Lu, G., Poon, W. S., Xie, D., Lin, M. C., and Kung, H. (2013) Transcriptional and epigenetic regulation of human microRNAs. *Cancer Lett.* **331**, 1–10
19. Lujambio, A., Ropero, S., Ballestar, E., Fraga, M. F., Cerrato, C., Setién, F., Casado, S., Suarez-Gauthier, A., Sanchez-Céspedes, M., Git, A., Gitt, A., Spiteri, I., Das, P. P., Caldas, C., Miska, E., and Esteller, M. (2007) Genetic unmasking of an epigenetically silenced microRNA in human cancer cells. *Cancer Res.* **67**, 1424–1429
20. Roman-Gomez, J., Agirre, X., Jiménez-Velasco, A., Arqueros, V., Vilas-Zornoza, A., Rodríguez-Otero, P., Martín-Subero, I., Garate, L., Cordeu, L., San José-Eneriz, E., Martín, V., Castillejo, J. A., Bandrés, E., Calasanz, M. J., Siebert, R., Heiniger, A., Torres,

- A., and Prosper, F. (2009) Epigenetic regulation of microRNAs in acute lymphoblastic leukemia. *J. Clin. Oncol. Off. J. Am. Soc. Clin. Oncol.* **27**, 1316–1322
21. Saito, Y., Liang, G., Egger, G., Friedman, J. M., Chuang, J. C., Coetzee, G. A., and Jones, P. A. (2006) Specific activation of microRNA-127 with downregulation of the proto-oncogene BCL6 by chromatin-modifying drugs in human cancer cells. *Cancer Cell* **9**, 435–443
 22. Wada, T., Kikuchi, J., and Furukawa, Y. (2012) Histone deacetylase 1 enhances microRNA processing via deacetylation of DGCR8. *EMBO Rep.* **13**, 142–149
 23. Morlando, M., Ballarino, M., Gromak, N., Pagano, F., Bozzoni, I., and Proudfoot, N. J. (2008) Primary microRNA transcripts are processed co-transcriptionally. *Nat. Struct. Mol. Biol.* **15**, 902–909
 24. Roth, B. M., Ishimaru, D., and Hennig, M. (2013) The core microprocessor component DiGeorge syndrome critical region 8 (DGCR8) is a nonspecific RNA-binding protein. *J. Biol. Chem.* **288**, 26785–26799
 25. Triboulet, R., Chang, H.-M., Lapierre, R. J., and Gregory, R. I. (2009) Post-transcriptional control of DGCR8 expression by the Microprocessor. *RNA N. Y. N* **15**, 1005–1011
 26. Gromak, N., Dienstbier, M., Macias, S., Plass, M., Eyraas, E., Cáceres, J. F., and Proudfoot, N. J. (2013) Drosha regulates gene expression independently of RNA cleavage function. *Cell Rep.* **5**, 1499–1510
 27. Macias, S., Plass, M., Stajuda, A., Michlewski, G., Eyraas, E., and Cáceres, J. F. (2012) DGCR8 HITS-CLIP reveals novel functions for the Microprocessor. *Nat. Struct. Mol. Biol.* **19**, 760–766
 28. Maurin, T., Cazalla, D., Yang, S., Jr, Bortolamiol-Becet, D., and Lai, E. C. (2012) RNase III-independent microRNA biogenesis in mammalian cells. *RNA N. Y. N* **18**, 2166–2173
 29. Tang, X., Zhang, Y., Tucker, L., and Ramratnam, B. (2010) Phosphorylation of the RNase III enzyme Drosha at Serine300 or Serine302 is required for its nuclear localization. *Nucleic Acids Res.* **38**, 6610–6619

30. Herbert, K. M., Pimienta, G., DeGregorio, S. J., Alexandrov, A., and Steitz, J. A. (2013) Phosphorylation of DGCR8 Increases Its Intracellular Stability and Induces a Progrowth miRNA Profile. *Cell Rep.* **5**, 1070–1081
31. Gwizdek, C., Ossareh-Nazari, B., Brownawell, A. M., Doglio, A., Bertrand, E., Macara, I. G., and Dargemont, C. (2003) Exportin-5 mediates nuclear export of minihelix-containing RNAs. *J. Biol. Chem.* **278**, 5505–5508
32. Basyuk, E., Suavet, F., Doglio, A., Bordonné, R., and Bertrand, E. (2003) Human let-7 stem-loop precursors harbor features of RNase III cleavage products. *Nucleic Acids Res.* **31**, 6593–6597
33. Melo, S. A., Moutinho, C., Roperio, S., Calin, G. A., Rossi, S., Spizzo, R., Fernandez, A. F., Davalos, V., Villanueva, A., Montoya, G., Yamamoto, H., Schwartz Jr, S., and Esteller, M. (2010) A Genetic Defect in Exportin-5 Traps Precursor MicroRNAs in the Nucleus of Cancer Cells. *Cancer Cell* **18**, 303–315
34. Drinnenberg, I. A., Weinberg, D. E., Xie, K. T., Mower, J. P., Wolfe, K. H., Fink, G. R., and Bartel, D. P. (2009) RNAi in budding yeast. *Science* **326**, 544–550
35. Ma, J.-B., Ye, K., and Patel, D. J. (2004) Structural basis for overhang-specific small interfering RNA recognition by the PAZ domain. *Nature* **429**, 318–322
36. Macrae, I. J., Zhou, K., Li, F., Repic, A., Brooks, A. N., Cande, W. Z., Adams, P. D., and Doudna, J. A. (2006) Structural basis for double-stranded RNA processing by Dicer. *Science* **311**, 195–198
37. Bernstein, E., Kim, S. Y., Carmell, M. A., Murchison, E. P., Alcorn, H., Li, M. Z., Mills, A. A., Elledge, S. J., Anderson, K. V., and Hannon, G. J. (2003) Dicer is essential for mouse development. *Nat. Genet.* **35**, 215–217
38. Merritt, W. M., Lin, Y. G., Han, L. Y., Kamat, A. A., Spannuth, W. A., Schmandt, R., Urbauer, D., Pennacchio, L. A., Cheng, J.-F., Nick, A. M., Deavers, M. T., Mourad-Zeidan, A., Wang, H., Mueller, P., Lenburg, M. E., Gray, J. W., Mok, S., Birrer, M. J., Lopez-Berestein, G., Coleman, R. L., Bar-Eli, M., and Sood, A. K. (2008) Dicer, Drosha, and outcomes in patients with ovarian cancer. *N. Engl. J. Med.* **359**, 2641–2650

39. Yan, M., Huang, H.-Y., Wang, T., Wan, Y., Cui, S.-D., Liu, Z.-Z., and Fan, Q.-X. (2012) Dysregulated expression of dicer and drosha in breast cancer. *Pathol. Oncol. Res. POR* **18**, 343–348
40. Zhang, B., Chen, H., Zhang, L., Dakhova, O., Zhang, Y., Lewis, M. T., Creighton, C. J., Ittmann, M. M., and Xin, L. (2013) A dosage-dependent pleiotropic role of Dicer in prostate cancer growth and metastasis. *Oncogene*
41. Su, X., Chakravarti, D., Cho, M. S., Liu, L., Gi, Y. J., Lin, Y.-L., Leung, M. L., El-Naggar, A., Creighton, C. J., Suraokar, M. B., Wistuba, I., and Flores, E. R. (2010) TAp63 suppresses metastasis through coordinate regulation of Dicer and miRNAs. *Nature* **467**, 986–990
42. Lee, H. Y., Zhou, K., Smith, A. M., Noland, C. L., and Doudna, J. A. (2013) Differential roles of human Dicer-binding proteins TRBP and PACT in small RNA processing. *Nucleic Acids Res.* **41**, 6568–6576
43. Koscianska, E., Starega-Roslan, J., and Krzyzosiak, W. J. (2011) The role of Dicer protein partners in the processing of microRNA precursors. *PLoS One* **6**, e28548
44. Paroo, Z., Ye, X., Chen, S., and Liu, Q. (2009) Phosphorylation of the human microRNA-generating complex mediates MAPK/Erk signaling. *Cell* **139**, 112–122
45. Chendrimada, T. P., Gregory, R. I., Kumaraswamy, E., Norman, J., Cooch, N., Nishikura, K., and Shiekhattar, R. (2005) TRBP recruits the Dicer complex to Ago2 for microRNA processing and gene silencing. *Nature* **436**, 740–744
46. Tomari, Y., Matranga, C., Haley, B., Martinez, N., and Zamore, P. D. (2004) A protein sensor for siRNA asymmetry. *Science* **306**, 1377–1380
47. Preall, J. B., and Sontheimer, E. J. (2005) RNAi: RISC gets loaded. *Cell* **123**, 543–545
48. Schwarz, D. S., Hutvagner, G., Du, T., Xu, Z., Aronin, N., and Zamore, P. D. (2003) Asymmetry in the assembly of the RNAi enzyme complex. *Cell* **115**, 199–208
49. Khvorovova, A., Reynolds, A., and Jayasena, S. D. (2003) Functional siRNAs and miRNAs exhibit strand bias. *Cell* **115**, 209–216

50. Chen, C.-Y. A., Zheng, D., Xia, Z., and Shyu, A.-B. (2009) Ago-TNRC6 triggers microRNA-mediated decay by promoting two deadenylation steps. *Nat. Struct. Mol. Biol.* **16**, 1160–1166
51. Huntzinger, E., Kuzuoglu-Öztürk, D., Braun, J. E., Eulalio, A., Wohlbold, L., and Izaurralde, E. (2013) The interactions of GW182 proteins with PABP and deadenylases are required for both translational repression and degradation of miRNA targets. *Nucleic Acids Res.* **41**, 978–994
52. Zeng, Y., Sankala, H., Zhang, X., and Graves, P. R. (2008) Phosphorylation of Argonaute 2 at serine-387 facilitates its localization to processing bodies. *Biochem. J.* **413**, 429–436
53. Rüdell, S., Wang, Y., Lenobel, R., Körner, R., Hsiao, H.-H., Urlaub, H., Patel, D., and Meister, G. (2011) Phosphorylation of human Argonaute proteins affects small RNA binding. *Nucleic Acids Res.* **39**, 2330–2343
54. Horman, S. R., Janas, M. M., Litterst, C., Wang, B., MacRae, I. J., Sever, M. J., Morrissey, D. V., Graves, P., Luo, B., Umeshima, S., Qi, H. H., Miraglia, L. J., Novina, C. D., and Orth, A. P. (2013) Akt-mediated phosphorylation of argonaute 2 downregulates cleavage and upregulates translational repression of MicroRNA targets. *Mol. Cell* **50**, 356–367
55. Shen, J., Xia, W., Khotskaya, Y. B., Huo, L., Nakanishi, K., Lim, S.-O., Du, Y., Wang, Y., Chang, W.-C., Chen, C.-H., Hsu, J. L., Wu, Y., Lam, Y. C., James, B. P., Liu, X., Liu, C.-G., Patel, D. J., and Hung, M.-C. (2013) EGFR modulates microRNA maturation in response to hypoxia through phosphorylation of AGO2. *Nature* **497**, 383–387
56. Rybak, A., Fuchs, H., Hadian, K., Smirnova, L., Wulczyn, E. A., Michel, G., Nitsch, R., Krappmann, D., and Wulczyn, F. G. (2009) The let-7 target gene mouse lin-41 is a stem cell specific E3 ubiquitin ligase for the miRNA pathway protein Ago2. *Nat. Cell Biol.* **11**, 1411–1420
57. Gibbins, D., Mostowy, S., Jay, F., Schwab, Y., Cossart, P., and Voinnet, O. (2012) Selective autophagy degrades DICER and AGO2 and regulates miRNA activity. *Nat. Cell Biol.* **14**, 1314–1321
58. Leung, A. K. L., Vyas, S., Rood, J. E., Bhutkar, A., Sharp, P. A., and Chang, P. (2011) Poly (ADP-Ribose) Regulates Stress Responses and MicroRNA Activity in the Cytoplasm. *Mol. Cell* **42**, 489–499

59. Qi, H. H., Ongusaha, P. P., Myllyharju, J., Cheng, D., Pakkanen, O., Shi, Y., Lee, S. W., Peng, J., and Shi, Y. (2008) Prolyl 4-hydroxylation regulates Argonaute 2 stability. *Nature* **455**, 421–424
60. Gruber, J. J., Zatechka, D. S., Sabin, L. R., Yong, J., Lum, J. J., Kong, M., Zong, W.-X., Zhang, Z., Lau, C.-K., Rawlings, J., Cherry, S., Ihle, J. N., Dreyfuss, G., and Thompson, C. B. (2009) Ars2 links the nuclear cap-binding complex to RNA interference and cell proliferation. *Cell* **138**, 328–339
61. Sabin, L. R., Zhou, R., Gruber, J. J., Lukinova, N., Bambina, S., Berman, A., Lau, C.-K., Thompson, C. B., and Cherry, S. (2009) Ars2 regulates both miRNA- and siRNA-dependent silencing and suppresses RNA virus infection in *Drosophila*. *Cell* **138**, 340–351
62. Viswanathan, S. R., Daley, G. Q., and Gregory, R. I. (2008) Selective blockade of microRNA processing by Lin28. *Science* **320**, 97–100
63. Hagan, J. P., Piskounova, E., and Gregory, R. I. (2009) Lin28 recruits the TUTase Zcchc11 to inhibit let-7 maturation in mouse embryonic stem cells. *Nat. Struct. Mol. Biol.* **16**, 1021–1025
64. Thornton, J. E., Chang, H.-M., Piskounova, E., and Gregory, R. I. (2012) Lin28-mediated control of let-7 microRNA expression by alternative TUTases Zcchc11 (TUT4) and Zcchc6 (TUT7). *RNA N. Y. N* **18**, 1875–1885
65. Heo, I., Joo, C., Kim, Y.-K., Ha, M., Yoon, M.-J., Cho, J., Yeom, K.-H., Han, J., and Kim, V. N. (2009) TUT4 in concert with Lin28 suppresses microRNA biogenesis through pre-microRNA uridylation. *Cell* **138**, 696–708
66. Lehrbach, N. J., Armisen, J., Lightfoot, H. L., Murfitt, K. J., Bugaut, A., Balasubramanian, S., and Miska, E. A. (2009) LIN-28 and the poly(U) polymerase PUP-2 regulate let-7 microRNA processing in *Caenorhabditis elegans*. *Nat. Struct. Mol. Biol.* **16**, 1016–1020
67. Ustianenko, D., Hrossova, D., Potesil, D., Chalupnikova, K., Hrazdilova, K., Pachernik, J., Cetkowska, K., Uldrijan, S., Zdrahal, Z., and Vanacova, S. (2013) Mammalian DIS3L2 exoribonuclease targets the uridylated precursors of let-7 miRNAs. *RNA N. Y. N* **19**, 1632–1638

68. Fukuda, T., Yamagata, K., Fujiyama, S., Matsumoto, T., Koshida, I., Yoshimura, K., Mihara, M., Naitou, M., Endoh, H., Nakamura, T., Akimoto, C., Yamamoto, Y., Katagiri, T., Foulds, C., Takezawa, S., Kitagawa, H., Takeyama, K., O'Malley, B. W., and Kato, S. (2007) DEAD-box RNA helicase subunits of the Drosha complex are required for processing of rRNA and a subset of microRNAs. *Nat. Cell Biol.* **9**, 604–611
69. Davis, B. N., Hilyard, A. C., Lagna, G., and Hata, A. (2008) SMAD proteins control DROSHA-mediated microRNA maturation. *Nature* **454**, 56–61
70. Suzuki, H. I., Yamagata, K., Sugimoto, K., Iwamoto, T., Kato, S., and Miyazono, K. (2009) Modulation of microRNA processing by p53. *Nature* **460**, 529–533
71. Yu, B., Bi, L., Zheng, B., Ji, L., Chevalier, D., Agarwal, M., Ramachandran, V., Li, W., Lagrange, T., Walker, J. C., and Chen, X. (2008) The FHA domain proteins DAWDLE in Arabidopsis and SNIP1 in humans act in small RNA biogenesis. *Proc. Natl. Acad. Sci. U. S. A.* **105**, 10073–10078
72. Michlewski, G., Guil, S., Semple, C. A., and Cáceres, J. F. (2008) Posttranscriptional regulation of miRNAs harboring conserved terminal loops. *Mol. Cell* **32**, 383–393
73. Nicastro, G., García-Mayoral, M. F., Hollingworth, D., Kelly, G., Martin, S. R., Briata, P., Gherzi, R., and Ramos, A. (2012) Noncanonical G recognition mediates KSRP regulation of let-7 biogenesis. *Nat. Struct. Mol. Biol.* **19**, 1282–1286
74. Michlewski, G., and Cáceres, J. F. (2010) Antagonistic role of hnRNP A1 and KSRP in the regulation of let-7a biogenesis. *Nat. Struct. Mol. Biol.* **17**, 1011–1018
75. Trabucchi, M., Briata, P., Garcia-Mayoral, M., Haase, A. D., Filipowicz, W., Ramos, A., Gherzi, R., and Rosenfeld, M. G. (2009) The RNA-binding protein KSRP promotes the biogenesis of a subset of microRNAs. *Nature* **459**, 1010–1014
76. Zhang, X., Wan, G., Berger, F. G., He, X., and Lu, X. (2011) The ATM kinase induces microRNA biogenesis in the DNA damage response. *Mol. Cell* **41**, 371–383
77. Ruggiero, T., Trabucchi, M., De Santa, F., Zupo, S., Harfe, B. D., McManus, M. T., Rosenfeld, M. G., Briata, P., and Gherzi, R. (2009) LPS induces KH-type splicing regulatory protein-dependent processing of microRNA-155 precursors in macrophages. *FASEB J. Off. Publ. Fed. Am. Soc. Exp. Biol.* **23**, 2898–2908

78. Yamagata, K., Fujiyama, S., Ito, S., Ueda, T., Murata, T., Naitou, M., Takeyama, K.-I., Minami, Y., O'Malley, B. W., and Kato, S. (2009) Maturation of microRNA is hormonally regulated by a nuclear receptor. *Mol. Cell* **36**, 340–347
79. Paris, O., Ferraro, L., Grober, O. M. V., Ravo, M., De Filippo, M. R., Giurato, G., Nassa, G., Tarallo, R., Cantarella, C., Rizzo, F., Di Benedetto, A., Mottolese, M., Benes, V., Ambrosino, C., Nola, E., and Weisz, A. (2012) Direct regulation of microRNA biogenesis and expression by estrogen receptor beta in hormone-responsive breast cancer. *Oncogene* **31**, 4196–4206
80. Sakamoto, S., Aoki, K., Higuchi, T., Todaka, H., Morisawa, K., Tamaki, N., Hatano, E., Fukushima, A., Taniguchi, T., and Agata, Y. (2009) The NF90-NF45 complex functions as a negative regulator in the microRNA processing pathway. *Mol. Cell Biol.* **29**, 3754–3769
81. Shiohama, A., Sasaki, T., Noda, S., Minoshima, S., and Shimizu, N. (2007) Nucleolar localization of DGCR8 and identification of eleven DGCR8-associated proteins. *Exp. Cell Res.* **313**, 4196–4207
82. Cheloufi, S., Dos Santos, C. O., Chong, M. M. W., and Hannon, G. J. (2010) A dicer-independent miRNA biogenesis pathway that requires Ago catalysis. *Nature* **465**, 584–589
83. Cifuentes, D., Xue, H., Taylor, D. W., Patnode, H., Mishima, Y., Cheloufi, S., Ma, E., Mane, S., Hannon, G. J., Lawson, N. D., Wolfe, S. A., and Giraldez, A. J. (2010) A novel miRNA processing pathway independent of Dicer requires Argonaute2 catalytic activity. *Science* **328**, 1694–1698
84. Yang, J.-S., Maurin, T., Robine, N., Rasmussen, K. D., Jeffrey, K. L., Chandwani, R., Papapetrou, E. P., Sadelain, M., O'Carroll, D., and Lai, E. C. (2010) Conserved vertebrate mir-451 provides a platform for Dicer-independent, Ago2-mediated microRNA biogenesis. *Proc. Natl. Acad. Sci. U. S. A.* **107**, 15163–15168
85. Yoda, M., Cifuentes, D., Izumi, N., Sakaguchi, Y., Suzuki, T., Giraldez, A. J., and Tomari, Y. (2013) Poly(A)-specific ribonuclease mediates 3'-end trimming of Argonaute2-cleaved precursor microRNAs. *Cell Rep.* **5**, 715–726
86. Xie, M., Li, M., Vilborg, A., Lee, N., Shu, M.-D., Yartseva, V., Šestan, N., and Steitz, J. A. (2013) Mammalian 5'-capped microRNA precursors that generate a single microRNA. *Cell* **155**, 1568–1580

87. Okamura, K., Hagen, J. W., Duan, H., Tyler, D. M., and Lai, E. C. (2007) The mirtron pathway generates microRNA-class regulatory RNAs in *Drosophila*. *Cell* **130**, 89–100
88. Ruby, J. G., Jan, C. H., and Bartel, D. P. (2007) Intronic microRNA precursors that bypass Drosha processing. *Nature* **448**, 83–86
89. Kim, U., Wang, Y., Sanford, T., Zeng, Y., and Nishikura, K. (1994) Molecular cloning of cDNA for double-stranded RNA adenosine deaminase, a candidate enzyme for nuclear RNA editing. *Proc. Natl. Acad. Sci. U. S. A.* **91**, 11457–11461
90. Yang, W., Chendrimada, T. P., Wang, Q., Higuchi, M., Seeburg, P. H., Shiekhattar, R., and Nishikura, K. (2006) Modulation of microRNA processing and expression through RNA editing by ADAR deaminases. *Nat. Struct. Mol. Biol.* **13**, 13–21
91. Kawahara, Y., Megraw, M., Kreider, E., Iizasa, H., Valente, L., Hatzigeorgiou, A. G., and Nishikura, K. (2008) Frequency and fate of microRNA editing in human brain. *Nucleic Acids Res.* **36**, 5270–5280
92. Choudhury, Y., Tay, F. C., Lam, D. H., Sandanaraj, E., Tang, C., Ang, B.-T., and Wang, S. (2012) Attenuated adenosine-to-inosine editing of microRNA-376a* promotes invasiveness of glioblastoma cells. *J. Clin. Invest.* **122**, 4059–4076
93. Newman, M. A., Mani, V., and Hammond, S. M. (2011) Deep sequencing of microRNA precursors reveals extensive 3' end modification. *RNA* **17**, 1795–1803
94. Katoh, T., Sakaguchi, Y., Miyauchi, K., Suzuki, T., Kashiwabara, S.-I., Baba, T., and Suzuki, T. (2009) Selective stabilization of mammalian microRNAs by 3' adenylation mediated by the cytoplasmic poly(A) polymerase GLD-2. *Genes Dev.* **23**, 433–438
95. Burroughs, A. M., Ando, Y., de Hoon, M. J. L., Tomaru, Y., Nishibu, T., Ukekawa, R., Funakoshi, T., Kurokawa, T., Suzuki, H., Hayashizaki, Y., and Daub, C. O. (2010) A comprehensive survey of 3' animal miRNA modification events and a possible role for 3' adenylation in modulating miRNA targeting effectiveness. *Genome Res.* **20**, 1398–1410

96. Yu, B., Yang, Z., Li, J., Minakhina, S., Yang, M., Padgett, R. W., Steward, R., and Chen, X. (2005) Methylation as a crucial step in plant microRNA biogenesis. *Science* **307**, 932–935
97. Li, J., Yang, Z., Yu, B., Liu, J., and Chen, X. (2005) Methylation protects miRNAs and siRNAs from a 3'-end uridylation activity in Arabidopsis. *Curr. Biol. CB* **15**, 1501–1507
98. Xhemalce, B., Robson, S. C., and Kouzarides, T. (2012) Human RNA Methyltransferase BCDIN3D Regulates MicroRNA Processing. *Cell* **151**, 278–288
99. Wyman, S. K., Knouf, E. C., Parkin, R. K., Fritz, B. R., Lin, D. W., Dennis, L. M., Krouse, M. A., Webster, P. J., and Tewari, M. (2011) Post-transcriptional generation of miRNA variants by multiple nucleotidyl transferases contributes to miRNA transcriptome complexity. *Genome Res.* **21**, 1450–1461
100. Krol, J., Loedige, I., and Filipowicz, W. (2010) The widespread regulation of microRNA biogenesis, function and decay. *Nat. Rev. Genet.* **11**, 597–610
101. Ramachandran, V., and Chen, X. (2008) Degradation of microRNAs by a family of exoribonucleases in Arabidopsis. *Science* **321**, 1490–1492
102. Chatterjee, S., and Großhans, H. (2009) Active turnover modulates mature microRNA activity in *Caenorhabditis elegans*. *Nature* **461**, 546–549
103. Rohrbaugh, M., Ramos, E., Nguyen, D., Price, M., Wen, Y., and Lai, Z. C. (2002) Notch activation of yan expression is antagonized by RTK/pointed signaling in the *Drosophila* eye. *Curr. Biol. CB* **12**, 576–581
104. Li, X., Cassidy, J. J., Reinke, C. A., Fischboeck, S., and Carthew, R. W. (2009) A microRNA imparts robustness against environmental fluctuation during development. *Cell* **137**, 273–282
105. Chou, Y.-T., Lin, H.-H., Lien, Y.-C., Wang, Y.-H., Hong, C.-F., Kao, Y.-R., Lin, S.-C., Chang, Y.-C., Lin, S.-Y., Chen, S.-J., Chen, H.-C., Yeh, S.-D., and Wu, C.-W. (2010) EGFR promotes lung tumorigenesis by activating miR-7 through a Ras/ERK/Myc pathway that targets the Ets2 transcriptional repressor ERF. *Cancer Res.* **70**, 8822–8831

106. Osella, M., Bosia, C., Corá, D., and Caselle, M. (2011) The role of incoherent microRNA-mediated feedforward loops in noise buffering. *PLoS Comput. Biol.* **7**, e1001101
107. Marson, A., Levine, S. S., Cole, M. F., Frampton, G. M., Brambrink, T., Johnstone, S., Guenther, M. G., Johnston, W. K., Wernig, M., Newman, J., Calabrese, J. M., Dennis, L. M., Volkert, T. L., Gupta, S., Love, J., Hannett, N., Sharp, P. A., Bartel, D. P., Jaenisch, R., and Young, R. A. (2008) Connecting microRNA Genes to the Core Transcriptional Regulatory Circuitry of Embryonic Stem Cells. *Cell* **134**, 521–533
108. Woods, K., Thomson, J. M., and Hammond, S. M. (2007) Direct regulation of an oncogenic micro-RNA cluster by E2F transcription factors. *J. Biol. Chem.* **282**, 2130–2134
109. Brosh, R., Shalgi, R., Liran, A., Landan, G., Korotayev, K., Nguyen, G. H., Enerly, E., Johnsen, H., Baganim, Y., Solomon, H., Goldstein, I., Madar, S., Goldfinger, N., Børresen - Dale, A.-L., Ginsberg, D., Harris, C. C., Pilpel, Y., Oren, M., and Rotter, V. (2008) p53-repressed miRNAs are involved with E2F in a feed-forward loop promoting proliferation. *Mol. Syst. Biol.* **4** [online] <http://msb.embopress.org/content/4/1/229> (Accessed April 9, 2014).
110. Gregory, P. A., Bert, A. G., Paterson, E. L., Barry, S. C., Tsykin, A., Farshid, G., Vadas, M. A., Khew-Goodall, Y., and Goodall, G. J. (2008) The miR-200 family and miR-205 regulate epithelial to mesenchymal transition by targeting ZEB1 and SIP1. *Nat. Cell Biol.* **10**, 593–601
111. Bracken, C. P., Gregory, P. A., Kolesnikoff, N., Bert, A. G., Wang, J., Shannon, M. F., and Goodall, G. J. (2008) A double-negative feedback loop between ZEB1-SIP1 and the microRNA-200 family regulates epithelial-mesenchymal transition. *Cancer Res.* **68**, 7846–7854
112. Inui, M., Martello, G., and Piccolo, S. (2010) MicroRNA control of signal transduction. *Nat. Rev. Mol. Cell Biol.* **11**, 252–263
113. Salmena, L., Poliseno, L., Tay, Y., Kats, L., and Pandolfi, P. P. (2011) A ceRNA hypothesis: the Rosetta Stone of a hidden RNA language? *Cell* **146**, 353–358
114. Karreth, F. A., Tay, Y., Perna, D., Ala, U., Tan, S. M., Rust, A. G., DeNicola, G., Webster, K. A., Weiss, D., Perez-Mancera, P. A., Krauthammer, M., Halaban, R., Provero, P., Adams, D. J., Tuveson, D. A., and Pandolfi, P. P. (2011) In vivo identification of tumor-

suppressive PTEN ceRNAs in an oncogenic BRAF-induced mouse model of melanoma. *Cell* **147**, 382–395

115. Esquela-Kerscher, A., and Slack, F. J. (2006) Oncomirs — microRNAs with a role in cancer. *Nat. Rev. Cancer* **6**, 259–269
116. Calin, G. A., and Croce, C. M. (2006) MicroRNA signatures in human cancers. *Nat. Rev. Cancer* **6**, 857–866
117. He, L., and Hannon, G. J. (2004) MicroRNAs: small RNAs with a big role in gene regulation. *Nat. Rev. Genet.* **5**, 522–531
118. Garding, A., Bhattacharya, N., Claus, R., Ruppel, M., Tschuch, C., Filarsky, K., Idler, I., Zucknick, M., Caudron-Herger, M., Oakes, C., Fleig, V., Keklikoglou, I., Allegra, D., Serra, L., Thakurela, S., Tiwari, V., Weichenhan, D., Benner, A., Radlwimmer, B., Zentgraf, H., Wiemann, S., Rippe, K., Plass, C., Döhner, H., Lichter, P., Stilgenbauer, S., and Mertens, D. (2013) Epigenetic upregulation of lncRNAs at 13q14.3 in leukemia is linked to the In Cis downregulation of a gene cluster that targets NF-κB. *PLoS Genet.* **9**, e1003373
119. Cimmino, A., Calin, G. A., Fabbri, M., Iorio, M. V., Ferracin, M., Shimizu, M., Wojcik, S. E., Aqeilan, R. I., Zupo, S., Dono, M., Rassenti, L., Alder, H., Volinia, S., Liu, C.-G., Kipps, T. J., Negrini, M., and Croce, C. M. (2005) miR-15 and miR-16 induce apoptosis by targeting BCL2. *Proc. Natl. Acad. Sci. U. S. A.* **102**, 13944–13949
120. Xia, L., Zhang, D., Du, R., Pan, Y., Zhao, L., Sun, S., Hong, L., Liu, J., and Fan, D. (2008) miR-15b and miR-16 modulate multidrug resistance by targeting BCL2 in human gastric cancer cells. *Int. J. Cancer J. Int. Cancer* **123**, 372–379
121. Garzon, R., Pichiorri, F., Palumbo, T., Visentini, M., Aqeilan, R., Cimmino, A., Wang, H., Sun, H., Volinia, S., Alder, H., Calin, G. A., Liu, C.-G., Andreeff, M., and Croce, C. M. (2007) MicroRNA gene expression during retinoic acid-induced differentiation of human acute promyelocytic leukemia. *Oncogene* **26**, 4148–4157
122. Martello, G., Zacchigna, L., Inui, M., Montagner, M., Adorno, M., Mamidi, A., Morsut, L., Soligo, S., Tran, U., Dupont, S., Cordenonsi, M., Wessely, O., and Piccolo, S. (2007) MicroRNA control of Nodal signalling. *Nature* **449**, 183–188

123. Korpala, M., and Kang, Y. (2008) The emerging role of miR-200 family of microRNAs in epithelial-mesenchymal transition and cancer metastasis. *RNA Biol.* **5**, 115–119
124. Williams, L. V., Veliceasa, D., Vinokour, E., and Volpert, O. V. (2013) miR-200b inhibits prostate cancer EMT, growth and metastasis. *PLoS One* **8**, e83991
125. Paterson, E. L., Kazenwadel, J., Bert, A. G., Khew-Goodall, Y., Ruzkiewicz, A., and Goodall, G. J. (2013) Down-regulation of the miRNA-200 family at the invasive front of colorectal cancers with degraded basement membrane indicates EMT is involved in cancer progression. *Neoplasia N. Y. N* **15**, 180–191
126. Li, X., Roslan, S., Johnstone, C. N., Wright, J. A., Bracken, C. P., Anderson, M., Bert, A. G., Selth, L. A., Anderson, R. L., Goodall, G. J., Gregory, P. A., and Khew-Goodall, Y. (2013) MiR-200 can repress breast cancer metastasis through ZEB1-independent but moesin-dependent pathways. *Oncogene*
127. Gravgaard, K. H., Lyng, M. B., Laenkholm, A.-V., Søkilde, R., Nielsen, B. S., Litman, T., and Ditzel, H. J. (2012) The miRNA-200 family and miRNA-9 exhibit differential expression in primary versus corresponding metastatic tissue in breast cancer. *Breast Cancer Res. Treat.* **134**, 207–217
128. Korpala, M., Ell, B. J., Buffa, F. M., Ibrahim, T., Blanco, M. A., Celià-Terrassa, T., Mercatali, L., Khan, Z., Goodarzi, H., Hua, Y., Wei, Y., Hu, G., Garcia, B. A., Ragoussis, J., Amadori, D., Harris, A. L., and Kang, Y. (2011) Direct targeting of Sec23a by miR-200s influences cancer cell secretome and promotes metastatic colonization. *Nat. Med.* **17**, 1101–1108
129. Liu, Y.-N., Yin, J. J., Abou-Kheir, W., Hynes, P. G., Casey, O. M., Fang, L., Yi, M., Stephens, R. M., Seng, V., Sheppard-Tillman, H., Martin, P., and Kelly, K. (2013) MiR-1 and miR-200 inhibit EMT via Slug-dependent and tumorigenesis via Slug-independent mechanisms. *Oncogene* **32**, 296–306
130. Niranjanakumari, S., Lasda, E., Brazas, R., and Garcia-Blanco, M. A. (2002) Reversible cross-linking combined with immunoprecipitation to study RNA–protein interactions in vivo. *Methods* **26**, 182–190
131. Keene, J. D., Komisarow, J. M., and Friedersdorf, M. B. (2006) RIP-Chip: the isolation and identification of mRNAs, microRNAs and protein components of ribonucleoprotein complexes from cell extracts. *Nat. Protoc.* **1**, 302–307

132. Zhao, J., Ohsumi, T. K., Kung, J. T., Ogawa, Y., Grau, D. J., Sarma, K., Song, J. J., Kingston, R. E., Borowsky, M., and Lee, J. T. (2010) Genome-wide identification of polycomb-associated RNAs by RIP-seq. *Mol. Cell* **40**, 939–953
133. Ule, J., Jensen, K. B., Ruggiu, M., Mele, A., Ule, A., and Darnell, R. B. (2003) CLIP identifies Nova-regulated RNA networks in the brain. *Science* **302**, 1212–1215
134. Licatalosi, D. D., Mele, A., Fak, J. J., Ule, J., Kayikci, M., Chi, S. W., Clark, T. A., Schweitzer, A. C., Blume, J. E., Wang, X., Darnell, J. C., and Darnell, R. B. (2008) HITS-CLIP yields genome-wide insights into brain alternative RNA processing. *Nature* **456**, 464–469
135. Hafner, M., Landthaler, M., Burger, L., Khorshid, M., Hausser, J., Berninger, P., Rothballer, A., Ascano, M., Jr, Jungkamp, A.-C., Munschauer, M., Ulrich, A., Wardle, G. S., Dewell, S., Zavolan, M., and Tuschl, T. (2010) Transcriptome-wide identification of RNA-binding protein and microRNA target sites by PAR-CLIP. *Cell* **141**, 129–141
136. Hafner, M., Landthaler, M., Burger, L., Khorshid, M., Hausser, J., Berninger, P., Rothballer, A., Ascano, M., Jungkamp, A.-C., Munschauer, M., Ulrich, A., Wardle, G. S., Dewell, S., Zavolan, M., and Tuschl, T. (2010) PAR-CLIP--a method to identify transcriptome-wide the binding sites of RNA binding proteins. *J. Vis. Exp. JoVE*
137. König, J., Zarnack, K., Rot, G., Curk, T., Kayikci, M., Zupan, B., Turner, D. J., Luscombe, N. M., and Ule, J. (2010) iCLIP reveals the function of hnRNP particles in splicing at individual nucleotide resolution. *Nat. Struct. Mol. Biol.* **17**, 909–915
138. Slobodin, B., and Gerst, J. E. (2010) A novel mRNA affinity purification technique for the identification of interacting proteins and transcripts in ribonucleoprotein complexes. *RNA* **16**, 2277–2290
139. Castello, A., Fischer, B., Eichelbaum, K., Horos, R., Beckmann, B. M., Strein, C., Davey, N. E., Humphreys, D. T., Preiss, T., Steinmetz, L. M., Krijgsveld, J., and Hentze, M. W. (2012) Insights into RNA biology from an atlas of mammalian mRNA-binding proteins. *Cell* **149**, 1393–1406
140. Castello, A., Horos, R., Strein, C., Fischer, B., Eichelbaum, K., Steinmetz, L. M., Krijgsveld, J., and Hentze, M. W. (2013) System-wide identification of RNA-binding proteins by interactome capture. *Nat. Protoc.* **8**, 491–500

141. Curanovic, D., Cohen, M., Singh, I., Slagle, C. E., Leslie, C. S., and Jaffrey, S. R. (2013) Global profiling of stimulus-induced polyadenylation in cells using a poly(A) trap. *Nat. Chem. Biol.* **9**, 671–673
142. Chu, C., Qu, K., Zhong, F. L., Artandi, S. E., and Chang, H. Y. (2011) Genomic maps of long noncoding RNA occupancy reveal principles of RNA-chromatin interactions. *Mol. Cell* **44**, 667–678
143. Engreitz, J. M., Pandya-Jones, A., McDonel, P., Shishkin, A., Sirokman, K., Surka, C., Kadri, S., Xing, J., Goren, A., Lander, E. S., Plath, K., and Guttman, M. (2013) The Xist lncRNA exploits three-dimensional genome architecture to spread across the X chromosome. *Science* **341**, 1237973
144. Porcheddu, A., and Giacomelli, G. (2005) Peptide nucleic acids (PNAs), a chemical overview. *Curr. Med. Chem.* **12**, 2561–2599
145. Ohtsuki, T., Fujimoto, T., Kamimukai, M., Kumano, C., Kitamatsu, M., and Sisido, M. (2008) Isolation of small RNAs using biotinylated PNAs. *J. Biochem. (Tokyo)* **144**, 415–418
146. Wu, H., Xu, H., Miraglia, L. J., and Crooke, S. T. (2000) Human RNase III is a 160-kDa protein involved in preribosomal RNA processing. *J. Biol. Chem.* **275**, 36957–36965
147. Bernstein, D. A., Vyas, V. K., Weinberg, D. E., Drinnenberg, I. A., Bartel, D. P., and Fink, G. R. (2012) *Candida albicans* Dicer (CaDcr1) is required for efficient ribosomal and spliceosomal RNA maturation. *Proc. Natl. Acad. Sci. U. S. A.* **109**, 523–528
148. Liang, X.-H., and Crooke, S. T. (2011) Depletion of key protein components of the RISC pathway impairs pre-ribosomal RNA processing. *Nucleic Acids Res.* **39**, 4875–4889
149. Teng, Y., Girvan, A. C., Casson, L. K., Pierce, W. M., Jr, Qian, M., Thomas, S. D., and Bates, P. J. (2007) AS1411 alters the localization of a complex containing protein arginine methyltransferase 5 and nucleolin. *Cancer Res.* **67**, 10491–10500
150. Landthaler, M., Yalcin, A., and Tuschl, T. (2004) The human DiGeorge syndrome critical region gene 8 and its *D. melanogaster* homolog are required for miRNA biogenesis. *Curr. Biol. CB* **14**, 2162–2167

151. Ogawa-Goto, K., Tanaka, K., Ueno, T., Tanaka, K., Kurata, T., Sata, T., and Irie, S. (2007) p180 is involved in the interaction between the endoplasmic reticulum and microtubules through a novel microtubule-binding and bundling domain. *Mol. Biol. Cell* **18**, 3741–3751
152. Lee, Y., and Kim, V. N. (2007) In vitro and in vivo assays for the activity of Drosha complex. *Methods Enzymol.* **427**, 89–106
153. Guil, S., and Cáceres, J. F. (2007) The multifunctional RNA-binding protein hnRNP A1 is required for processing of miR-18a. *Nat. Struct. Mol. Biol.* **14**, 591–596
154. Jalal, C., Uhlmann-Schiffler, H., and Stahl, H. (2007) Redundant role of DEAD box proteins p68 (Ddx5) and p72/p82 (Ddx17) in ribosome biogenesis and cell proliferation. *Nucleic Acids Res.* **35**, 3590–3601
155. Sinkkonen, L., Hugenschmidt, T., Filipowicz, W., and Svoboda, P. (2010) Dicer is associated with ribosomal DNA chromatin in mammalian cells. *PloS One* **5**, e12175
156. Ganesan, G., and Rao, S. M. R. (2008) A novel noncoding RNA processed by Drosha is restricted to nucleus in mouse. *RNA N. Y. N* **14**, 1399–1410
157. Ginisty, H., Amalric, F., and Bouvet, P. (1998) Nucleolin functions in the first step of ribosomal RNA processing. *EMBO J.* **17**, 1476–1486
158. Otake, Y., Soundararajan, S., Sengupta, T. K., Kio, E. A., Smith, J. C., Pineda-Roman, M., Stuart, R. K., Spicer, E. K., and Fernandes, D. J. (2007) Overexpression of nucleolin in chronic lymphocytic leukemia cells induces stabilization of bcl2 mRNA. *Blood* **109**, 3069–3075
159. Mi, Y., Thomas, S. D., Xu, X., Casson, L. K., Miller, D. M., and Bates, P. J. (2003) Apoptosis in leukemia cells is accompanied by alterations in the levels and localization of nucleolin. *J. Biol. Chem.* **278**, 8572–8579
160. Joo, E. J., Yang, H., Park, Y., Park, N. Y., Toida, T., Linhardt, R. J., and Kim, Y. S. (2010) Induction of nucleolin translocation by acharan sulfate in A549 human lung adenocarcinoma. *J. Cell. Biochem.* **110**, 1272–1278

161. Mourmouras, V., Cevenini, G., Cosci, E., Epistolato, M. C., Biagioli, M., Barbagli, L., Luzi, P., Mannucci, S., and Miracco, C. (2009) Nucleolin protein expression in cutaneous melanocytic lesions. *J. Cutan. Pathol.* **36**, 637–646
162. González, V., and Hurley, L. H. (2010) The C-terminus of nucleolin promotes the formation of the c-MYC G-quadruplex and inhibits c-MYC promoter activity. *Biochemistry (Mosc.)* **49**, 9706–9714
163. Chang, T.-C., Yu, D., Lee, Y.-S., Wentzel, E. A., Arking, D. E., West, K. M., Dang, C. V., Thomas-Tikhonenko, A., and Mendell, J. T. (2008) Widespread microRNA repression by Myc contributes to tumorigenesis. *Nat. Genet.* **40**, 43–50
164. Daniely, Y., Dimitrova, D. D., and Borowiec, J. A. (2002) Stress-dependent nucleolin mobilization mediated by p53-nucleolin complex formation. *Mol. Cell. Biol.* **22**, 6014–6022
165. Gopal, Y. N. V., Arora, T. S., and Van Dyke, M. W. (2007) Parthenolide specifically depletes histone deacetylase 1 protein and induces cell death through ataxia telangiectasia mutated. *Chem. Biol.* **14**, 813–823
166. Politz, J. C. R., Hogan, E. M., and Pederson, T. (2009) MicroRNAs with a nucleolar location. *RNA N. Y. N* **15**, 1705–1715
167. Politz, J. C. R., Zhang, F., and Pederson, T. (2006) MicroRNA-206 colocalizes with ribosome-rich regions in both the nucleolus and cytoplasm of rat myogenic cells. *Proc. Natl. Acad. Sci. U. S. A.* **103**, 18957–18962
168. Créancier, L., Prats, H., Zanibellato, C., Amalric, F., and Bugler, B. (1993) Determination of the functional domains involved in nucleolar targeting of nucleolin. *Mol. Biol. Cell* **4**, 1239–1250
169. Allain, F. H., Bouvet, P., Dieckmann, T., and Feigon, J. (2000) Molecular basis of sequence-specific recognition of pre-ribosomal RNA by nucleolin. *EMBO J.* **19**, 6870–6881
170. Lee, Y., Ahn, C., Han, J., Choi, H., Kim, J., Yim, J., Lee, J., Provost, P., Rådmark, O., Kim, S., and Kim, V. N. (2003) The nuclear RNase III Drosha initiates microRNA processing. *Nature* **425**, 415–419

171. Chaffer, C. L., Marjanovic, N. D., Lee, T., Bell, G., Kleer, C. G., Reinhardt, F., D'Alessio, A. C., Young, R. A., and Weinberg, R. A. (2013) Poised chromatin at the ZEB1 promoter enables breast cancer cell plasticity and enhances tumorigenicity. *Cell* **154**, 61–74
172. Wright, J. A., Richer, J. K., and Goodall, G. J. (2010) microRNAs and EMT in mammary cells and breast cancer. *J. Mammary Gland Biol. Neoplasia* **15**, 213–223
173. Chang, C.-J., Chao, C.-H., Xia, W., Yang, J.-Y., Xiong, Y., Li, C.-W., Yu, W.-H., Rehman, S. K., Hsu, J. L., Lee, H.-H., Liu, M., Chen, C.-T., Yu, D., and Hung, M.-C. (2011) p53 regulates epithelial-mesenchymal transition and stem cell properties through modulating miRNAs. *Nat. Cell Biol.* **13**, 317–323
174. Lu, J., Guo, H., Treekitkarnmongkol, W., Li, P., Zhang, J., Shi, B., Ling, C., Zhou, X., Chen, T., Chiao, P. J., Feng, X., Seewaldt, V. L., Muller, W. J., Sahin, A., Hung, M.-C., and Yu, D. (2009) 14-3-3zeta Cooperates with ErbB2 to promote ductal carcinoma in situ progression to invasive breast cancer by inducing epithelial-mesenchymal transition. *Cancer Cell* **16**, 195–207
175. Danes, C. G., Wyszomierski, S. L., Lu, J., Neal, C. L., Yang, W., and Yu, D. (2008) 14-3-3 zeta down-regulates p53 in mammary epithelial cells and confers luminal filling. *Cancer Res.* **68**, 1760–1767
176. Kwon, S. C., Yi, H., Eichelbaum, K., Föhr, S., Fischer, B., You, K. T., Castello, A., Krijgsveld, J., Hentze, M. W., and Kim, V. N. (2013) The RNA-binding protein repertoire of embryonic stem cells. *Nat. Struct. Mol. Biol.* **20**, 1122–1130
177. Igloi, G. L. (2003) Single-nucleotide polymorphism detection using peptide nucleic acids. *Expert Rev. Mol. Diagn.* **3**, 17–26
178. Nielsen, E. (2006) RNA targeting using peptide nucleic acid. *Handb. Exp. Pharmacol.*, 395–403
179. Armitage, B. A. (2003) The impact of nucleic acid secondary structure on PNA hybridization. *Drug Discov. Today* **8**, 222–228
180. Nielsen, P. E. (2004) PNA Technology. *Mol. Biotechnol.* **26**, 233–248
181. Nielsen, P. E. (2002) PNA technology. *Methods Mol. Biol. Clifton NJ* **208**, 3–26

182. Rezaee, M., Isokawa, K., Halligan, N., Markwald, R. R., and Krug, E. L. (1993) Identification of an extracellular 130-kDa protein involved in early cardiac morphogenesis. *J. Biol. Chem.* **268**, 14404–14411
183. Krug, E. L., Rezaee, M., Isokawa, K., Turner, D. K., Litke, L. L., Wunsch, A. M., Bain, J. L., Riley, D. A., Capehart, A. A., and Markwald, R. R. (1995) Transformation of cardiac endothelium into cushion mesenchyme is dependent on ES/130: temporal, spatial, and functional studies in the early chick embryo. *Cell. Mol. Biol. Res.* **41**, 263–277
184. Langley, R., Leung, E., Morris, C., Berg, R., McDonald, M., Weaver, A., Parry, D. A., Ni, J., Su, J., Gentz, R., Spurr, N., and Krissansen, G. W. (1998) Identification of multiple forms of 180-kDa ribosome receptor in human cells. *DNA Cell Biol.* **17**, 449–460
185. Kim, Y. J., Lee, M. C., Kim, S. J., and Chun, J. Y. (2000) Identification and characterization of multiple isoforms of a mouse ribosome receptor. *Gene* **261**, 337–344
186. Bai, J.-Z., Leung, E., Holloway, H., and Krissansen, G. W. (2008) Alternatively spliced forms of the P180 ribosome receptor differ in their ability to induce the proliferation of rough endoplasmic reticulum. *Cell Biol. Int.* **32**, 473–483
187. Ueno, T., Kaneko, K., Sata, T., Hattori, S., and Ogawa-Goto, K. (2012) Regulation of polysome assembly on the endoplasmic reticulum by a coiled-coil protein, p180. *Nucleic Acids Res.* **40**, 3006–3017
188. Chang, J., Chance, M. R., Nicholas, C., Ahmed, N., Guilmeau, S., Flandez, M., Wang, D., Byun, D.-S., Nasser, S., Albanese, J. M., Corner, G. A., Heerdt, B. G., Wilson, A. J., Augenlicht, L. H., and Mariadason, J. M. (2008) Proteomic changes during intestinal cell maturation in vivo. *J. Proteomics* **71**, 530–546
189. Telikicherla, D., Marimuthu, A., Kashyap, M. K., Ramachandra, Y. L., Mohan, S., Roa, J. C., Maharudraiah, J., and Pandey, A. (2012) Overexpression of ribosome binding protein 1 (RRBP1) in breast cancer. *Clin. Proteomics* **9**, 7
190. Chen, X., Iliopoulos, D., Zhang, Q., Tang, Q., Greenblatt, M. B., Hatziapostolou, M., Lim, E., Tam, W. L., Ni, M., Chen, Y., Mai, J., Shen, H., Hu, D. Z., Adoro, S., Hu, B., Song, M., Tan, C., Landis, M. D., Ferrari, M., Shin, S. J., Brown, M., Chang, J. C., Liu, X. S., and Glimcher, L. H. (2014) XBP1 promotes triple-negative breast cancer by controlling the HIF1 α pathway. *Nature* **508**, 103–107

191. Tellez, C. S., Juri, D. E., Do, K., Bernauer, A. M., Thomas, C. L., Damiani, L. A., Tessema, M., Leng, S., and Belinsky, S. A. (2011) EMT and stem cell-like properties associated with miR-205 and miR-200 epigenetic silencing are early manifestations during carcinogen-induced transformation of human lung epithelial cells. *Cancer Res.* **71**, 3087–3097
192. Huppertz, I., Attig, J., D'Ambrogio, A., Easton, L. E., Sibley, C. R., Sugimoto, Y., Tajnik, M., König, J., and Ule, J. (2014) iCLIP: protein-RNA interactions at nucleotide resolution. *Methods San Diego Calif* **65**, 274–287
193. Craene, B. D., and Berx, G. (2013) Regulatory networks defining EMT during cancer initiation and progression. *Nat. Rev. Cancer* **13**, 97–110
194. Gregory, P. A., Bracken, C. P., Smith, E., Bert, A. G., Wright, J. A., Roslan, S., Morris, M., Wyatt, L., Farshid, G., Lim, Y.-Y., Lindeman, G. J., Shannon, M. F., Drew, P. A., Khew-Goodall, Y., and Goodall, G. J. (2011) An autocrine TGF-beta/ZEB/miR-200 signaling network regulates establishment and maintenance of epithelial-mesenchymal transition. *Mol. Biol. Cell* **22**, 1686–1698
195. Wang, G., Guo, X., Hong, W., Liu, Q., Wei, T., Lu, C., Gao, L., Ye, D., Zhou, Y., Chen, J., Wang, J., Wu, M., Liu, H., and Kang, J. (2013) Critical regulation of miR-200/ZEB2 pathway in Oct4/Sox2-induced mesenchymal-to-epithelial transition and induced pluripotent stem cell generation. *Proc. Natl. Acad. Sci. U. S. A.* **110**, 2858–2863
196. Hurteau, G. J., Carlson, J. A., Roos, E., and Brock, G. J. (2009) Stable expression of miR-200c alone is sufficient to regulate TCF8 (ZEB1) and restore E-cadherin expression. *Cell Cycle Georget. Tex* **8**, 2064–2069
197. Kim, T., Veronese, A., Pichiorri, F., Lee, T. J., Jeon, Y.-J., Volinia, S., Pineau, P., Marchio, A., Palatini, J., Suh, S.-S., Alder, H., Liu, C.-G., Dejean, A., and Croce, C. M. (2011) p53 regulates epithelial-mesenchymal transition through microRNAs targeting ZEB1 and ZEB2. *J. Exp. Med.* **208**, 875–883
198. Wellner, U., Schubert, J., Burk, U. C., Schmalhofer, O., Zhu, F., Sonntag, A., Waldvogel, B., Vannier, C., Darling, D., zur Hausen, A., Brunton, V. G., Morton, J., Sansom, O., Schüler, J., Stemmler, M. P., Herzberger, C., Hopt, U., Keck, T., Brabletz, S., and Brabletz, T. (2009) The EMT-activator ZEB1 promotes tumorigenicity by repressing stemness-inhibiting microRNAs. *Nat. Cell Biol.* **11**, 1487–1495

199. Hovanesian, A. G., Soundaramourty, C., El Khoury, D., Nondier, I., Svab, J., and Krust, B. (2010) Surface expressed nucleolin is constantly induced in tumor cells to mediate calcium-dependent ligand internalization. *PLoS One* **5**, e15787
200. Wu, D., Zhang, P., Liu, R., Sang, Y., Zhou, C., Xu, G., Yang, J., Tong, A., and Wang, C. Phosphorylation and changes in the distribution of nucleolin promote tumor metastasis via the PI3K/Akt pathway in colorectal carcinoma. *FEBS Lett.* Available online 5 April 2014, ISSN 0014-5793
201. Girvan, A. C., Teng, Y., Casson, L. K., Thomas, S. D., Jülicher, S., Ball, M. W., Klein, J. B., Pierce, W. M., Jr, Barve, S. S., and Bates, P. J. (2006) AGRO100 inhibits activation of nuclear factor-kappaB (NF-kappaB) by forming a complex with NF-kappaB essential modulator (NEMO) and nucleolin. *Mol. Cancer Ther.* **5**, 1790–1799
202. Reyes-Reyes, E. M., Teng, Y., and Bates, P. J. (2010) A new paradigm for aptamer therapeutic AS1411 action: uptake by macropinocytosis and its stimulation by a nucleolin-dependent mechanism. *Cancer Res.* **70**, 8617–8629
203. Pichiorri, F., Palmieri, D., De Luca, L., Consiglio, J., You, J., Rocci, A., Talabere, T., Piovan, C., Lagana, A., Cascione, L., Guan, J., Gasparini, P., Balatti, V., Nuovo, G., Coppola, V., Hofmeister, C. C., Marcucci, G., Byrd, J. C., Volinia, S., Shapiro, C. L., Freitas, M. A., and Croce, C. M. (2013) In vivo NCL targeting affects breast cancer aggressiveness through miRNA regulation. *J. Exp. Med.* **210**, 951–968
204. Shimono, Y., Zabala, M., Cho, R. W., Lobo, N., Dalerba, P., Qian, D., Diehn, M., Liu, H., Panula, S. P., Chiao, E., Dirbas, F. M., Somlo, G., Pera, R. A. R., Lao, K., and Clarke, M. F. (2009) Downregulation of miRNA-200c links breast cancer stem cells with normal stem cells. *Cell* **138**, 592–603
205. Pérez-Pomares, J. M., Macías, D., García-Garrido, L., and Muñoz-Chápuli, R. (1997) Contribution of the primitive epicardium to the subepicardial mesenchyme in hamster and chick embryos. *Dev. Dyn. Off. Publ. Am. Assoc. Anat.* **210**, 96–105
206. Larriba, M. J., Casado-Vela, J., Pendás-Franco, N., Peña, R., García de Herreros, A., Berciano, M. T., Lafarga, M., Casal, J. I., and Muñoz, A. (2010) Novel Snail1 Target Proteins in Human Colon Cancer Identified by Proteomic Analysis. *PLoS ONE* **5**, e10221
207. Tsai, H.-Y., Yang, Y.-F., Wu, A. T., Yang, C.-J., Liu, Y.-P., Jan, Y.-H., Lee, C.-H., Hsiao, Y.-W., Yeh, C.-T., Shen, C.-N., Lu, P.-J., Huang, M.-S., and Hsiao, M. (2013) Endoplasmic

reticulum ribosome-binding protein 1 (RRBP1) overexpression is frequently found in lung cancer patients and alleviates intracellular stress-induced apoptosis through the enhancement of GRP78. *Oncogene* **32**, 4921–4931

208. Shaffer, A. L., Shapiro-Shelef, M., Iwakoshi, N. N., Lee, A.-H., Qian, S.-B., Zhao, H., Yu, X., Yang, L., Tan, B. K., Rosenwald, A., Hurt, E. M., Petroulakis, E., Sonenberg, N., Yewdell, J. W., Calame, K., Glimcher, L. H., and Staudt, L. M. (2004) XBP1, downstream of Blimp-1, expands the secretory apparatus and other organelles, and increases protein synthesis in plasma cell differentiation. *Immunity* **21**, 81–93
209. Becker, F., Block-Alper, L., Nakamura, G., Harada, J., Wittrup, K. D., and Meyer, D. I. (1999) Expression of the 180-kD ribosome receptor induces membrane proliferation and increased secretory activity in yeast. *J. Cell Biol.* **146**, 273–284
210. Hyde, M., Block-Alper, L., Felix, J., Webster, P., and Meyer, D. I. (2002) Induction of secretory pathway components in yeast is associated with increased stability of their mRNA. *J. Cell Biol.* **156**, 993–1001
211. Kosaka, N., Yoshioka, Y., Tominaga, N., Hagiwara, K., Katsuda, T., and Ochiya, T. (2014) Dark side of the exosome: the role of the exosome in cancer metastasis and targeting the exosome as a strategy for cancer therapy. *Future Oncol. Lond. Engl.* **10**, 671–681
212. Obbard, D. J., Gordon, K. H. J., Buck, A. H., and Jiggins, F. M. (2009) The evolution of RNAi as a defence against viruses and transposable elements. *Philos. Trans. R. Soc. B Biol. Sci.* **364**, 99–115

Vita

Brian Frederick Pickering was born on April 24, 1982 in Canandaigua, New York to Fred and Barbara Pickering. In high school he spent three years conducting research at the New York State Department of Health and Skidmore College while competing in the Westinghouse competition. After graduating from Schuylerville High School in Schuylerville, New York in June of 2000 he enrolled at Texas A&M University, College Station, Texas where he studied bacterial chemotaxis through developing microfluidic flow chambers under the guidance of Dr. Michael Manson. He received a Bachelor of Science degree in Biology from Texas A&M in May, 2004. He then enrolled in the Biodefense Ph.D. program at George Mason University in Fairfax, Virginia, where he developed vaccines and therapeutics against the biothreat agents *Bacillus anthracis*, *Yersinia pestis*, and *Francisella tularensis* under the supervision of Dr. Ken Alibek. During his doctoral studies he appeared on the Discovery Channel show “Ultimate Weapons” discussing the threat of biological weapons and testified before the Congressional Joint Armed Services Committee on the potential impact of avian influenza. He successfully defended his thesis and graduated in January, 2007. He worked for a brief time for a biotechnology company, AFG Biosolutions, Inc. in Germantown, Virginia and went on to be a founder in a biopharmaceutical company, MaxWell Biopharma, Inc., in Kiev, Ukraine. In 2007 he began his second Ph.D. at the University of Texas at Houston Graduate School of Biomedical Science working for two years in the lab of Michael Van Dyke, Ph.D. and later joining the lab of Dihua Yu, MD, Ph.D. where he studied the regulation of microRNA biogenesis.